A NUMERICAL STUDY ON BLOCK SHEAR FAILURE OF STEEL TENSION MEMBERS

A THESIS SUBMITTED TO
THE GRADUATE SCHOOL OF NATURAL AND APPLIED SCIENCES
OF
MIDDLE EAST TECHNICAL UNIVERSITY

BY

EMRE KARA

IN PARTIAL FULFILLMENT OF THE REQUIREMENTS
FOR
THE DEGREE OF MASTER OF SCIENCE
IN
CIVIL ENGINEERING

JULY 2005

Approval of the Graduate School of Natural and Applied Sciences.

Prof. Dr. Canan Özgen
Director

I certify that this thesis satisfies all the requirements as a thesis for the degree of Master of Science.

Prof. Dr. Erdal Çokça
Head of Department

This is to certify that we have read this thesis and that in our opinion it is fully adequate, in scope and quality, as a thesis for the degree of Master of Science.

Assoc. Prof. Dr. Cem Topkaya
Supervisor

Examining Committee Members

Prof. Dr. Tanvir Wasti	(METU, CE)	
Assoc. Prof. Dr. Cem Topkaya	(METU, CE)	
Asst. Prof. Dr. Ahmet Türer	(METU, CE)	
Asst. Prof. Dr. Alp Caner	(METU, CE)	
Hasan Başaran	(PROMER ENG.)	

I hereby declare that all information in this document has been obtained and presented in accordance with academic rules and ethical conduct. I also declare that, as required by these rules and conduct, I have fully cited and referenced all material and results that are not original to this work.

Name, Last Name: Emre KARA

Signature :

ABSTRACT

A NUMERICAL STUDY ON BLOCK SHEAR FAILURE OF STEEL TENSION MEMBERS

Kara, Emre

M.S., Department of Civil Engineering

Supervisor : Assoc. Prof. Dr. Cem Topkaya

July 2005, 76 pages

Block shear is a limit state that should be accounted for during the design of the steel tension members. This failure mechanism combines a tension failure on one plane and a shear plane on a perpendicular plane. Although current design specifications present equations to predict block shear load capacities of the connections, they fail in predicting the failure modes. Block shear failure of a structural connection along a staggered path may be the governing failure mode. Code treatments for stagger in a block shear path are not exactly defined. A parametric study has been conducted and over a thousand finite element analyses were performed to identify the parameters affecting the block shear failure in connections with multiple bolt lines and staggered holes. The quality of the specification equations were assessed by comparing the code predictions with finite element results. In addition, based on the analytical findings new equations were developed and are presented herein.

Keywords: block shear, multiple bolt lines, staggered bolts, finite elements, tension members.

ÖZ

ÇELİK ÇEKME ELEMANLARININ BLOK KESME DAVRANIŞLARI ÜZERİNE BİR NÜMERİK ÇALIŞMA

Kara, Emre

Yüksek Lisans, İnşaat Mühendisliği Bölümü

Tez Yöneticisi : Doç. Dr. Cem Topkaya

Temmuz 2005, 76 sayfa

Blok kesme dayanımı çelik çekme elemanlarının tasarımında göz önüne alınması gereken limit durumlardan biridir. Blok kesme kapasitesi bir planda çekme, bu plana dik diğer bir planda kesme kapasitelerine ulaşılması sonucu elde edilir. Mevcut tasarım şartnameleri, bağlantıların blok kesme yük kapasitelerini tahmin etmeye yarayan formüller sunmaktadır. Ancak bu formüller doğru kapasite ulaşım modunu tahmin edememektedirler. Şaşırtmalı civatalı bağlantılarda da şaşırtma güzergahında blok kesme kapasitesine ulaşılabilmektedir. Ancak, şaşırtmalı civatalı bağlantılar için var olan tasarım kuralları tam olarak blok kesme güzergahını tanımlamamışlardır. Çoklu ve şaşırtmalı civatalı bağlantıların blok kesme kapasitesini etkileyen parametreleri incelemek için bini aşkın sonlu elemanlar analizini içeren bir çalışma yapılmıştır. Şartnamelerin sunduğu formüllerin kalitesi sonlu eleman analiz sonuçlarıyla yapılan karşılaştırmalarla ortaya çıkmıştır. Buna ek olarak, analitik bulgular üzerine yeni formüller geliştirilmiş ve bu çalışmada sunulmuştur.

Anahtar Sözcükler: blok kesme, çoklu dizinli civatalar, şaşırtmalı civatalar, sonlu elemanlar, çelik çekme elemanlar.

ACKNOWLEDGMENTS

The research presented in this thesis has been made possible with contributions from many individuals to whom I am indebted. This study was performed under the supervision of Dr. Cem Topkaya. I would like to express my sincere appreciation for his invaluable support, guidance and insights throughout my study. It has been a privilege for me to work under his guidance. I am very grateful to him for always keeping me motivated and showing his great interest at every step of my thesis. It would have been much harder for me to finish this study without his invaluable support.

I would like to thank my employer Ali Rıza Bakır for his understanding during my thesis study.

I would like to thank to Cenker Söğütlüoğlu not only for his friendship but also for his endless support and help during my study.

I would like to thank my dearest friend Sermin Oğuz, for being such an invaluable person throughout my life and for all the things she has done for me. Without her support, everything would be harder for me.

I would like to thank to my family, for their love, support and understanding during my life even they have been further away from me. I am greatly indebted to them for everything that they have done for me.

This study is dedicated to the memory of Sevdat Kaya with whom I passed most of my time during my university life and who departed this life at an early age.

TABLE OF CONTENTS

PAGE

PLAGIARISM iii

ABSTRACT iv

ÖZ v

ACKNOWLEDGMENTS vi

TABLE OF CONTENTS vii

CHAPTER

1. INTRODUCTION 1

1.1 Background 1

1.2 Previous Studies 4

1.2.1 Experimental Studies 4

1.2.1.1 Study of Ricles and Yura (1983) 4

1.2.1.2 Study of Hardash and Bjorhovde (1985) 4

1.2.1.3 Study of Epstein (1993) 5

1.2.1.4 Study of Gross (1995) 5

1.2.1.5 Study of Orbison (1998) 5

1.2.2 Statistical Studies 6

1.2.2.1 Study of Cunnigham (1995) 6

1.2.2.2 Study of Kulak and Grondin (2001) 6

PAGE

1.2.3 Finite Element Studies 7

1.2.3.1 Study of Epstein and Chamarajanagar (1996) 7

1.2.3.2 Study of Kulak and Wu (1997) 7

1.2.3.3 Study of Topkaya (2004) 8

1.3 Problem Statement 9

2. FINITE ELEMENT METHODOLOGY AND COMPARISONS WITH EXPERIMENTAL FINDINGS 10

2.1 Finite Element Methodology 10

2.2 Finite Element Analysis Predictions 12

3. ANALYSIS OF CONNECTIONS WITH MULTIPLE BOLT LINES 19

3.1 Results of the Analysis Cases 22

3.2 Discussion of the Results 28

3.2.1 Effect of End Distance 28

3.2.2 Effect of Pitch Distance 29

3.2.3 Effect of Connection Length 30

3.2.4 Effect of Ultimate-to-Yield Ratio 33

3.2.5 Effect of Block Aspect Ratio 33

3.3 Assessment of the Existing Capacity Prediction Equations 35

4. ANALYSIS OF STAGGER EFFECTS 44

4.1 Introduction 44

4.2 Investigation of Stagger with Triangular Pattern 45

PAGE

4.2.1 Results of the Analysis Cases 47

4.2.2 Assessment of the Existing Capacity Equations 49

4.2.3 Development of the Block Shear Capacity Prediction Equations for Staggered Connections 54

4.3 Investigation of Negative and Positive Stagger Pattern 61

4.2.1 Results of the Analysis Cases 63

4.2.2 Assessment of the Existing Capacity Equations 65

5. SUMMARY AND CONCLUSIONS 72

5.1 Summary 72

5.2 Conclusions 73

REFERENCES……..……75

CHAPTER 1

INTRODUCTION

1.1 Background

Tension members with bolted ends are frequently used as principal structural members in trusses and lateral bracing systems. These members are designed to resist yielding of the gross section, rupture of the minimum net section and block shear failure during the life time of the structure.

Block shear is known to be a potential failure mode which can control the load capacity of several different types of bolted connections, including shear connections at the ends of coped beams, tension member connections and gusset plates. It is a limit state that combines a tension failure on one plane and a shear failure on a perpendicular plane. Typical block shear failure mechanisms for a single angle tension member and gusset plate are shown in Figure 1.1. The 'block' of the connected plate bounded by the bolt holes tears out in this failure mechanism in which tensile force is developed along the upper edge of the block (tension plane) and a shear force develops along the bolt line (shear plane).

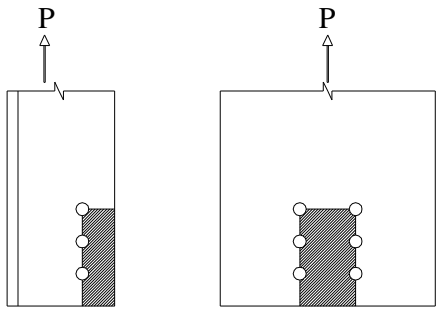

(a) Angle Connection (b) Gusset Plate Connection
Figure 1.1 : Typical Block Shear Failure Paths

The AISC- LRFD (2001) and ASD (1989) specifications present equations to predict the block shear rupture strength. The AISC-LRFD procedure assumes that when one plane, either tension or shear, reaches ultimate strength the other plane develops full yield. This assumption results in two possible failure mechanisms in which the controlling mode is the one having a larger fracture strength term. In the first mechanism, it is assumed that failure load is reached when rupture occurs along the net tension plane and full yield is developed along the gross shear plane. Conversely, the second failure mode assumes that rupture occurs along the net shear plane while full yield is developed at the gross tension plane. Based on these assumptions, the nominal block shear capacity is calculated as follows:

if $F_u A_{nt} \geq (0.6F_u)A_{nv}$

then $R_n = [F_u A_{nt} + (0.6F_y)A_{gv}] \leq [F_u A_{nt} + (0.6F_u)A_{nv}]$ (1.1)

and if $(0.6F_u)A_{nv} > F_u A_{nt}$

then $R_n = [(0.6F_u)A_{nv} + F_y A_{gt}] \leq [(0.6F_u)A_{nv} + F_u A_{nt}]$ (1.2)

where

F_y = tensile yield strength

F_u = tensile ultimate strength

A_{nt} = net area subjected to tension

A_{nv} = net area subjected to shear

A_{gt} = gross area subjected to tension

A_{gv} = gross area subjected to shear

R_n = nominal block shear resistance

A_{nt}, A_{nv}, A_{gt}, A_{gv} are shown in Figure 1.2 below.

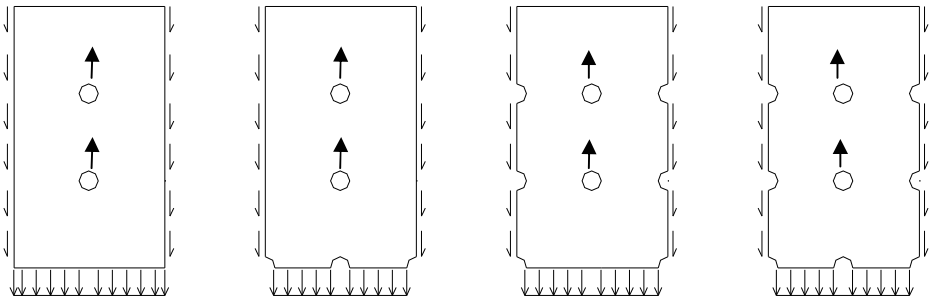

a) Tensile gross area; shear gross area

(b) Tensile net area; shear gross area

c) Tensile gross area; shear net area

d) Tensile net area; shear net area

Figure1.2 : Representation of A_{nt} , A_{nv} , A_{gt} , A_{gv}

The LRFD procedure has an upper limit on the nominal strength such that its value could not exceed the value determined by considering the simultaneous fracture at the net shear and tension planes. In order to calculate the design strength, the nominal strength given by Equations 1.1 or 1.2 is multiplied by a resistance factor (ϕ) which is equal to 0.75.

On the other hand, in the AISC-ASD (1989) procedure, failure is assumed to occur when rupture of the net section and shear planes occur simultaneously. A factor of safety of 2 is used according to this specification. The ASD nominal load capacity without a safety factor is calculated as follows:

$$R_n = F_u A_{nt} + 0.6 F_u A_{nv} \tag{1.3}$$

1.2 Previous Studies

1.2.1 Experimental Studies

1.2.1.1 Study of Ricles and Yura (1983)

Full scale testing of double-row bolted-web connections were performed on coped and uncoped ASTM grade A36 W460X89 specimens by Ricles and Yura (1983). The major variables were end and edge distances, slot length, and number of holes. 3/4-A325 (19mm) bolts and a hole diameter of 21 mm were used in the connections. The minimum edge and end distances were 25 mm. It was indicated that shear resistance is developed on the gross section rather than the net section.

1.2.1.2 Study of Hardash and Bjorhovde (1985)

Hardash and Bjorhovde (1985) tested 28 specimens to develop an improved design method for gusset plates. Gage between lines of bolts, edge distance, bolt spacing and number of bolts were considered as the strength parameters. Gusset plates fastened with two lines of bolts were tested. Test specimens had a gage length of 51, 76 and 101 mm, edge distance of 25, 38 mm, and pitch distance of 38 and 51 mm. Connections had two to five bolts in a bolt line and diameter of bolt holes were 14 and 17 mm. The average material properties of 27 specimens had a yield strength of 229 MPa and an ultimate strength of 323 MPa. One specimen had a yield strength value of 341 MPa and ultimate strength of 444 MPa. Test plates had a basic failure mode consisting of tensile failure across the last row of bolts, along with an elongation of the bolt holes.

Load deformation curves of the each test specimens was obtained and it was observed that the drop in strength from the ultimate load to second strength plateau corresponded approximately to the ultimate strength of the net area at the last row of bolts. Ultimate shear resistance was more difficult to define, because, the shear stress behavior varied among the test specimens. Shear stress was found to be dependent on the connection length and a new block shear capacity equation, which includes the connection length factor, was developed.

1.2.1.3 Study of Epstein (1993)

Epstein (1993) performed an experimental study on double-row, staggered, and unstaggered bolted connections of structural steel angles. The basic connections to be tested were pairs of angles, 8 mm thick, connected by two rows of 8 mm diameter bolts in two rows on a 150 mm leg. Outstanding legs of the angles vary between 90, 210 and 150 mm. An end and edge distances of 38 mm, a bolt diameter of 19 mm were used in the connections. The effect of several parameters in the connection geometry was investigated. Test results were compared with the current code provisions and a revised treatment was suggested by inclusion of a shear lag factor to the equation.

1.2.1.4. Study of Gross (1995)

Gross (1995) tested ten A588 Grade 50 and three A36 steel single angle tension members with various leg sizes that failed in block shear. A588 Grade 50 steel had a yield and ultimate strength of 427 and 545 MPa and A36 steel had a yield and ultimate strength value of 310 and 469 MPa, respectively. Bolt holes having a diameter of 21 mm and a bolt hole spacing of 64 mm and an end distance of 38 mm was used in all specimens. The edge distance was varied between 32, 38, 44 and 50mm. Test results were compared with the AISC-ASD and AISC-LRFD equation predictions and it was observed that code treatments accurately predict failure loads for A36 and A588 specimens.

1.2.1.5 Study of Orbison (1998)

Orbison (1998) tested 12 specimens that failed in block shear. Three of these analyzed specimens were L6X4X5/16 tension members having varying edge distances of 50.8 mm, 63.5 mm and 76.2 mm. Nine of the specimens were WT7X11 tension members with two, three or four bolt end connections having varying edge distances of 63.5 mm, 76.2 mm. A490 bolts in bearing, 25.4 mm in diameter and snug-tight, were used for all specimen connections. A pitch distance of 76.2 mm and an end distance of 63.5 mm were used. Experimental failure loads were compared

with code treatments. Recommendations were given based on the ultimate load and the strain variation along the tension plane that was measured during the experiments.

1.2.2 Statistical Studies

1.2.2.1 Study of Cunnigham (1995)

Cunnigham (1995) performed a statistical study to assess the American block shear load capacity predictions. Even though, both ASD and LRFD equations predicts the failure loads with a reasonable level of accuracy on average, it was observed that both the ASD and LRFD block shear predictions have drawbacks in terms of anticipated failure modes. It is evident from the test results that tension and shear planes do not rupture simultaneously as assumed in ASD specification. In LRFD predictions, the equation (Equation 1.2) with shear fracture term governed, but experiments showed a failure mode similar to described in the equation (Equation 1.1) with tensile fracture term. Thus, Cunnigham set the geometric and material parameters that had been investigated and studied several other parameters such as in-plane shear eccentricity and tension eccentricity. Some equations, which include different types of failure modes and variables, were presented to predict block shear load capacity.

1.2.2.2 Study of Kulak and Grondin (2001)

Kulak and Grondin (2001) performed a statistical study on evaluation of LRFD rules for block shear capacities in bolted connections with test results. It was stated that there were two equations to predict the block shear capacity but the one including the shear ultimate strength in combination with the tensile yield strength seemed unlikely. Examination of the test results on gusset plates reveals that there is not sufficient tensile ductility to permit shear fracture to occur.

After reviewing the test results, it was observed that failure modes seen in gusset plates and coped beams are significantly different and use of Equations 1.1 and 1.2 gives conservative predictions for gusset plates but they are not satisfactory for the case of coped beams. In angles block shear capacity is predicted well by these equations. As a conclusion, Kulak and Grondin (2001) recommended different equations for predicting the block shear capacities for gusset plates and coped beams to use.

1.2.3 Finite Element Studies

1.2.3.1 Study of Epstein and Chamarajanagar (1996)

Epstein and Chamarajangar (1996) studied the effects of stagger and shear lag on the failure load of angles in this study. Angles were modeled with 20 node brick elements and elastic-perfectly plastic stress strain curve for steel was used in this analysis. A strain based criterion was used to determine the failure load of the member. The nondimensionalized finite element results were compared with the full scale testing results.

1.2.3.2 Study of Kulak and Wu (1997)

Kulak and Wu (1997) observed the shear lag effect on the net section rupture of the single and double angle tension members. For practical reasons it is unusual to be able to connect the all legs of the angle and the influence of only one of the connected leg to the tensile capacity of the connection is termed as shear lag. ANSYS was used in the analysis and quadrilateral shell elements that can include plasticity were used to model the angles and elastic quadrilateral shell elements were used to define the gusset plates. Kulak and Wu (1997) included the material and geometric nonlinearities in the analysis. The failure load was considered as the load corresponding to the last converged load step. The failure loads obtained from finite element modeling were compared with the full scale testing.

1.2.3.3 Study of Topkaya (2004)

Topkaya (2004) aimed to develop simple block shear capacity equations that are based on principles of mechanics in this study. A parametric study was conducted to identify important parameters that influence the block shear response. Specimens tested by three independent research teams were modeled and analyzed. Analysis was performed with a finite element program "ANSYS". Gusset plates were modeled with six node triangular plane stress elements, whereas angles and tee sections were modeled with ten node tetrahedral elements. These element types were capable of showing high material and geometric nonlinearities. The nonlinear stress-strain behavior of steel was modeled using von Mises yield criterion with isotropic hardening. A generic true stress- true strain response was used in all analysis. Throughout the analysis the Newton-Raphson method is used to trace the entire nonlinear load-deflection response and failure load was assumed to be the maximum load reached during the loading history.

Topkaya (2004) presented three equations based on the analysis performed to predict block shear load capacity:

$$R_n = \left(0.25 + 0.35 \frac{F_u}{F_y} - \frac{Cl}{2800} \right) F_y A_{gv} + F_u A_{nt} \tag{1.4}$$

where Cl is the connection length in mm.

$$R_n = \left(0.20 + 0.35 \frac{F_u}{F_y} \right) F_y A_{gv} + F_u A_{nt} \tag{1.5}$$

$$R_n = 0.48 F_u A_{gv} + F_u A_{nt} \tag{1.6}$$

1.3. Problem Statement

Block shear failure is one of the main criteria to be considered while designing some of the steel members. American provisions for determining design load capacities for this type of failure mode first appeared in AISC-LRFD and AISC-ASD specifications. Over the past decades, very limited experimental and analytical researches have been conducted to predict the block shear load capacities of different types of connections. In 2004, Topkaya presented a finite element parametric study on block shear failure of steel tension members with nonstaggered holes and presented simple block shear load capacity equations. It was stated that further research was needed to determine the applicability of Topkaya's (2004) findings to block shear failure of connections having staggered hole and multiple bolt line connections. This thesis aims to present a numerical parametric study to investigate the block shear failure load capacities of the connection geometries mentioned above.

To ensure the reliability of the finite element analysis, comparison between the finite element analysis and the experimental studies will be presented for the gusset plates, angles and tee section with non-staggered bolted connections by using the methodology developed by Topkaya (2004). The quality of the current block shear capacity equations specified in the AISC-LRFD and AISC-ASD specifications and Topkaya's research will be assessed by making comparisons with experimental findings. After ensuring the reliability of the finite element analysis predictions, new numerical investigations will be performed to identify the important parameters which influence the block shear response of multiple bolt line and staggered hole connections.

If necessary, by using the obtained analytical findings new equations will be presented to predict the block shear load capacities of the aforementioned connections.

CHAPTER 2

FINITE ELEMENT METHODOLOGY AND COMPARISONS WITH EXPERIMENTAL FINDINGS

In this study, finite element method is employed to investigate the behavior of structural members subject to block shear failure mode. An accurate prediction of the block shear failure load is essential to develop design equations and to evaluate the existing ones. For this purpose an analysis methodology similar to that in Topkaya's (2004) study was employed and some of the analysis that was performed by Topkaya was reproduced in this chapter. A general purpose finite element program ANSYS was used to perform the analyses.

2.1 Finite Element Methodology

In this methodology, gusset plates are modeled by using six node triangular plane stress elements. On the other hand, angles and tee sections are modeled using ten node tetrahedral elements. Six node triangular elements have a quadratic displacement behavior and are well suited to model irregular meshes. The element is defined by six nodes having two degrees of freedom at each node: translations in the nodal x and y directions and they are capable of representing large deformation geometric and material nonlinearities. Three dimensional elements are defined by 10 nodes having three degrees of freedom at each node: translations in the nodal x, y, and z directions. The element has plasticity, hyperelasticity, creep, stress stiffening, large deflection and large strain capabilities.

The nonlinear stress-strain behavior of steel is modeled using von Mises yield criterion with isotropic hardening. A generic true-stress true-strain response is used

in all analysis. In this generic response the material behaves elastic until yield point. A yield plateau follows the elastic portion. Strain hardening commences at a true strain value of 0.02 and varies linearly until the true ultimate stress reached. The true-strain at true ultimate stress is assumed to be 0.1. After the true ultimate stress is reached there is a constant stress plateau until the material is assumed to break at a true strain of 0.3. True strain is expressed as $\varepsilon=\ln(l/l_0)$, in where l is the deformed length and l_0 is the initial length. For small-strain regions of response, true strain and engineering strain are essentially identical. As a result true yield stress is assigned as engineering yield stress value. To convert strain from small (engineering) strain to logarithmic strain, $\varepsilon_{ln} = \ln(1 + \varepsilon_{eng})$ is used. From this point on, the relation, $\sigma_{true} = \sigma_{eng}(1 + \varepsilon_{eng})$, is used to convert engineering stress to true stress. As a result, ultimate engineering stress value is increased by 10% to find out the true ultimate stress. The generic true-stress true-strain curve is given in Figure 2.1.

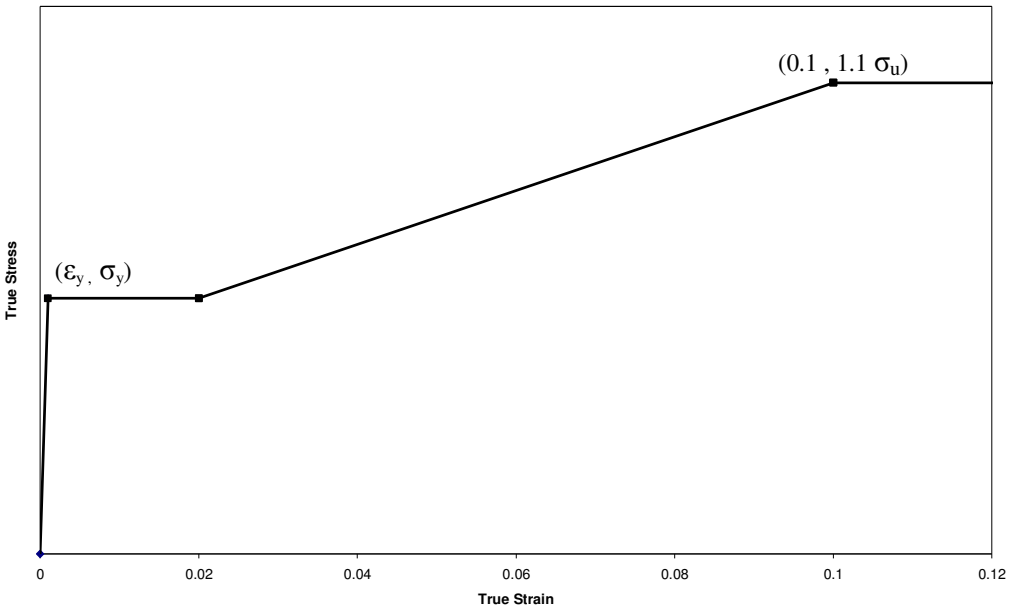

Figure 2.1 : Generic True-Stress True-Strain Material Response for Steel

Usually half length of the specimen is modeled if specimens possess a symmetry plane along the length. Similarly, for cross sections that possess a symmetry plane like the tees, only half of the cross section is modeled. In an effort to reduce the computational cost, end connection details which are used to apply loading are not modeled. In order to simulate the end reactions, nodes that lie on the half circumference of each hole where bolts come into contact are restrained against displacement in two directions in the plane of the plate. A longitudinal displacement boundary condition is applied at the opposite end of the member.

Throughout the analysis the Newton-Raphson method is used to trace the entire nonlinear load-deflection response. The failure load is assumed to be the maximum load reached during the loading history. In most of the experiments failure was triggered by significant amount of necking of the tension plane. In the finite element analysis substantial amount of necking was observed near the vicinity of the leading bolt hole at the ultimate load. A representative finite element analysis on a gusset plate is presented in Figure 2.2 along with the load-displacement response obtained. The comparisons of the finite element predictions with the experimental findings will be presented in the following section.

2.2 Finite Element Analysis Predictions

Predicting block shear capacity with finite element analysis was assessed by making comparisons with experimental findings. Aforementioned experimental tests of three independent research teams on gusset plates, angles and tees are considered in this section. A finite element mesh was prepared for 28 gusset plate test specimens of Hardash and Bjorhovde (1985), 13 angle specimens of Gross (1995) and 3 angle and 9 tee section specimens of Orbison (1998) according to the same procedure explained before. Ultimate load values were documented for each case. Figure 2.3 shows representative deformed finite element meshes for a gusset plate and an angle specimen. The displacement of a block of material could be easily seen in the half

plate model (Figure 2.3a). In addition, the necking behavior of the tension plane could be observed easily in the angle model (Figure 2.3b).

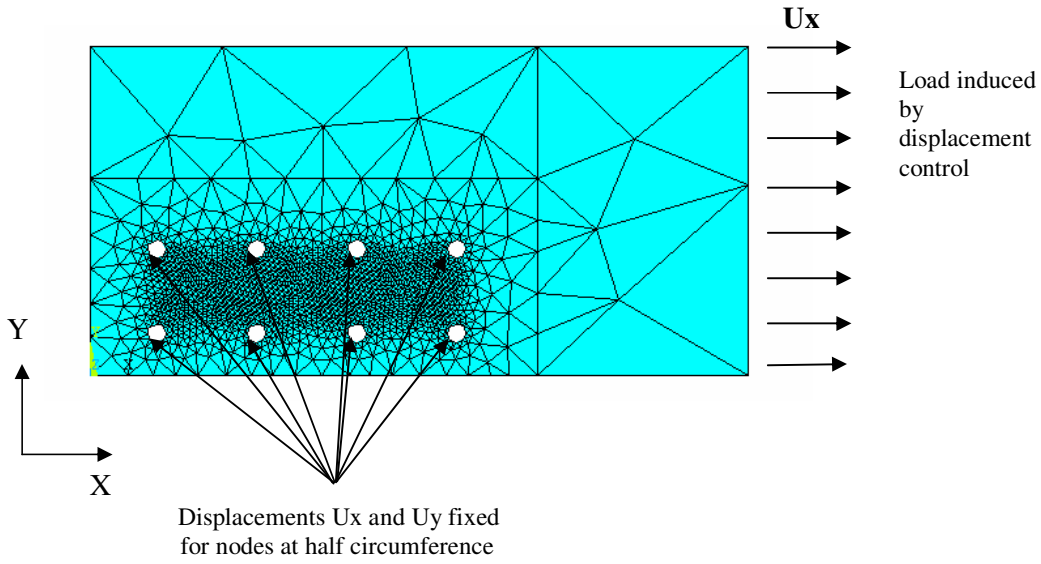

(a) Model of Half Plate

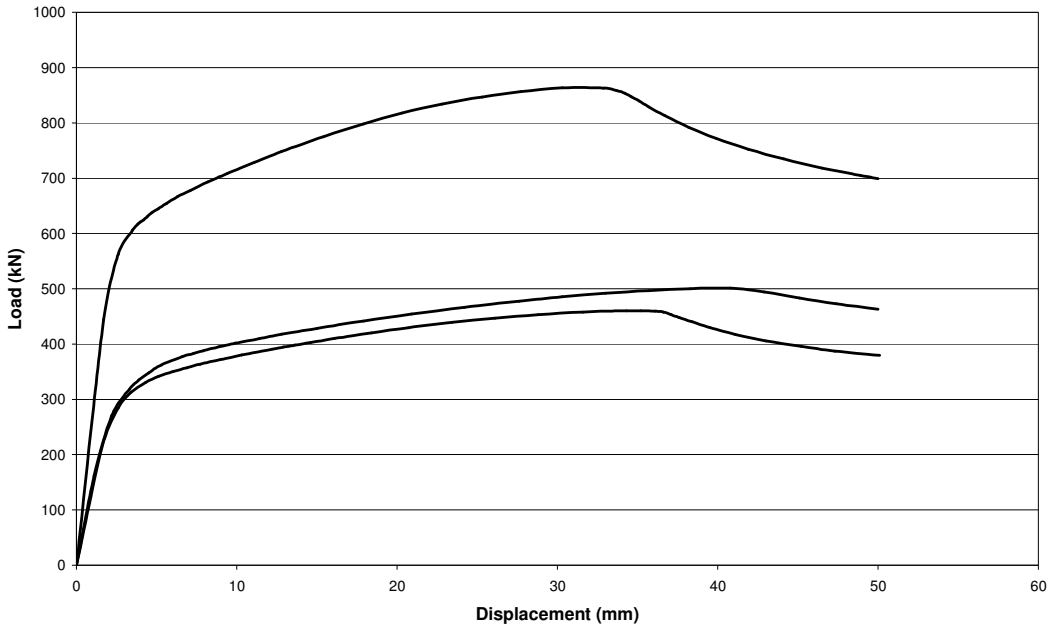

(b) Typical Load-Displacement Responses

Figure 2.2 : Representative Finite Element Analysis of a Gusset Plate

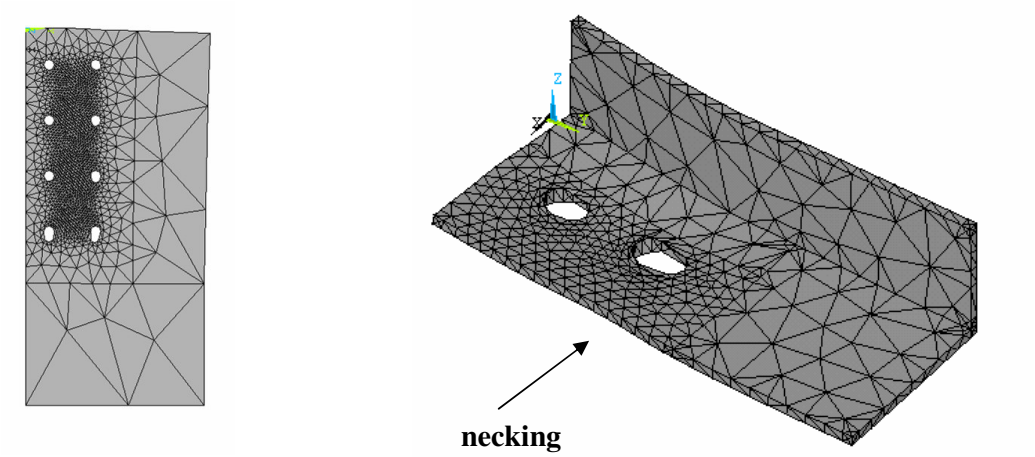

a) Half Gusset Plate b) Angle Section

Figure 2.3 : Representative Deformed Shapes

Comparison of the finite element analysis results with experimental results of totally 53 specimens are presented in Table 2.1. and in Figure 2.4. In this figure experimental failure loads are plotted against the finite element analysis predictions. Diagonal line represents the full agreement with the FEM results with experimental results. Data points appearing below the diagonal line indicates that FEM predictions overestimate the ultimate load capacity of the specimen (FEM results are unconservative) while points above the diagonal line indicates that FEM predictions underestimates the ultimate load capacity of the specimen (FEM results are conservative). For statistical evaluations professional factors of each tested specimens are calculated. Professional factor is the ratio of experimental ultimate load (P_{exp}) to predicted ultimate load (P_{pred}) as Hardash and Bjorhovde (1985) stated. Professional factor of unity represents a perfect agreement between the experimental loads with predicted load. If the equation prediction overestimates the failure load, professional factor is less than unity. Conversely, if the equation prediction underestimates the load, professional factor is greater than unity. Professional factor is presented in Equation 2.1 below:

$$PF = \frac{P_{\exp}}{P_{pred}} \qquad (2.1)$$

The statistical analyses of the predictions are presented in Table 2.2. It is evident from the Figure 2.4 and Table 2.2 that finite element method provides good load capacity predictions. Mean of the professional factor is 0.990 which means finite element predictions underestimates the experimental failure loads in general and standard deviation of the professional factors of 53 cases is very low.

Similar types of comparisons were performed to assess the LRFD and ASD procedure's load capacity predictions. In calculating the LRFD and ASD failure loads bolt hole sizes were taken as 2 mm larger than the nominal bolt hole diameter. Comparison of LRFD and ASD predictions with experimental findings are presented in Figures 2.5 and 2.6, respectively. Also, statistical measures of the predictions are presented in Table 2.2. For the 53 specimens mostly the equation with shear fracture term governed, although, fracture occurred at the net section for all of the 53 tested specimens. From this point on it can be said that LRFD procedure does not capture the failure mode of the specimens. According to the statistical measures and figures both LRFD and ASD procedures provides conservative predictions of the failure loads on average. Finite element method predicts more closely the failure loads when compared with both LRFD and ASD procedures. Also, standard deviations of the proof loads of LRFD and ASD predictions are higher than that of finite element method. This means finite element predictions give much closer results with less scatter compared to the code treatments. The same finite element procedure will be employed for studying the multiple bolt lines and stagger effects in the following chapters.

Table.2.1 : Test Results, AISC-LRFD, ASD and FEA Predictions

Test #	Orbison's T.R. (kN)	FEA Pr. (kN)	ASD Pr. (kN)	LRFD Pr. (kN)
1	362.1	380.2	361.2	360.3
2	444.8	447.0	394.5	379.9
3	500.0	485.0	449.0	453.3
4	264.7	265.1	247.8	247.3
5	311.8	297.8	274.0	265.5
6	345.2	318.5	303.8	309.6
7	379.0	357.8	359.0	350.5
8	427.5	384.2	388.8	372.3
9	491.1	463.4	415.0	390.1
10	452.8	460.1	412.3	404.8
11	520.4	481.0	453.7	435.9
12	578.2	566.0	496.8	471.0

Test #	Gross's T.R. (kN)	FEA Pr. (kN)	ASD Pr. (kN)	LRFD Pr. (kN)
1	199.3	209.1	185.5	186.4
2	257.1	280.0	263.3	264.7
3	232.6	274.0	247.3	251.8
4	231.3	274.0	237.1	248.2
5	391.4	394.8	374.5	375.0
6	317.6	338.2	330.5	341.6
7	215.7	251.0	215.7	231.7
8	298.9	331.4	303.8	319.4
9	284.6	290.0	235.7	246.9
10	374.5	397.1	404.8	420.3
11	390.5	395.9	410.1	420.3
12	426.1	432.2	431.9	436.8
13	448.4	448.0	448.8	452.4

Test #	Hardash's T.R. (kN)	FEA Pr. (kN)	ASD Pr. (kN)	LRFD Pr. (kN)
1	242.9	216.4	175.3	175.3
2	245.5	231.8	199.0	197.1
3	300.7	279.5	225.0	225.0
4	327.4	323.1	284.3	281.1
5	318.0	303.9	254.6	254.6
6	360.7	356.5	313.9	302.1
7	338.9	345.0	274.4	274.4
8	371.0	382.5	333.7	330.5
9	358.5	350.7	304.1	304.1
10	399.9	395.5	363.4	351.5
11	374.5	387.9	323.8	323.8
12	407.4	428.8	359.4	359.4
13	353.6	356.3	280.6	280.6
14	422.6	422.4	369.6	365.1
15	379.0	367.8	310.2	310.2
16	443.9	428.6	367.1	367.1
17	391.9	410.1	330.0	330.0
18	687.2	696.2	615.2	615.2
19	413.2	422.2	359.7	359.7
20	532.4	477.8	416.5	416.5
21	467.0	468.9	379.5	379.5
22	511.1	527.7	468.5	463.9
23	487.5	478.5	409.1	409.1
24	524.9	557.2	507.0	491.2
25	467.5	476.6	385.6	385.6
26	583.6	525.9	464.7	464.7
27	498.2	476.6	415.3	415.3
28	559.1	576.2	534.0	519.5

Table 2.2 : Professional Factor Statistics for FEA, LRFD and ASD Predictions

	Professional factor		
	Finite Element	AISC-LRFD	AISC-ASD
Mean	0.990	1.174	1.150
Standard deviation	0.062	0.138	0.128
Maximum	1.122	1.458	1.458
Minimum	0.844	0.925	0.925

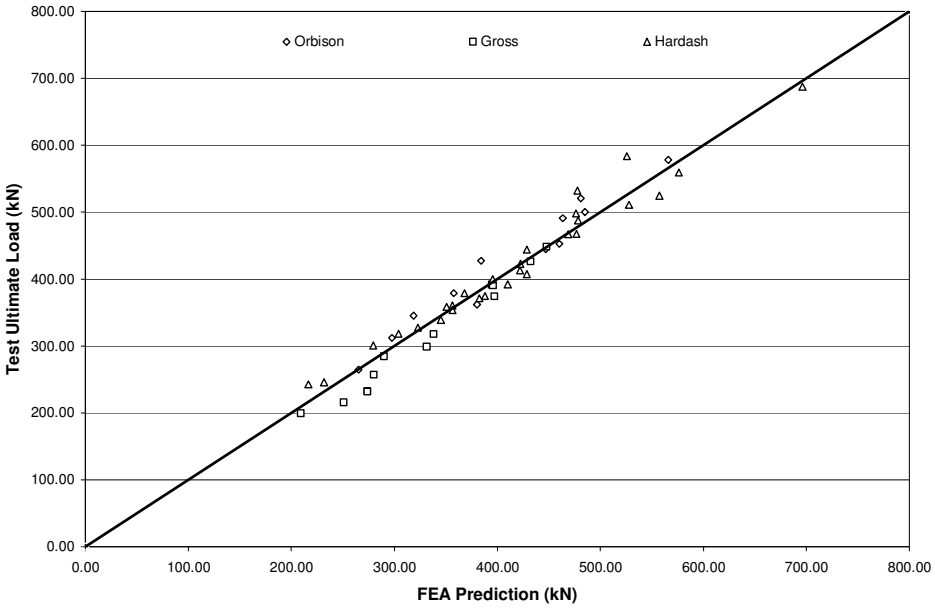

Figure 2.4 : Comparison of Finite Element Analysis Predictions with Experimental Findings

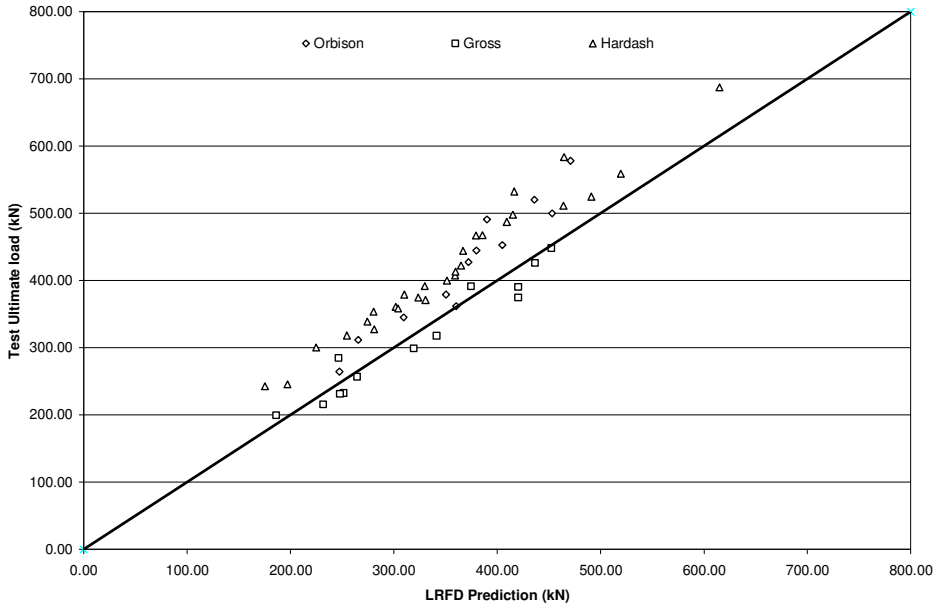

Figure 2.5 : Comparison of LRFD Procedure Predictions with Experimental Findings

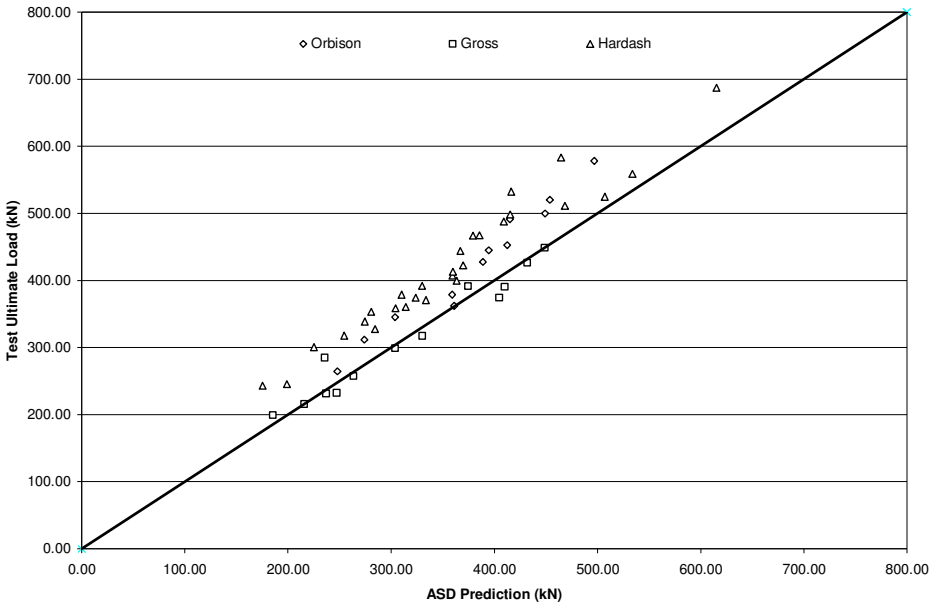

Figure 2.6 : Comparison of ASD Procedure Predictions with Experimental Findings

CHAPTER 3

ANALYSIS OF CONNECTIONS WITH MULTIPLE BOLT LINES

In this chapter, a parametric study has been conducted to understand the effects of some variables on block shear capacity in gusset plates with multiple bolt line connections. The procedure explained in Chapter 2 was used in all analyses. Geometric and material variables are defined as the spacing between bolts, end distances, number of bolt lines, number of bolts per a bolt line, bolt pitch, yield strength (F_y) and ultimate strength (F_u) of the material. Two-dimensional plane stress elements are used in the modeling to reduce the computational cost. Only half of the member is modeled because of the symmetry. Therefore, rollers are placed along the symmetry axis. As indicated in Chapter 2, half circumference of the each bolt hole is restrained in two directions. Ultimate load is defined as the maximum load reached in the loading history.

A total of 576 nonlinear finite element analyses were performed to investigate the block shear capacity of the multiple bolt line connections. Three and four bolt line connections with two, three and four bolts per bolt line were modeled as shown in Figure 3.1.

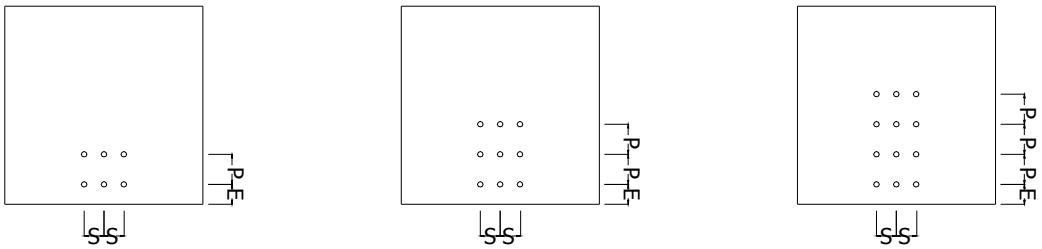

i. 2 bolts per bolt line case ii. 3 bolts per bolt line case iii. 4 bolts per bolt line case

a) 3 Bolt Line Case

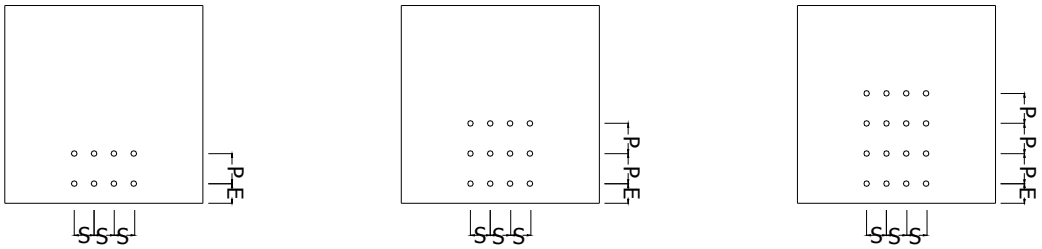

i. 2 bolts per bolt line case ii. 3 bolts per bolt line case iii. 4 bolts per bolt line case

b) 4 Bolt Line Case

Figure 3.1 : Bolt Arrangements of Analyzed Gusset Plates
(P=Pitch Distance, E=End Distance, S=Spacing)

Analyzed specimens had dimensions of 500 mm in width and length, an end distance of 25, 50 mm and a spacing of 38, 50, 64 mm. End distance is the distance from the end of the gusset plate to the center of the bolt which is closest to the end of the plate. Spacing is the distance between the bolt centers in the horizontal direction and pitch distance is the distance between the bolts along the connection length. In all the analyses 14 mm diameter bolt holes were defined and to assure the minimum hole spacing provisions, a bolt pitch greater than or equal to three times the bolt diameter was defined. A pitch distance of 38, 50, and 64 mm were used in the analyses. For these 576 cases ultimate strength of the material was assigned as 352 MPa. Yield strength values of the materials were chosen as 210, 252 and 293 MPa, which results in ultimate to yield ratios of 1.68, 1.4 and 1.2 respectively. The combinations of these variables considered in the study are listed in Table 3.1.

Table 3.1 : Combinations of the Variables Used in Parametric Study

End distance	Spacing	Pitch distance	F_u/F_y
Hole diameter (14mm)			
3 bolt line case			
2bolt case			
25	38/50/64/76	38/50/64/76	1.68/1.4/1.2
50	38/50/64/76	38/50/64/76	1.68/1.4/1.2
3bolt case			
25	38/50/64/76	38/50/64/76	1.68/1.4/1.2
50	38/50/64/76	38/50/64/76	1.68/1.4/1.2
4bolt case			
25	38/50/64/76	38/50/64/76	1.68/1.4/1.2
50	38/50/64/76	38/50/64/76	1.68/1.4/1.2
4 bolt line case			
2bolt case			
25	38/50/64/76	38/50/64/76	1.68/1.4/1.2
50	38/50/64/76	38/50/64/76	1.68/1.4/1.2
3bolt case			
25	38/50/64/76	38/50/64/76	1.68/1.4/1.2
50	38/50/64/76	38/50/64/76	1.68/1.4/1.2
4bolt case			
25	38/50/64/76	38/50/64/76	1.68/1.4/1.2
50	38/50/64/76	38/50/64/76	1.68/1.4/1.2
Total number of cases			576

All dimensions are in mm

3.1 Results of the Analysis Cases

The results of the analysis are presented in Tables 3.2 to 3.7.

a) 3-Bolt Line Case

i. 2 Bolt Case

Table 3.2 : Test Results of 2 Bolt for 3 Bolt Line

Run#	E (mm)	P (mm)	S (mm)	Fu (Mpa)	Fy (Mpa)	U.L. (kN)	Fef / Fy	CL (mm)
1	25	38	38	352	210	35.1	0.69	63
2	25	38	50	352	210	43.2	0.67	63
3	25	38	64	352	210	52.4	0.65	63
4	25	38	76	352	210	59.2	0.59	63
5	25	50	38	352	210	38.0	0.67	75
6	25	50	50	352	210	46.0	0.66	75
7	25	50	64	352	210	54.6	0.62	75
8	25	50	76	352	210	62.0	0.58	75
9	25	64	38	352	210	41.6	0.66	89
10	25	64	50	352	210	50.1	0.66	89
11	25	64	64	352	210	57.9	0.61	89
12	25	64	76	352	210	65.9	0.60	89
13	25	76	38	352	210	44.6	0.65	101
14	25	76	50	352	210	51.6	0.62	101
15	25	76	64	352	210	60.4	0.59	101
16	25	76	76	352	210	68.2	0.58	101
17	50	38	38	352	210	41.3	0.66	88
18	50	38	50	352	210	49.2	0.65	88
19	50	38	64	352	210	57.8	0.61	88
20	50	38	76	352	210	65.2	0.58	88
21	50	50	38	352	210	44.1	0.65	100
22	50	50	50	352	210	51.6	0.62	100
23	50	50	64	352	210	60.5	0.60	100
24	50	50	76	352	210	67.7	0.57	100
25	50	64	38	352	210	47.4	0.64	114
26	50	64	50	352	210	54.9	0.62	114
27	50	64	64	352	210	64.1	0.60	114
28	50	64	76	352	210	70.5	0.56	114
29	50	76	38	352	210	50.0	0.63	126
30	50	76	50	352	210	57.7	0.61	126
31	50	76	64	352	210	67.1	0.60	126
32	50	76	76	352	210	73.0	0.55	126
33	25	38	38	352	252	37.1	0.63	63
34	25	38	50	352	252	45.1	0.62	63
35	25	38	64	352	252	53.8	0.59	63
36	25	38	76	352	252	61.0	0.55	63
37	25	50	38	352	252	40.3	0.62	75
38	25	50	50	352	252	47.7	0.59	75
39	25	50	64	352	252	56.2	0.56	75
40	25	50	76	352	252	63.4	0.52	75
41	25	64	38	352	252	44.2	0.61	89
42	25	64	50	352	252	51.0	0.57	89
43	25	64	64	352	252	61.3	0.58	89
44	25	64	76	352	252	67.1	0.52	89
45	25	76	38	352	252	47.8	0.61	101
46	25	76	50	352	252	55.1	0.58	101
47	25	76	64	352	252	63.6	0.56	101
48	25	76	76	352	252	70.5	0.53	101
49	50	38	38	352	252	43.8	0.61	88
50	50	38	50	352	252	51.9	0.60	88
51	50	38	64	352	252	60.3	0.57	88
52	50	38	76	352	252	67.6	0.54	88
53	50	50	38	352	252	47.1	0.60	100
54	50	50	50	352	252	54.6	0.58	100
55	50	50	64	352	252	63.9	0.57	100
56	50	50	76	352	252	70.1	0.52	100
57	50	64	38	352	252	50.8	0.59	114
58	50	64	50	352	252	58.6	0.58	114
59	50	64	64	352	252	67.5	0.56	114
60	50	64	76	352	252	74.3	0.53	114
61	50	76	38	352	252	54.1	0.59	126
62	50	76	50	352	252	61.6	0.57	126
63	50	76	64	352	252	71.0	0.56	126
64	50	76	76	352	252	77.2	0.53	126
65	25	38	38	352	293	38.7	0.59	63
66	25	38	50	352	293	46.8	0.58	63
67	25	38	64	352	293	56.1	0.57	63
68	25	38	76	352	293	64.3	0.56	63
69	25	50	38	352	293	42.2	0.57	75
70	25	50	50	352	293	50.2	0.57	75
71	25	50	64	352	293	59.1	0.54	75
72	25	50	76	352	293	66.8	0.53	75
73	25	64	38	352	293	46.8	0.57	89
74	25	64	50	352	293	54.2	0.55	89
75	25	64	64	352	293	64.0	0.55	89
76	25	64	76	352	293	70.7	0.52	89
77	25	76	38	352	293	50.8	0.57	101
78	25	76	50	352	293	58.4	0.56	101
79	25	76	64	352	293	67.6	0.55	101
80	25	76	76	352	293	75.2	0.53	101
81	50	38	38	352	293	46.5	0.57	88
82	50	38	50	352	293	54.7	0.57	88
83	50	38	64	352	293	63.5	0.55	88
84	50	38	76	352	293	71.3	0.54	88
85	50	50	38	352	293	50.1	0.57	100
86	50	50	50	352	293	57.9	0.55	100
87	50	50	64	352	293	67.2	0.55	100
88	50	50	76	352	293	74.3	0.52	100
89	50	64	38	352	293	54.4	0.56	114
90	50	64	50	352	293	62.3	0.55	114
91	50	64	64	352	293	71.4	0.54	114
92	50	64	76	352	293	74.5	0.46	114
93	50	76	38	352	293	58.0	0.56	126
94	50	76	50	352	293	65.7	0.55	126
95	50	76	64	352	293	75.3	0.54	126
96	50	76	76	352	293	82.8	0.53	126

ii. 3 Bolt Case

Table 3.3 : Test Results of 3 Bolt for 3 Bolt Line

Run#	E (mm)	P (mm)	S (mm)	Fu (Mpa)	Fy (Mpa)	U.L. (kN)	Fef / Fy	CL (mm)
1	25	38	38	352	210	45.0	0.66	101
2	25	38	50	352	210	53.1	0.66	101
3	25	38	64	352	210	62.4	0.64	101
4	25	38	76	352	210	70.1	0.62	101
5	25	50	38	352	210	50.5	0.64	125
6	25	50	50	352	210	58.8	0.64	125
7	25	50	64	352	210	69.0	0.64	125
8	25	50	76	352	210	74.7	0.59	125
9	25	64	38	352	210	57.4	0.63	153
10	25	64	50	352	210	64.3	0.61	153
11	25	64	64	352	210	74.0	0.60	153
12	25	64	76	352	210	81.8	0.59	153
13	25	76	38	352	210	62.1	0.61	177
14	25	76	50	352	210	71.3	0.62	177
15	25	76	64	352	210	79.1	0.59	177
16	25	76	76	352	210	88.0	0.60	177
17	50	38	38	352	210	50.7	0.64	126
18	50	38	50	352	210	59.0	0.64	126
19	50	38	64	352	210	68.8	0.63	126
20	50	38	76	352	210	76.1	0.61	126
21	50	50	38	352	210	56.4	0.63	150
22	50	50	50	352	210	64.5	0.62	150
23	50	50	64	352	210	74.1	0.62	150
24	50	50	76	352	210	80.9	0.59	150
25	50	64	38	352	210	62.5	0.61	178
26	50	64	50	352	210	71.1	0.61	178
27	50	64	64	352	210	79.8	0.60	178
28	50	64	76	352	210	85.0	0.55	178
29	50	76	38	352	210	67.2	0.59	202
30	50	76	50	352	210	75.5	0.59	202
31	50	76	64	352	210	83.3	0.57	202
32	50	76	76	352	210	90.1	0.55	202
33	25	38	38	352	252	47.5	0.60	101
34	25	38	50	352	252	56.0	0.60	101
35	25	38	64	352	252	65.6	0.60	101
36	25	38	76	352	252	72.8	0.57	101
37	25	50	38	352	252	54.3	0.59	125
38	25	50	50	352	252	62.3	0.59	125
39	25	50	64	352	252	71.8	0.58	125
40	25	50	76	352	252	79.0	0.56	125
41	25	64	38	352	252	62.1	0.59	153
42	25	64	50	352	252	69.9	0.58	153
43	25	64	64	352	252	78.6	0.56	153
44	25	64	76	352	252	86.3	0.55	153
45	25	76	38	352	252	68.1	0.57	177
46	25	76	50	352	252	75.9	0.57	177
47	25	76	64	352	252	84.7	0.56	177
48	25	76	76	352	252	93.2	0.56	177

Run#	E (mm)	P (mm)	S (mm)	Fu (Mpa)	Fy (Mpa)	U.L. (kN)	Fef / Fy	CL (mm)
49	50	38	38	352	252	53.9	0.58	126
50	50	38	50	352	252	62.9	0.59	126
51	50	38	64	352	252	72.1	0.58	126
52	50	38	76	352	252	79.5	0.56	126
53	50	50	38	352	252	60.9	0.58	150
54	50	50	50	352	252	69.2	0.58	150
55	50	50	64	352	252	78.3	0.57	150
56	50	50	76	352	252	85.5	0.55	150
57	50	64	38	352	252	68.3	0.57	178
58	50	64	50	352	252	76.8	0.57	178
59	50	64	64	352	252	85.7	0.56	178
60	50	64	76	352	252	92.4	0.54	178
61	50	76	38	352	252	74.0	0.56	202
62	50	76	50	352	252	82.4	0.56	202
63	50	76	64	352	252	90.5	0.54	202
64	50	76	76	352	252	97.2	0.53	202
65	25	38	38	352	293	50.5	0.57	101
66	25	38	50	352	293	59.1	0.57	101
67	25	38	64	352	293	68.7	0.57	101
68	25	38	76	352	293	77.1	0.57	101
69	25	50	38	352	293	57.8	0.56	125
70	25	50	50	352	293	66.6	0.56	125
71	25	50	64	352	293	75.9	0.56	125
72	25	50	76	352	293	84.0	0.55	125
73	25	64	38	352	293	66.2	0.55	153
74	25	64	50	352	293	74.8	0.55	153
75	25	64	64	352	293	84.2	0.55	153
76	25	64	76	352	293	93.1	0.55	153
77	25	76	38	352	293	74.1	0.55	177
78	25	76	50	352	293	82.0	0.55	177
79	25	76	64	352	293	90.6	0.53	177
80	25	76	76	352	293	98.0	0.52	177
81	50	38	38	352	293	57.8	0.55	126
82	50	38	50	352	293	66.3	0.56	126
83	50	38	64	352	293	76.1	0.55	126
84	50	38	76	352	293	84.6	0.55	126
85	50	50	38	352	293	64.9	0.55	150
86	50	50	50	352	293	74.0	0.55	150
87	50	50	64	352	293	83.4	0.55	150
88	50	50	76	352	293	92.2	0.55	150
89	50	64	38	352	293	73.4	0.54	178
90	50	64	50	352	293	82.2	0.54	178
91	50	64	64	352	293	90.8	0.53	178
92	50	64	76	352	293	99.1	0.53	178
93	50	76	38	352	293	80.8	0.54	202
94	50	76	50	352	293	89.0	0.54	202
95	50	76	64	352	293	98.5	0.53	202
96	50	76	76	352	293	106.6	0.53	202

iii. 4 Bolt Case

Table 3.4. Test Results of 4 Bolt for 3 Bolt Line

Run#	E (mm)	P (mm)	S (mm)	Fu (Mpa)	Fy (Mpa)	U.L. (kN)	Fef / Fy	CL (mm)
1	25	38	38	352	210	56.2	0.67	139
2	25	38	50	352	210	67.1	0.71	139
3	25	38	64	352	210	77.7	0.73	139
4	25	38	76	352	210	85.7	0.72	139
5	25	50	38	352	210	65.6	0.66	175
6	25	50	50	352	210	74.4	0.67	175
7	25	50	64	352	210	86.6	0.70	175
8	25	50	76	352	210	94.8	0.70	175
9	25	64	38	352	210	74.8	0.64	217
10	25	64	50	352	210	84.5	0.65	217
11	25	64	64	352	210	95.2	0.66	217
12	25	64	76	352	210	104.5	0.67	217
13	25	76	38	352	210	82.0	0.61	253
14	25	76	50	352	210	89.8	0.61	253
15	25	76	64	352	210	100.5	0.61	253
16	25	76	76	352	210	111.1	0.63	253
17	50	38	38	352	210	62.0	0.66	164
18	50	38	50	352	210	72.3	0.68	164
19	50	38	64	352	210	84.5	0.72	164
20	50	38	76	352	210	91.7	0.70	164
21	50	50	38	352	210	70.7	0.64	200
22	50	50	50	352	210	79.5	0.64	200
23	50	50	64	352	210	92.6	0.68	200
24	50	50	76	352	210	99.5	0.66	200
25	50	64	38	352	210	79.0	0.61	242
26	50	64	50	352	210	88.7	0.62	242
27	50	64	64	352	210	98.7	0.62	242
28	50	64	76	352	210	107.6	0.63	242
29	50	76	38	352	210	86.3	0.59	278
30	50	76	50	352	210	94.6	0.59	278
31	50	76	64	352	210	102.9	0.58	278
32	50	76	76	352	210	112.8	0.59	278
33	25	38	38	352	252	60.2	0.62	139
34	25	38	50	352	252	69.7	0.63	139
35	25	38	64	352	252	79.7	0.63	139
36	25	38	76	352	252	87.4	0.62	139
37	25	50	38	352	252	70.9	0.61	175
38	25	50	50	352	252	79.0	0.61	175
39	25	50	64	352	252	90.0	0.62	175
40	25	50	76	352	252	97.7	0.61	175
41	25	64	38	352	252	81.6	0.59	217
42	25	64	50	352	252	90.5	0.60	217
43	25	64	64	352	252	99.7	0.59	217
44	25	64	76	352	252	109.1	0.60	217
45	25	76	38	352	252	90.7	0.58	253
46	25	76	50	352	252	98.2	0.57	253
47	25	76	64	352	252	106.8	0.56	253
48	25	76	76	352	252	116.4	0.57	253
49	50	38	38	352	252	66.9	0.61	164
50	50	38	50	352	252	76.3	0.62	164
51	50	38	64	352	252	86.9	0.63	164
52	50	38	76	352	252	94.3	0.61	164
53	50	50	38	352	252	76.3	0.59	200
54	50	50	50	352	252	85.3	0.59	200
55	50	50	64	352	252	96.5	0.61	200
56	50	50	76	352	252	103.2	0.59	200
57	50	64	38	352	252	86.8	0.57	242
58	50	64	50	352	252	96.0	0.58	242
59	50	64	64	352	252	104.6	0.57	242
60	50	64	76	352	252	112.2	0.56	242
61	50	76	38	352	252	96.0	0.56	278
62	50	76	50	352	252	103.6	0.56	278
63	50	76	64	352	252	110.5	0.54	278
64	50	76	76	352	252	119.5	0.54	278
65	25	38	38	352	293	64.0	0.58	139
66	25	38	50	352	293	73.3	0.59	139
67	25	38	64	352	293	83.2	0.59	139
68	25	38	76	352	293	90.8	0.58	139
69	25	50	38	352	293	75.1	0.57	175
70	25	50	50	352	293	83.9	0.57	175
71	25	50	64	352	293	94.4	0.58	175
72	25	50	76	352	293	102.5	0.57	175
73	25	64	38	352	293	88.0	0.56	217
74	25	64	50	352	293	97.2	0.56	217
75	25	64	64	352	293	106.2	0.56	217
76	25	64	76	352	293	114.7	0.56	217
77	25	76	38	352	293	98.9	0.55	253
78	25	76	50	352	293	106.8	0.55	253
79	25	76	64	352	293	115.2	0.54	253
80	25	76	76	352	293	123.2	0.54	253
81	50	38	38	352	293	71.5	0.57	164
82	50	38	50	352	293	80.7	0.58	164
83	50	38	64	352	293	89.9	0.57	164
84	50	38	76	352	293	99.0	0.58	164
85	50	50	38	352	293	82.4	0.56	200
86	50	50	50	352	293	91.1	0.56	200
87	50	50	64	352	293	102.3	0.57	200
88	50	50	76	352	293	109.3	0.56	200
89	50	64	38	352	293	94.1	0.54	242
90	50	64	50	352	293	104.0	0.55	242
91	50	64	64	352	293	112.6	0.55	242
92	50	64	76	352	293	120.0	0.54	242
93	50	76	38	352	293	105.3	0.54	278
94	50	76	50	352	293	113.3	0.54	278
95	50	76	64	352	293	120.2	0.52	278
96	50	76	76	352	293	127.4	0.51	278

b) 4-Bolt Line Case

i. 2 Bolt Case

Table 3.5 : Test Results of 2 Bolt for 4 Bolt Line

Run#	E (mm)	P (mm)	S (mm)	Fu (Mpa)	Fy (Mpa)	U.L. (kN)	Fef / Fy	CL (mm)
1	25	38	38	352	210	44.0	0.71	63
2	25	38	50	352	210	55.6	0.66	63
3	25	38	64	352	210	69.8	0.64	63
4	25	38	76	352	210	80.3	0.56	63
5	25	50	38	352	210	47.1	0.69	75
6	25	50	50	352	210	58.5	0.65	75
7	25	50	64	352	210	71.5	0.59	75
8	25	50	76	352	210	82.8	0.55	75
9	25	64	38	352	210	50.3	0.67	89
10	25	64	50	352	210	61.6	0.63	89
11	25	64	64	352	210	75.1	0.60	89
12	25	64	76	352	210	85.4	0.53	89
13	25	76	38	352	210	53.7	0.67	101
14	25	76	50	352	210	65.1	0.64	101
15	25	76	64	352	210	78.3	0.60	101
16	25	76	76	352	210	88.1	0.53	101
17	50	38	38	352	210	50.8	0.69	88
18	50	38	50	352	210	63.3	0.68	88
19	50	38	64	352	210	76.2	0.63	88
20	50	38	76	352	210	87.7	0.60	88
21	50	50	38	352	210	53.3	0.67	100
22	50	50	50	352	210	65.5	0.65	100
23	50	50	64	352	210	78.8	0.62	100
24	50	50	76	352	210	90.3	0.59	100
25	50	64	38	352	210	57.1	0.66	114
26	50	64	50	352	210	68.0	0.63	114
27	50	64	64	352	210	82.3	0.62	114
28	50	64	76	352	210	91.4	0.54	114
29	50	76	38	352	210	59.8	0.65	126
30	50	76	50	352	210	71.8	0.64	126
31	50	76	64	352	210	83.2	0.57	126
32	50	76	76	352	210	92.8	0.52	126
33	25	38	38	352	252	46.3	0.66	63
34	25	38	50	352	252	58.2	0.63	63
35	25	38	64	352	252	73.6	0.65	63
36	25	38	76	352	252	84.9	0.61	63
37	25	50	38	352	252	49.9	0.65	75
38	25	50	50	352	252	61.4	0.62	75
39	25	50	64	352	252	75.0	0.59	75
40	25	50	76	352	252	85.9	0.54	75
41	25	64	38	352	252	53.6	0.63	89
42	25	64	50	352	252	65.0	0.60	89
43	25	64	64	352	252	77.7	0.56	89
44	25	64	76	352	252	88.8	0.52	89
45	25	76	38	352	252	56.9	0.62	101
46	25	76	50	352	252	68.1	0.59	101
47	25	76	64	352	252	81.2	0.56	101
48	25	76	76	352	252	91.2	0.51	101
49	50	38	38	352	252	53.3	0.63	88
50	50	38	50	352	252	65.6	0.62	88
51	50	38	64	352	252	78.7	0.58	88
52	50	38	76	352	252	90.1	0.56	88
53	50	50	38	352	252	56.5	0.62	100
54	50	50	50	352	252	68.3	0.60	100
55	50	50	64	352	252	81.6	0.57	100
56	50	50	76	352	252	93.2	0.55	100
57	50	64	38	352	252	60.3	0.61	114
58	50	64	50	352	252	71.3	0.58	114
59	50	64	64	352	252	85.4	0.57	114
60	50	64	76	352	252	95.0	0.51	114
61	50	76	38	352	252	63.8	0.61	126
62	50	76	50	352	252	75.3	0.59	126
63	50	76	64	352	252	87.4	0.54	126
64	50	76	76	352	252	97.1	0.50	126
65	25	38	38	352	293	48.3	0.62	63
66	25	38	50	352	293	60.7	0.61	63
67	25	38	64	352	293	76.1	0.63	63
68	25	38	76	352	293	87.6	0.60	63
69	25	50	38	352	293	52.2	0.61	75
70	25	50	50	352	293	64.1	0.59	75
71	25	50	64	352	293	77.8	0.57	75
72	25	50	76	352	293	88.7	0.53	75
73	25	64	38	352	293	56.4	0.60	89
74	25	64	50	352	293	68.4	0.58	89
75	25	64	64	352	293	81.8	0.56	89
76	25	64	76	352	293	92.0	0.51	89
77	25	76	38	352	293	60.3	0.59	101
78	25	76	50	352	293	71.9	0.57	101
79	25	76	64	352	293	84.8	0.54	101
80	25	76	76	352	293	94.8	0.49	101
81	50	38	38	352	293	56.1	0.60	88
82	50	38	50	352	293	68.7	0.59	88
83	50	38	64	352	293	83.2	0.59	88
84	50	38	76	352	293	94.0	0.55	88
85	50	50	38	352	293	60.0	0.59	100
86	50	50	50	352	293	72.0	0.58	100
87	50	50	64	352	293	85.6	0.56	100
88	50	50	76	352	293	97.5	0.55	100
89	50	64	38	352	293	64.1	0.58	114
90	50	64	50	352	293	75.3	0.56	114
91	50	64	64	352	293	89.6	0.55	114
92	50	64	76	352	293	99.9	0.52	114
93	50	76	38	352	293	67.8	0.58	126
94	50	76	50	352	293	79.8	0.57	126
95	50	76	64	352	293	92.1	0.53	126
96	50	76	76	352	293	102.4	0.50	126

ii. 3 Bolt Case

Table 3.6 : Test Results of 3 Bolt for 4 Bolt Line

Run#	E (mm)	P (mm)	S (mm)	Fu (Mpa)	Fy (Mpa)	U.L. (kN)	Fef / Fy	CL (mm)
1	25	38	38	352	210	55.7	0.72	101
2	25	38	50	352	210	70.1	0.76	101
3	25	38	64	352	210	86.0	0.78	101
4	25	38	76	352	210	97.7	0.76	101
5	25	50	38	352	210	61.5	0.69	125
6	25	50	50	352	210	75.4	0.71	125
7	25	50	64	352	210	92.4	0.75	125
8	25	50	76	352	210	102.5	0.71	125
9	25	64	38	352	210	68.0	0.66	153
10	25	64	50	352	210	85.0	0.73	153
11	25	64	64	352	210	100.7	0.75	153
12	25	64	76	352	210	111.1	0.71	153
13	25	76	38	352	210	75.1	0.67	177
14	25	76	50	352	210	88.3	0.68	177
15	25	76	64	352	210	103.3	0.68	177
16	25	76	76	352	210	114.5	0.66	177
17	50	38	38	352	210	63.1	0.71	126
18	50	38	50	352	210	79.2	0.78	126
19	50	38	64	352	210	92.9	0.76	126
20	50	38	76	352	210	106.8	0.78	126
21	50	50	38	352	210	68.5	0.68	150
22	50	50	50	352	210	83.8	0.73	150
23	50	50	64	352	210	98.4	0.72	150
24	50	50	76	352	210	110.5	0.72	150
25	50	64	38	352	210	75.5	0.67	178
26	50	64	50	352	210	88.9	0.68	178
27	50	64	64	352	210	103.6	0.68	178
28	50	64	76	352	210	113.9	0.65	178
29	50	76	38	352	210	80.1	0.65	202
30	50	76	50	352	210	93.5	0.65	202
31	50	76	64	352	210	107.2	0.64	202
32	50	76	76	352	210	117.4	0.61	202
33	25	38	38	352	252	59.7	0.67	101
34	25	38	50	352	252	72.8	0.68	101
35	25	38	64	352	252	88.1	0.69	101
36	25	38	76	352	252	101.2	0.70	101
37	25	50	38	352	252	66.8	0.66	125
38	25	50	50	352	252	79.8	0.66	125
39	25	50	64	352	252	94.8	0.67	125
40	25	50	76	352	252	103.5	0.60	125
41	25	64	38	352	252	72.6	0.61	153
42	25	64	50	352	252	87.6	0.64	153
43	25	64	64	352	252	102.5	0.64	153
44	25	64	76	352	252	112.3	0.61	153
45	25	76	38	352	252	80.3	0.62	177
46	25	76	50	352	252	93.1	0.62	177
47	25	76	64	352	252	106.4	0.60	177
48	25	76	76	352	252	117.0	0.58	177
49	50	38	38	352	252	66.7	0.65	126
50	50	38	50	352	252	81.2	0.68	126
51	50	38	64	352	252	95.7	0.68	126
52	50	38	76	352	252	107.7	0.66	126
53	50	50	38	352	252	73.3	0.63	150
54	50	50	50	352	252	86.6	0.64	150
55	50	50	64	352	252	100.7	0.63	150
56	50	50	76	352	252	111.7	0.61	150
57	50	64	38	352	252	80.7	0.62	178
58	50	64	50	352	252	93.4	0.62	178
59	50	64	64	352	252	106.4	0.60	178
60	50	64	76	352	252	116.6	0.57	178
61	50	76	38	352	252	86.5	0.60	202
62	50	76	50	352	252	98.9	0.60	202
63	50	76	64	352	252	111.2	0.57	202
64	50	76	76	352	252	121.4	0.55	202
65	25	38	38	352	293	62.6	0.63	101
66	25	38	50	352	293	75.5	0.63	101
67	25	38	64	352	293	91.1	0.65	101
68	25	38	76	352	293	103.5	0.64	101
69	25	50	38	352	293	70.2	0.61	125
70	25	50	50	352	293	82.9	0.61	125
71	25	50	64	352	293	98.1	0.62	125
72	25	50	76	352	293	108.1	0.58	125
73	25	64	38	352	293	77.2	0.58	153
74	25	64	50	352	293	91.8	0.60	153
75	25	64	64	352	293	106.5	0.60	153
76	25	64	76	352	293	116.9	0.57	153
77	25	76	38	352	293	86.1	0.59	177
78	25	76	50	352	293	98.6	0.58	177
79	25	76	64	352	293	112.4	0.57	177
80	25	76	76	352	293	121.9	0.54	177
81	50	38	38	352	293	70.4	0.61	126
82	50	38	50	352	293	84.4	0.63	126
83	50	38	64	352	293	98.6	0.62	126
84	50	38	76	352	293	111.6	0.62	126
85	50	50	38	352	293	77.6	0.59	150
86	50	50	50	352	293	90.6	0.60	150
87	50	50	64	352	293	105.4	0.60	150
88	50	50	76	352	293	116.8	0.58	150
89	50	64	38	352	293	85.9	0.58	178
90	50	64	50	352	293	98.8	0.58	178
91	50	64	64	352	293	112.5	0.57	178
92	50	64	76	352	293	122.2	0.54	178
93	50	76	38	352	293	92.6	0.57	202
94	50	76	50	352	293	105.5	0.57	202
95	50	76	64	352	293	117.9	0.55	202
96	50	76	76	352	293	126.7	0.52	202

iii. 4 Bolt Case

Table 3.7 : Test Results of 4 Bolt for 4 Bolt Line

Run#	E (mm)	P (mm)	S (mm)	Fu (Mpa)	Fy (Mpa)	U.L. (kN)	Fef / Fy	CL (mm)
1	25	38	38	352	210	66.8	0.71	139
2	25	38	50	352	210	81.9	0.75	139
3	25	38	64	352	210	98.2	0.78	139
4	25	38	76	352	210	109.1	0.75	139
5	25	50	38	352	210	75.3	0.68	175
6	25	50	50	352	210	89.8	0.70	175
7	25	50	64	352	210	105.4	0.72	175
8	25	50	76	352	210	116.2	0.69	175
9	25	64	38	352	210	83.6	0.64	217
10	25	64	50	352	210	98.2	0.66	217
11	25	64	64	352	210	111.1	0.64	217
12	25	64	76	352	210	119.2	0.59	217
13	25	76	38	352	210	90.6	0.61	253
14	25	76	50	352	210	103.4	0.62	253
15	25	76	64	352	210	116.3	0.60	253
16	25	76	76	352	210	124.2	0.55	253
17	50	38	38	352	210	72.8	0.69	164
18	50	38	50	352	210	87.2	0.71	164
19	50	38	64	352	210	103.4	0.73	164
20	50	38	76	352	210	113.4	0.70	164
21	50	50	38	352	210	80.0	0.65	200
22	50	50	50	352	210	94.0	0.67	200
23	50	50	64	352	210	108.3	0.66	200
24	50	50	76	352	210	119.7	0.65	200
25	50	64	38	352	210	88.5	0.62	242
26	50	64	50	352	210	101.8	0.63	242
27	50	64	64	352	210	115.8	0.62	242
28	50	64	76	352	210	125.0	0.59	242
29	50	76	38	352	210	94.4	0.59	278
30	50	76	50	352	210	106.9	0.59	278
31	50	76	64	352	210	120.0	0.58	278
32	50	76	76	352	210	128.3	0.54	278
33	25	38	38	352	252	70.6	0.65	139
34	25	38	50	352	252	84.0	0.66	139
35	25	38	64	352	252	100.4	0.68	139
36	25	38	76	352	252	110.9	0.65	139
37	25	50	38	352	252	80.1	0.62	175
38	25	50	50	352	252	93.9	0.63	175
39	25	50	64	352	252	107.7	0.62	175
40	25	50	76	352	252	118.5	0.60	175
41	25	64	38	352	252	90.9	0.60	217
42	25	64	50	352	252	103.1	0.59	217
43	25	64	64	352	252	115.8	0.58	217
44	25	64	76	352	252	124.8	0.54	217
45	25	76	38	352	252	99.2	0.58	253
46	25	76	50	352	252	110.5	0.57	253
47	25	76	64	352	252	122.2	0.54	253
48	25	76	76	352	252	130.8	0.51	253
49	50	38	38	352	252	77.3	0.63	164
50	50	38	50	352	252	90.8	0.64	164
51	50	38	64	352	252	105.7	0.64	164
52	50	38	76	352	252	115.8	0.61	164
53	50	50	38	352	252	86.3	0.60	200
54	50	50	50	352	252	99.4	0.61	200
55	50	50	64	352	252	112.2	0.59	200
56	50	50	76	352	252	123.9	0.58	200
57	50	64	38	352	252	96.3	0.58	242
58	50	64	50	352	252	108.1	0.57	242
59	50	64	64	352	252	120.8	0.56	242
60	50	64	76	352	252	130.4	0.53	242
61	50	76	38	352	252	103.7	0.56	278
62	50	76	50	352	252	114.3	0.54	278
63	50	76	64	352	252	127.2	0.53	278
64	50	76	76	352	252	133.9	0.49	278
65	25	38	38	352	293	74.5	0.60	139
66	25	38	50	352	293	87.6	0.61	139
67	25	38	64	352	293	103.3	0.62	139
68	25	38	76	352	293	114.9	0.61	139
69	25	50	38	352	293	85.3	0.58	175
70	25	50	50	352	293	98.8	0.59	175
71	25	50	64	352	293	112.8	0.59	175
72	25	50	76	352	293	123.9	0.57	175
73	25	64	38	352	293	97.5	0.57	217
74	25	64	50	352	293	110.0	0.57	217
75	25	64	64	352	293	121.4	0.54	217
76	25	64	76	352	293	129.2	0.50	217
77	25	76	38	352	293	107.8	0.56	253
78	25	76	50	352	293	118.6	0.54	253
79	25	76	64	352	293	129.4	0.52	253
80	25	76	76	352	293	137.2	0.48	253
81	50	38	38	352	293	82.0	0.59	164
82	50	38	50	352	293	95.4	0.60	164
83	50	38	64	352	293	110.5	0.60	164
84	50	38	76	352	293	121.3	0.58	164
85	50	50	38	352	293	92.2	0.57	200
86	50	50	50	352	293	105.4	0.57	200
87	50	50	64	352	293	118.9	0.56	200
88	50	50	76	352	293	129.1	0.54	200
89	50	64	38	352	293	104.4	0.56	242
90	50	64	50	352	293	116.0	0.55	242
91	50	64	64	352	293	127.5	0.53	242
92	50	64	76	352	293	135.9	0.50	242
93	50	76	38	352	293	113.7	0.54	278
94	50	76	50	352	293	123.5	0.52	278
95	50	76	64	352	293	133.8	0.50	278
96	50	76	76	352	293	141.6	0.47	278

3.2 Discussion of the Results

In this section effects of parameters on block shear load capacity of gusset plates with multiple bolt lines will be presented. As explained before, 576 specimens were analyzed with the finite element method. In all analysis, it was observed that the net section plane reached to ultimate stress while there were significant amounts of yielding in gross shear plane. As indicated in Topkaya's (2004) study, the prediction equation should consider the contributions of the tension and shear planes and should be based on the premise that net tension plane reaches ultimate stress at failure. Based on this argument, shear stress developed at the gross shear plane is the only unknown in predicting the block shear capacity of the member. From this point on, parameters will be expressed as a function of effective shear stress (F_{ef}) normalized by yield stress (F_y), which is called as effective shear stress ratio ($F_{ef} / F_{y)}$. For all analysis, effective shear stress ratios were calculated by using the ultimate load values, net tension strength and gross shear area of the analyzed specimen and they are given in Tables 3.2 to 3.7.

3.2.1 Effect of End Distance

To investigate the effect of end distance on block shear load capacity, specimens with the same connection lengths are considered. Since shear stress develops along the shear plane, connection length is kept constant to eliminate its effect. Also, spacing is kept constant to eliminate the effect of the block aspect ratio, which is the ratio of the tension plane length to connection length. Analyzed specimens with connection length of 89 mm, 88mm, 101 mm, 100 mm with end distances of 25, 50, 25, 50 mm, respectively are compared and variation of effective shear stress ratio with end distance is presented in Figure 3.2. Only 2 bolts for 2 bolt line case with ultimate to yield strength value of 1.68 is presented in this figure and similar types of plots can be obtained if other ultimate to yield strength ratios and different bolt arrangements are considered. It can be seen from Figure 3.2, when connection length and spacing is same, effective shear stress does not depend much

on the end distance. This observation suggests that effect of end distance can be neglected.

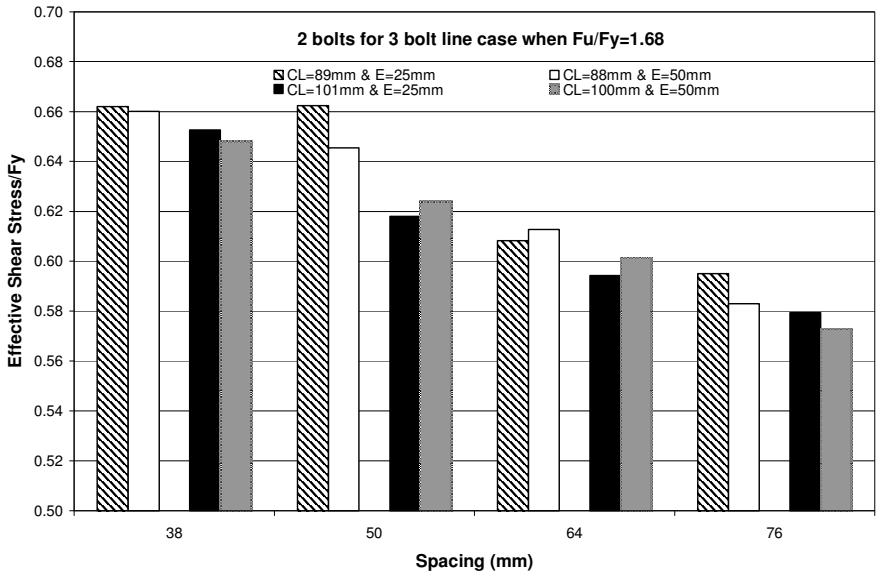

Figure 3.2 : Variation of Effective Shear Stress with End Distance

3.2.2 Effect of Pitch Distance

To investigate the effect of pitch distance on block shear load capacity, specimens with the same connection lengths are considered as explained in the previous section. Connection length and spacing are kept constant and variation of effective shear stress with pitch distance is presented in Figure 3.3. Only two bolts for 3 bolt line cases with ultimate to yield strength ratio of 1.68 is considered. Again, analyzed specimens with connection length of 89 mm, 88mm, 101 mm, 100 mm with pitch distances of 64, 38, 76, 50 mm, respectively are compared in this figure and similar types of plots can be obtained if other ultimate to yield strength ratios and different bolt arrangements are considered. It can be observed from Figure 3.3 that when connection length and spacing is kept nearly constant, effective shear stress does not depend much on the pitch distance. This observation suggests that effect of pitch distance can be neglected.

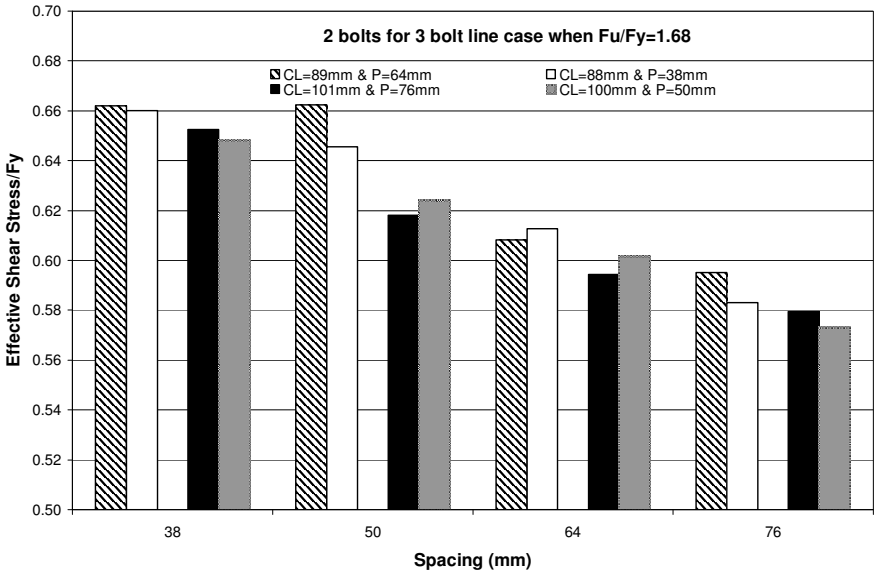

Figure 3.3 : Variation of Effective Shear Stress with Pitch Distance

3.2.3 Effect of Connection Length

Variation of effective shear stress normalized by yield stress as a function of connection length for different ultimate to yield stress ratios are plotted in Figures 3.4 to 3.7. A careful examination of the results reveals that, effective shear stress ratio is highly dependent on connection length. It is evident from the figures that, as connection length increases there is a decrease in the effective shear stress ratio for the specimens with same bolt line connection types. This phenomenon was pointed out by Hardash and Bjorhovde (1985) earlier. It is worthwhile to emphasize that the slope of the trend lines are different for three sets of yield strength values. For high ultimate-to-yield strength value the decrease in effective shear stress with an increase in connection length is much more pronounced than low ultimate to yield stress ratio.

In this study connection lengths up to 300 mm were investigated which encompass the practical cases.

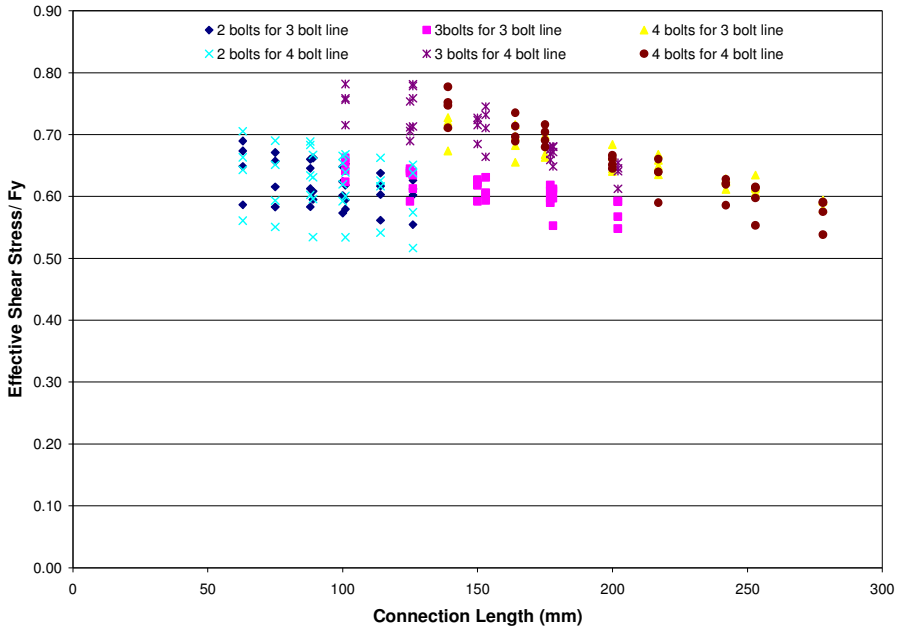

Figure 3.4 : Variation of Effective Shear Stress with Connection Length when Fu/Fy=1.68

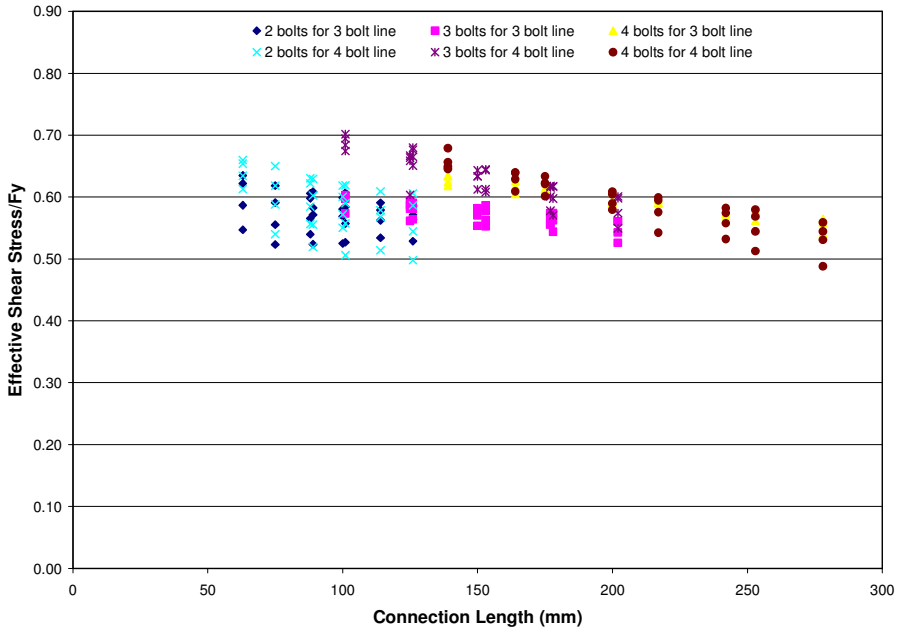

Figure 3.5 : Variation of Effective Shear Stress with Connection Length when Fu/Fy=1.4

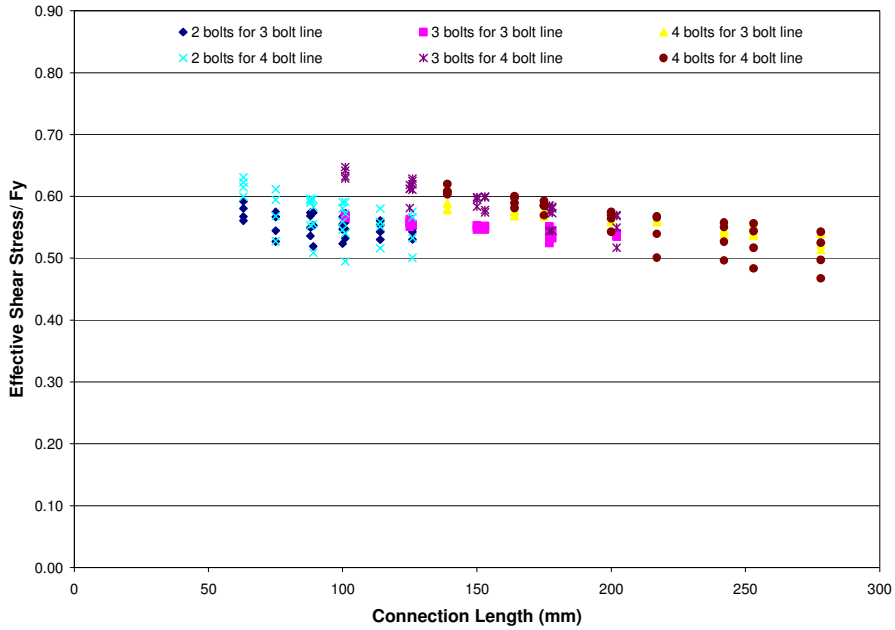

Figure 3.6 : Variation of Effective Shear Stress with Connection Length when Fu/Fy=1.2

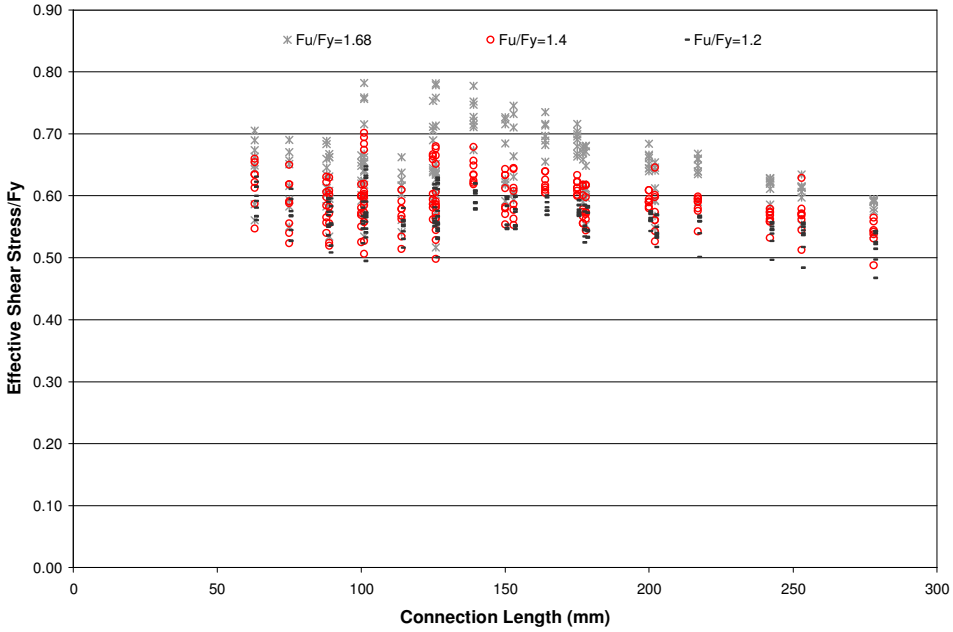

Figure 3.7 : Variation of Effective Shear Stress with Connection Length for All Analyzed Specimens

3.2.4 Effect of Ultimate-to-Yield Ratio

For the 576 previously mentioned finite element analyses the ultimate strength of the material was kept constant and the yield stress was varied to get ultimate-to-yield strength values of 1.68, 1.4 and 1.2. Variation of effective shear stress values for different ultimate-to-yield stress values are plotted in Figure 3.7. Investigation of the graph reveals that, as ultimate to yield ratio decreases, effective shear stress ratio decreases, also. The ultimate strength of the material was taken as 352 MPa and connections with yield stress values of 210 MPa gives the highest effective shear stress ratios in all cases. On the other hand, connections with yield stress values of 293 MPa gives the lowest effective shear stress values. For high ultimate-to-yield strength value the decrease in effective shear stress with connection length much more pronounced than low ultimate to yield stress ratio. This phenomenon was stated in Topkaya's (2004) study. So, it is evident that it is not accurate to use a single effective shear stress value as used in LRFD specification.

3.2.5 Effect of Block Aspect Ratio

Block aspect ratio is the ratio of gross tension length to the length of the connection. Gross tension length is a function of spacing between the holes. Connection length is a function of pitch and end distance. It is concluded that pitch and end distance does not affect the effective shear stress ratio from previous investigations. To investigate the effect of block aspect ratio, connection length is kept constant and spacing is varied. Variation of effective shear stress ratio with block aspect ratio is given in Figures 3.8 to 3.10. These figures represent the behavior of 2 bolts for 3 bolt line case. Similar results can be obtained for the other bolt arrangements. It can be concluded from these figures that, as spacing increases, effective shear stress ratio decreases for the same connection length. Also, the decrease is much more pronounced when connection length is short and ultimate to yield stress value is high. According to Figure 3.8, the effective shear stress ratio decreases about 14.5% when spacing between bolts increases from 38 mm to 76 mm for connection length of 63 mm for an ultimate to yield value of 1.68. On the other

hand, when connection length is 126 mm and ultimate to yield value is 1.2 the decrease in effective shear stress is about 0.05% for the same increase in spacing. Since not much variation in effective shear stress ratios were observed, effect of block aspect ratio on block shear capacity is neglected.

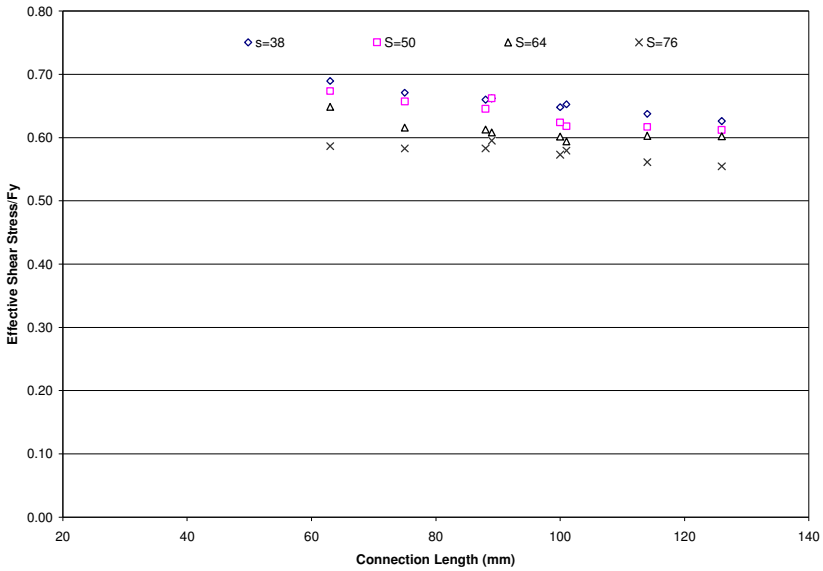

Figure 3.8 : Variation of Effective Shear Stress with Spacing for 2 Bolts for 3 Bolt Line, Fu/Fy=1.68

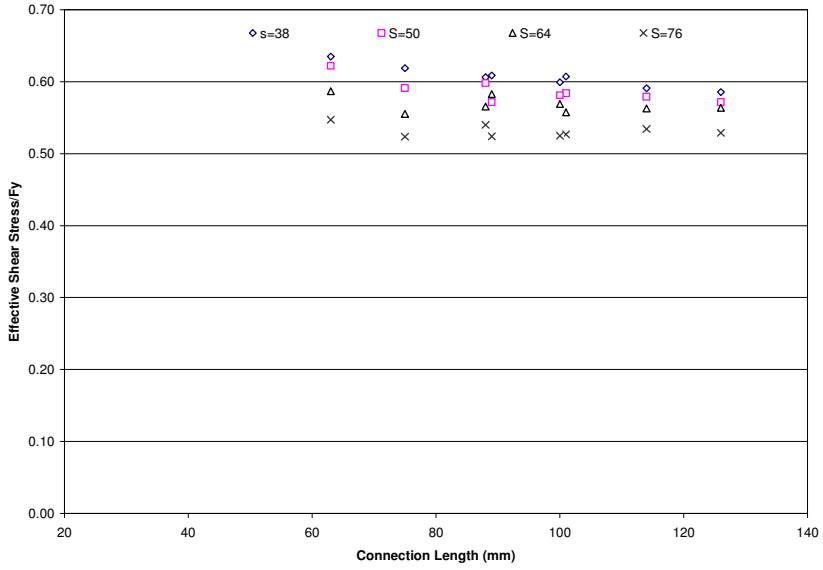

Figure 3.9 : Variation of Effective Shear Stress with Spacing for 2 bolts for 3 Bolt Line, Fu/Fy=1.4

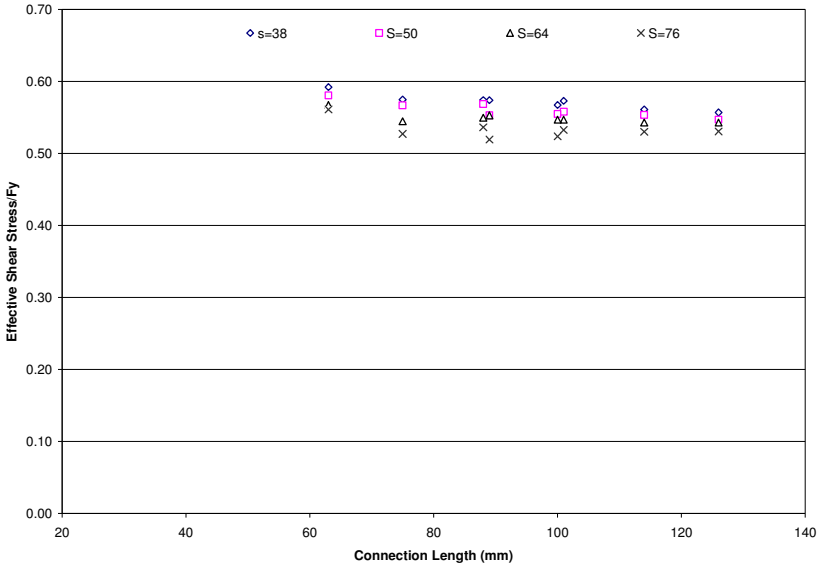

Figure 3.10 : Variation of Effective Shear Stress with Spacing for 2 Bolts for 3 Bolt Line, Fu/Fy=1.2

3.3 Assessment of the Existing Capacity Prediction Equations

The quality of the capacity prediction equations were assessed by making comparisons with the finite element results. In calculating the LRFD and ASD failure loads bolt hole sizes were not increased by 2 mm. Failure loads of equation predictions are plotted against the finite element analysis predictions in Figures 3.11 to 3.15. Data points appearing below the diagonal line indicate that equations overestimate the failure loads while points above the diagonal line indicate that equations underestimate the failure loads. Based on this analysis statistical measures of the predictions are given in Table 3.8. For each analyzed specimen a professional factor is calculated. Professional factor is the ratio of the finite element result to the predicted load capacity of the equations of the analyzed specimen. A perfect agreement between the predicted and analytical failure loads are expressed with a professional factor of unity. If the equation prediction overestimates the failure load, professional factor is less than unity. Conversely, if the equation prediction underestimates the load, professional factor is greater than unity.

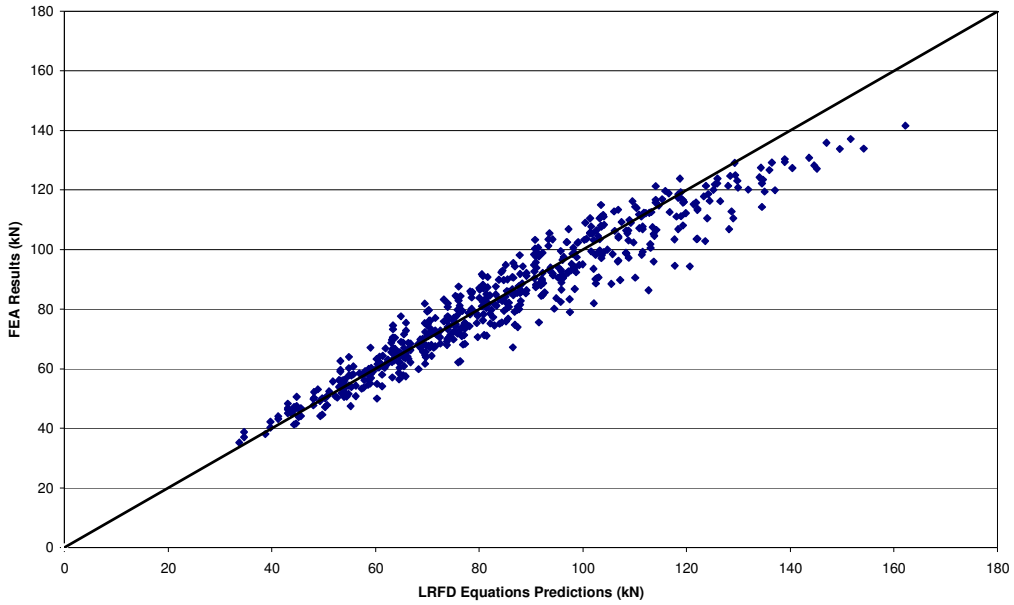

Figure 3.11 : Comparison of the LRFD Procedure Predictions with Finite Element Analysis Predictions

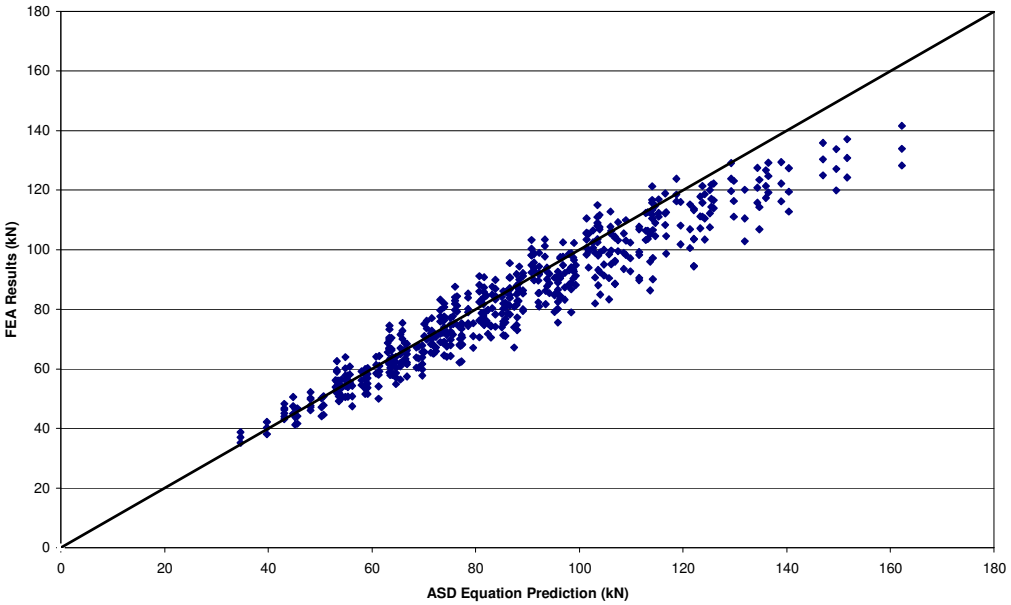

Figure 3.12 : Comparison of the ASD Procedure Predictions with FEA Predictions

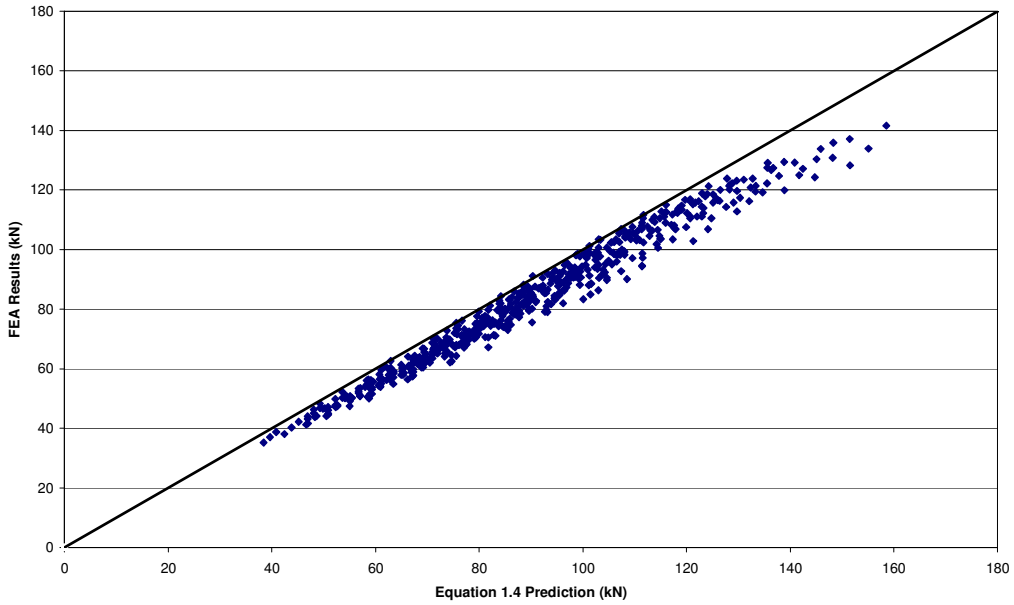

Figure 3.13 : Comparison of Equation 1.4 Predictions with FEA Predictions

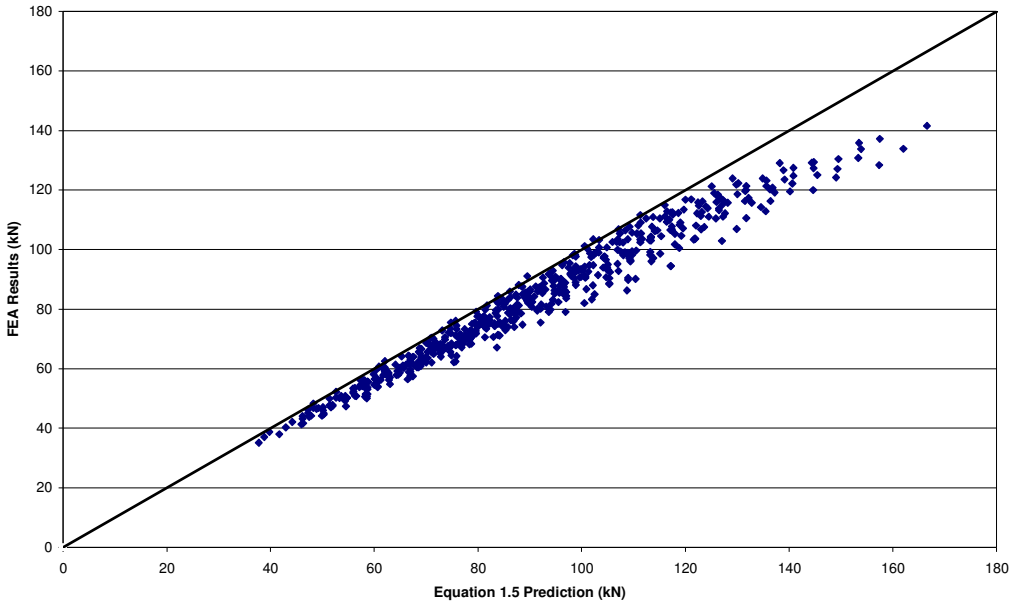

Figure 3.14 : Comparison of Equation 1.5 Predictions with FEA Predictions

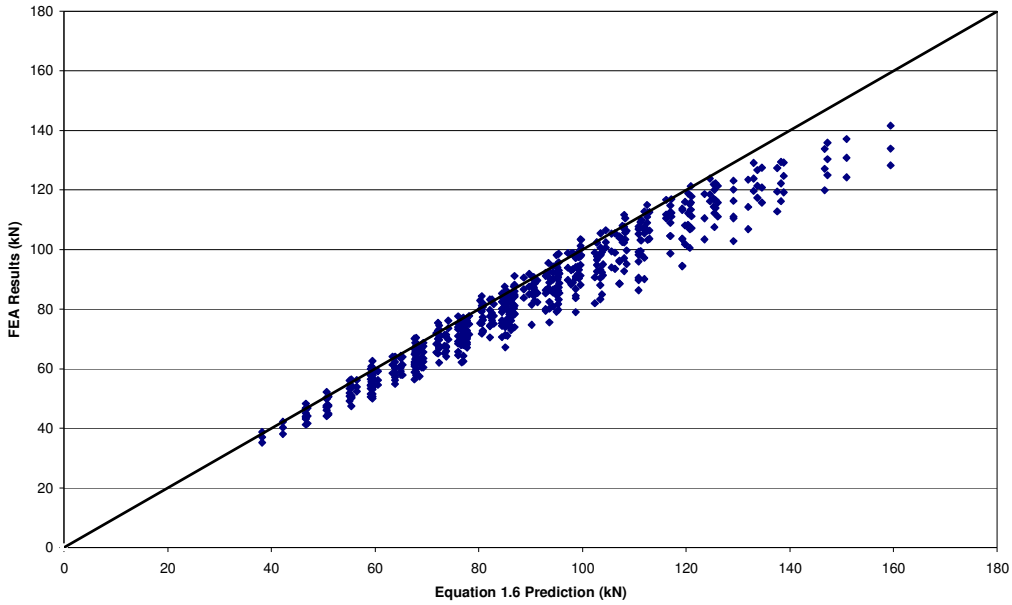

Figure 3.15: Comparison of Equation 1.6 Predictions with FEA Predictions

Table 3.8 : Professional Factor Statistics for LRFD, ASD, Topkaya's Predictions

	Professional factor				
	LRFD	ASD	Eq.1.4	Eq.1.5	Eq.1.6
Mean	0.989	0.962	0.925	0.920	0.934
Standard deviation	0.073	0.078	0.037	0.042	0.055
Maximum	1.197	1.176	1.008	1.018	1.052
Minimum	0.766	0.759	0.821	0.793	0.778

It is evident from Figures 3.11 and 3.12 and statistical measures that both ASD and LRFD procedure predicts the block shear load capacities with acceptable accuracies for 576 analyzed specimens. The average professional factor for LRFD procedure is 0.989 and the standard deviation is 7.3%. According to the maximum and minimum professional factors, predictions of 23.4% overstrength and 19.7% understrength are possible. In LRFD procedure usually the equation which assumes rupture in shear plane governs, while finite element findings tend to exhibit a failure mode of rupture in tension plane with yield in shear plane.

The average professional factor for ASD procedure is 0.962 and the standard deviation is 7.8%. According to the maximum and minimum professional factors, predictions of 24.1% overstrength and 17.6% understrength are possible. ASD procedure has a drawback in predicting the failure mode of the connection. ASD procedure assumes that rupture occurs simultaneously in tension and shear plane while actual observations are different.

As understood from the Figures 3.13 to 3.15 that equations developed by Topkaya mostly overestimates the failure loads for the multiple bolt line cases. The average professional factors for Topkaya's Equations are 0.925, 0.924, 0.934 and standard deviations are 3.7, 4.2, 5.5% respectively for these equations. For these three equations 22% overstrength and 5.2% understrength are possible. This indicates that average shear stress is smaller than the ones presented in those equations. Topkaya (2004) indicated that average effective shear stress value was 48% of ultimate strength value. For the 576 analyzed cases the effective shear stress is normalized by ultimate strength and the data points are presented in Figure 3.16. According to this figure the effective shear stress values fall within a band that is bounded by 31-54% of ultimate strength averaging a value of 43%.

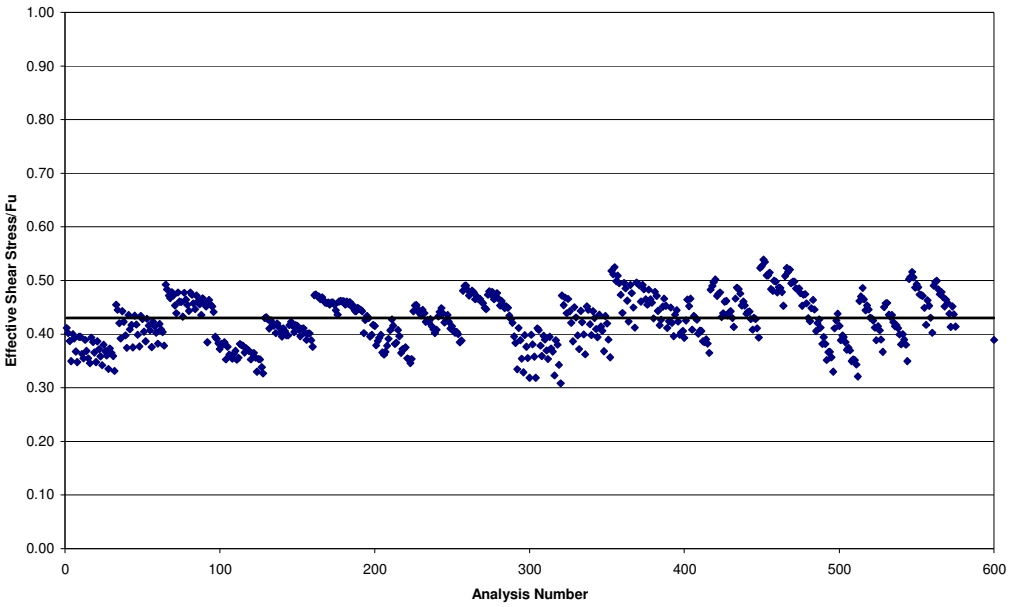

Figure 3.16 : Effective Shear Stress as a Function of Ultimate Strength

Topkaya used two typical edge boundary conditions in the analysis namely, boundary condition 1 (BC1) and boundary condition 2 (BC2) which are shown in Figure 3.17. Boundary condition 1 (BC1) represented the case of a gusset plate where half of the member was modeled and rollers were placed along the side which was close to the bolt holes. On the other hand, BC2 represented the case of a splice plate used to join the flanges of W-shapes. Since the bolts were symmetrically placed on both sides, only half of the plate was modeled and rollers were placed along the side which is farther away from the bolt holes.

Analysis of the results of two boundary conditions revealed that for the case of gusset plate represented by the BC1 the decrease in effective shear stress is much more pronounced than the case of splice plates which were represented by BC2. The difference in effective shear stress stayed below 10% between these two boundary conditions and for practical purposes Topkaya (2004) suggested that the effect of the difference between two boundary conditions could be ignored and used together to represent the general variation as a function of connection length and ultimate-to-yield ratio. This observation explains why Topkaya's equations overestimate the failure loads for multiple bolt lines even though standard deviations of these equations are low.

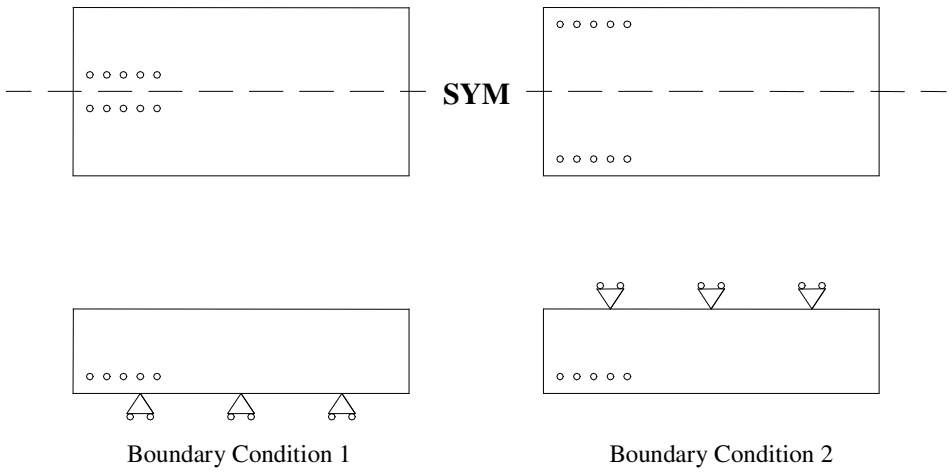

Figure 3.17 : Edge Boundary Conditions for Topkaya's Parametric Study

In the context of this thesis more refined equations were developed using regression analysis. The developed equations are presented in Equation 3.1 to Equation 3.3.

$$R_n = \left(0.41 + 0.17 \frac{F_u}{F_y} - \frac{Cl}{3090} \right) F_y A_{gv} + F_u A_{nt} \tag{3.1}$$

where Cl is the connection length in mm.

The coefficient determination (r^2) for the effective shear stress normalized by yield stress is 0.988 if the coefficients of Equation 3.1 are used. Cl is expressed in millimeters and if another system unit is used, the coefficient for connection length should be adjusted accordingly. Equation 3.1 is unit dependent and can be used in SI units.

A more simplified equation could be developed if the effective shear stress is based only on the ultimate-to-yield ratio. Regression analysis with rounding off the coefficients revealed that Equation 3.2 could also be a simple alternative of Equation 3.1.

$$R_n = \left(0.35 + 0.17 \frac{F_u}{F_y} \right) F_y A_{gv} + F_u A_{nt} \tag{3.2}$$

The coefficient of determination (r^2) for the effective shear stress normalized by yield stress is 0.985 if the coefficients of Equation 3.2 are used.

For the analyzed 576 analyses cases average effective shear stress value normalized with ultimate strength was found to be 0.43. Based on this observation a very simplified prediction equation was developed and is presented in Equation 3.3.

$$R_n = 0.43 \cdot F_u A_{gv} + F_u A_{nt} \tag{3.3}$$

Equations 3.2 and 3.3 can be used in all consistent system of units.

To investigate the quality of the developed prediction equations, comparisons of the load predictions and finite element analysis results for each case is presented in Figures 3.18 to 3.20 and the statistical measures of the predictions are given in Table 3.9.

It is evident from the figures and the statistical measures that the developed equations predict block shear load capacities with acceptable accuracy. The average professional factors are close to the unity and the standard deviations are less than 6%. According to the maximum and minimum professional factors 12% understrength and 15% overstrength are possible.

Table 3.9 : Professional Factor Statistics for Developed Equations

	Professional factor		
	Eq.3.1	Eq.3.2	Eq.3.3
Mean	0.999	1.006	0.993
Standard deviation	0.031	0.034	0.056
Maximum	1.091	1.106	1.119
Minimum	0.906	0.906	0.854

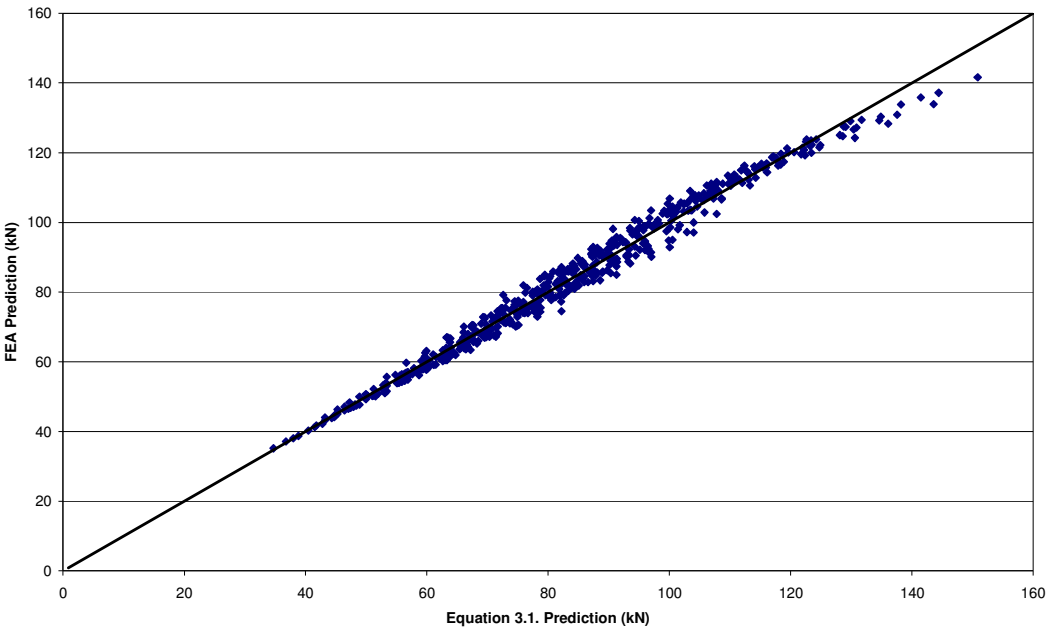

Figure 3.18 : Comparison of Equation 3.1 Predictions with FEA Predictions

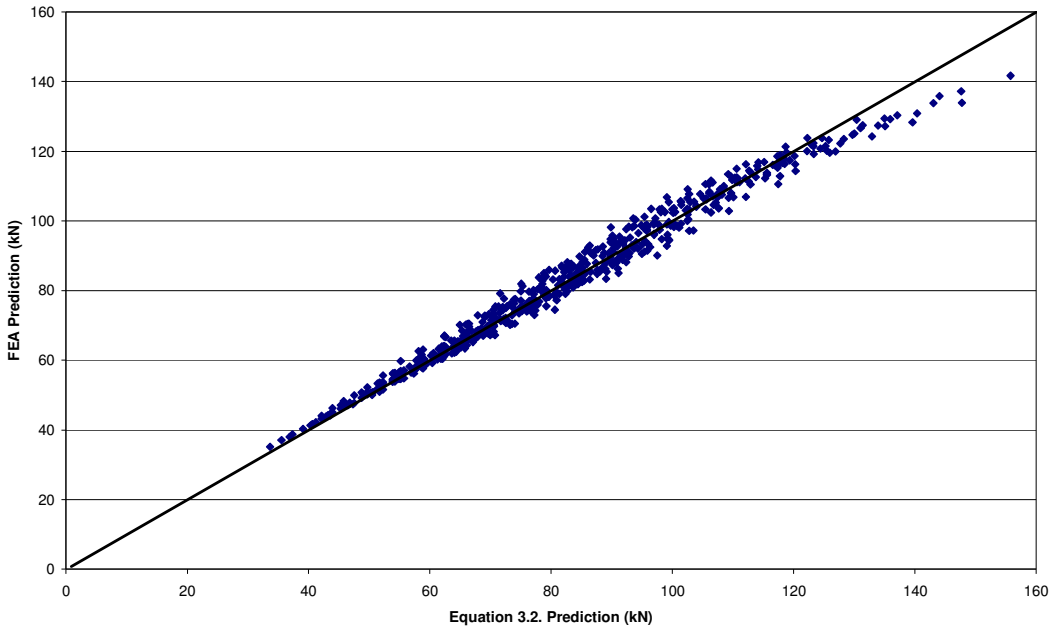

Figure 3.19 : Comparison of Equation 3.2 Predictions with FEA Predictions

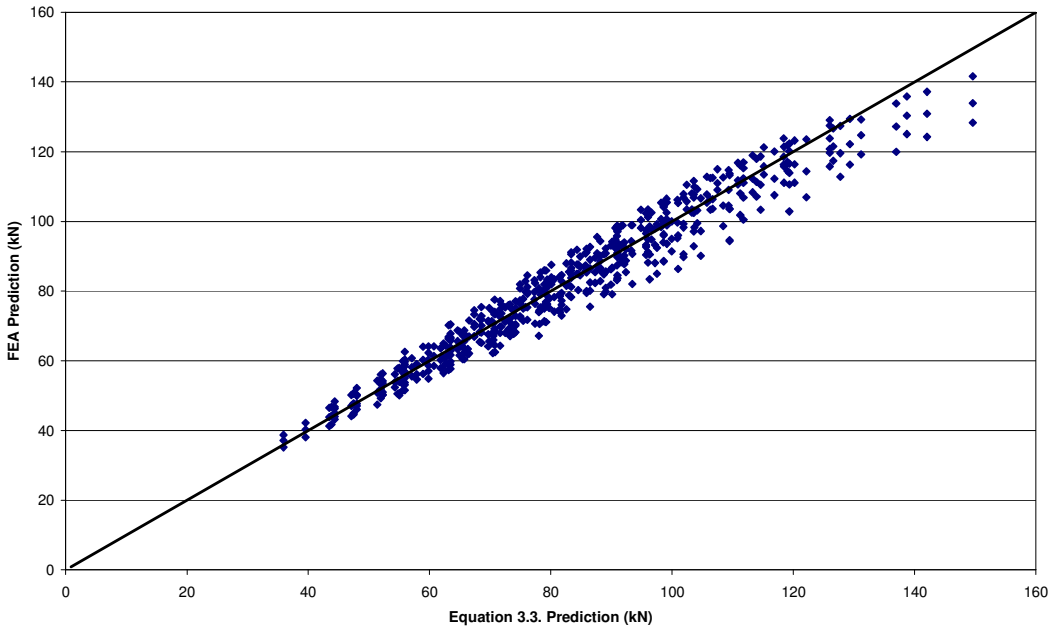

Figure 3.20 : Comparison of Equation 3.3 Predictions with FEA Predictions

CHAPTER 4

ANALYSIS OF STAGGER EFFECTS

4.1 Introduction

In the previous chapter a parametric study was successfully employed for preliminary studies of block shear failure for multiple bolt line connections. At the end of these investigations, effects of some variables on block shear capacity were defined and useful equations were developed. Previous study focused on block shear capacity of tension members with nonstaggered holes only. In this section effects of staggered bolts to block shear capacity will be investigated. Staggered holes are frequently used to connect the angles. For larger angles connected by one leg, two gage lines help to reduce the length of the connection. When two gage lines are present, staggered holes are used to provide AISC minimum spacing provisions and to increase the net tensile area of the section. Staggered holes may be required for certain geometries. For instance, when 19 mm or larger diameter bolts are used to connect a 127 mm angle leg, AISC provisions mandate stagger when bolts are used on two gage lines.

In this chapter a new parametric study is conducted to understand the stagger effects on block shear capacity of the connections. Since the existence of the outstanding leg creates out-of-plane eccentricity, only gusset plate connections is used in the analytical study to eliminate the effect of out-of plane eccentricity on block shear.

A total of 264 nonlinear finite element analyses were performed to investigate the block shear capacity of the connections with staggered holes. Two groups of

staggered hole patterns were analyzed. In the first group a triangular form of holes and in the second group negative and positive stagger patterns were used with four bolts having two gage lines. Analyses of these connections will be presented separately in the following sections.

In the finite element modeling phase of these specimens, the procedure explained in Chapter 2 was used in all analysis. Geometric and material variables are defined as the end distances, pitch distances, spacing and ultimate to yield strength (Fu/Fy) of the analyzed specimens.

4.2 Investigation of Stagger with Triangular Pattern

To evaluate the application of the block shear concept to gusset plates with staggered holes, it was decided to analyze plates with three holes in two gage lines. These holes are placed with a triangular form which results symmetrical gage (g1 and g2) and stagger (s_t) lines to occur, as shown in Figure 4.1.

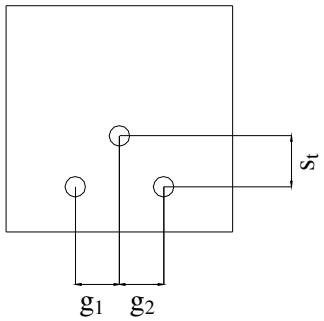

Figure 4.1 : Analyzed Specimens, Gage Length and Stagger Length

In this section, a total of 120 triangular shaped staggered connections were analyzed. Analyzed gusset plate specimens had a dimension of 500mm in width and length and thicknesses of the specimens were taken as unity. Two different hole diameters were used in the analysis. A total of 96 of the specimens had a hole diameter of 14mm and 24 of the specimens had a hole diameter of 27mm. Abovementioned 96 specimens had an end distance of 25, 50 mm., pitch distance of 38, 50, 64, 76 mm and spacing of 38, 50, 64, 76mm. Other 24 specimens had an end

distance of 50, 64 mm., spacing of 76, 150 mm. and a pitch distance of 50, 76 mm. As indicated in the Figure 4.2, end distance (E) is defined as the vertical distance from the end of the gusset plate to the center of the last holes, spacing (S) is the distance between the centers of the end bolts and pitch distance (P) is the inclined distance between the centers of the end holes and the top hole.

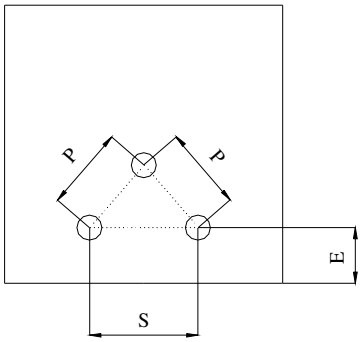

Figure 4.2 : General Analyzed Gusset Plate Configuration

All the analyzed specimens had an ultimate strength value of 352 MPa. To see the effect of ultimate to yield ratio yield strength values of the specimens, yield strength values were varied as 210, 252 and 293 MPa. These yield stress values correspond to ultimate to yield ratios of 1.68, 1.40 and 1.20 respectively. The combination of all the variables considered in this study is listed in Table 4.1.

Table 4.1 : Combinations of the Variables Used in Parametric Study

End distance	Spacing	Pitch distance	F_u/F_y
Hole diameter (14mm)			
First Set			
25	38/50/64/76	38/50/64/76	1.68/1.4/1.2
50	38/50/64/76	38/50/64/76	1.68/1.4/1.2
			96 cases
Hole diameter (27mm)			
Second Set			
50	76/150	76/150	1.68/1.4/1.2
64	76/150	76/150	1.68/1.4/1.2
			24 cases
Total number of cases			*120*

All dimensions are in mm

4.2.1 Results of the Analysis Cases

Previously mentioned geometries are used in the parametric study and Tables 4.2 and 4.3 show the results of 24 specimens with 27mm hole diameter and 96 specimens with 14mm hole diameter, respectively. In the tables below, end distances (E), pitch distances (P), spacing (S), ultimate strengths (F_u), yield strength (F_y) and ultimate loads (U.L) of each specimens are presented.

Table 4.2 : Analysis Results for Specimens with 27 mm. Diameter Holes

Run #	E (mm)	P (mm)	S (mm)	Fu (MPa)	Fy (MPa)	U.L (kN)
1	50	76	76	352	210	46.0
2	50	150	76	352	210	61.6
3	50	76	150	352	210	50.9
4	50	150	150	352	210	75.0
5	64	76	76	352	210	50.2
6	64	150	76	352	210	66.9
7	64	76	150	352	210	54.4
8	64	150	150	352	210	83.7
9	50	76	76	352	252	46.6
10	50	150	76	352	252	62.2
11	50	76	150	352	252	52.3
12	50	150	150	352	252	74.6
13	64	76	76	352	252	51.1
14	64	150	76	352	252	68.0
15	64	76	150	352	252	56.0
16	64	150	150	352	252	84.4
17	50	76	76	352	293	46.8
18	50	150	76	352	293	61.6
19	50	76	150	352	293	54.0
20	50	150	150	352	293	74.7
21	64	76	76	352	293	51.9
22	64	150	76	352	293	69.0
23	64	76	150	352	293	57.8
24	64	150	150	352	293	84.3

Table 4.3 : Analysis Results for Specimens with 14 mm. Diameter Holes

Run #	E (mm)	P (mm)	S (mm)	Fu (Mpa)	Fy (Mpa)	U.L. (kN)
1	25	38	38	352	210	24.3
2	25	38	50	352	210	24.0
3	25	38	64	352	210	25.7
4	25	38	76	352	210	26.4
5	25	50	38	352	210	29.5
6	25	50	50	352	210	29.9
7	25	50	64	352	210	31.3
8	25	50	76	352	210	31.0
9	25	64	38	352	210	31.6
10	25	64	50	352	210	33.2
11	25	64	64	352	210	36.0
12	25	64	76	352	210	37.0
13	25	76	38	352	210	31.2
14	25	76	50	352	210	34.9
15	25	76	64	352	210	38.6
16	25	76	76	352	210	38.9
17	50	38	38	352	210	33.0
18	50	38	50	352	210	31.7
19	50	38	64	352	210	33.1
20	50	38	76	352	210	32.9
21	50	50	38	352	210	38.5
22	50	50	50	352	210	36.7
23	50	50	64	352	210	38.6
24	50	50	76	352	210	39.1
25	50	64	38	352	210	43.2
26	50	64	50	352	210	45.1
27	50	64	64	352	210	44.6
28	50	64	76	352	210	47.4
29	50	76	38	352	210	46.6
30	50	76	50	352	210	48.1
31	50	76	64	352	210	50.5
32	50	76	76	352	210	50.5
33	25	38	38	352	210	24.5
34	25	38	50	352	210	24.4
35	25	38	64	352	210	25.9
36	25	38	76	352	210	27.1
37	25	50	38	352	210	29.0
38	25	50	50	352	210	30.1
39	25	50	64	352	210	30.7
40	25	50	76	352	210	31.4
41	25	64	38	352	210	31.6
42	25	64	50	352	210	33.8
43	25	64	64	352	210	36.2
44	25	64	76	352	210	37.1
45	25	76	38	352	210	31.5
46	25	76	50	352	210	38.7
47	25	76	64	352	210	38.6
48	25	76	76	352	210	38.9

Run #	E (mm)	P (mm)	S (mm)	Fu (Mpa)	Fy (Mpa)	U.L. (kN)
49	50	38	38	352	210	32.1
50	50	38	50	352	210	32.6
51	50	38	64	352	210	33.8
52	50	38	76	352	210	33.7
53	50	50	38	352	210	37.9
54	50	50	50	352	210	37.8
55	50	50	64	352	210	38.5
56	50	50	76	352	210	40.0
57	50	64	38	352	210	43.7
58	50	64	50	352	210	42.8
59	50	64	64	352	210	44.8
60	50	64	76	352	210	47.0
61	50	76	38	352	210	45.0
62	50	76	50	352	210	48.8
63	50	76	64	352	210	48.8
64	50	76	76	352	210	50.4
65	25	38	38	352	210	24.3
66	25	38	50	352	210	24.7
67	25	38	64	352	210	26.2
68	25	38	76	352	210	27.3
69	25	50	38	352	210	29.4
70	25	50	50	352	210	29.6
71	25	50	64	352	210	31.1
72	25	50	76	352	210	31.9
73	25	64	38	352	210	31.1
74	25	64	50	352	210	35.4
75	25	64	64	352	210	36.5
76	25	64	76	352	210	37.4
77	25	76	38	352	210	31.5
78	25	76	50	352	210	38.8
79	25	76	64	352	210	39.2
80	25	76	76	352	210	39.1
81	50	38	38	352	210	34.0
82	50	38	50	352	210	34.3
83	50	38	64	352	210	34.6
84	50	38	76	352	210	34.8
85	50	50	38	352	210	39.5
86	50	50	50	352	210	39.1
87	50	50	64	352	210	40.5
88	50	50	76	352	210	40.0
89	50	64	38	352	210	44.3
90	50	64	50	352	210	49.0
91	50	64	64	352	210	46.1
92	50	64	76	352	210	48.3
93	50	76	38	352	210	46.9
94	50	76	50	352	210	49.1
95	50	76	64	352	210	50.9
96	50	76	76	352	210	51.0

4.2.2 Assessment of the Existing Capacity Equations

AISC-LRFD and ASD codes present a $s_t^2/4g$ (developed by Cochrane (1922)) correction for stagger when dealing with net tension failure, but do not as yet explicitly deal with stagger effects when dealing with block shear. But, several recent manuals and textbooks (Munse and Chesson (1963), Yura (1988), Smith (1988)) all agree that it seems reasonable to incorporate long-standing $st^2/4g$ increase to net tensile width. Gage length and stagger was shown in Figure 4.1.

Net section for staggered holes is computed according to AISC-LRFD and ASD by the below Equation 4.1 ;

$$A_n = A_g - \sum d \cdot t + \sum \left[\frac{s_t}{4g}^2 \right] \cdot t \qquad (4.1)$$

where

A_n = net area of the staggered holes section

A_g =gross area of the section

t = thickness of the section

d =diameter of the holes

s_t =stagger

g =gage distance

Based on AISC-LRFD and ASD specifications block shear capacities of the analyzed 120 specimens are calculated. In the calculation of net tension plane $s_t^2/4g$ correction is used. The quality of the prediction equations was assessed by making comparisons with the finite element results. Failure loads of equation predictions are plotted against the finite element analysis predictions in Figures 4.3 to 4.6. Data points appearing below the diagonal line indicate that AISC-LRFD and ASD equations overestimate the failure loads while points above the diagonal line indicate that equations underestimate the failure loads. For each analyzed specimen a

professional factor is calculated and statistical measures of the predictions are presented in Table 4.4.

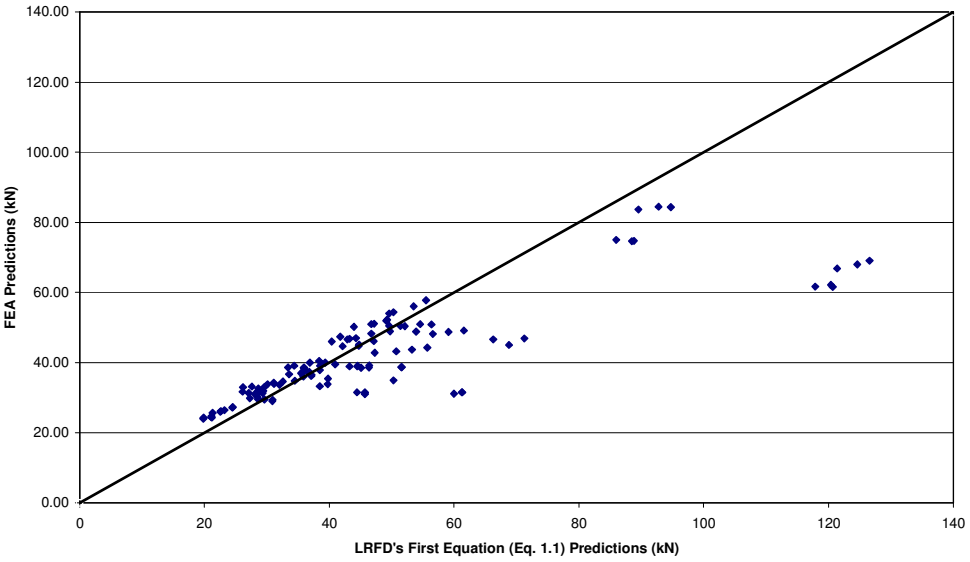

Figure 4.3 : Comparison of the LRFD's First Equation (Equation 1.1) Predictions with FEA Prediction

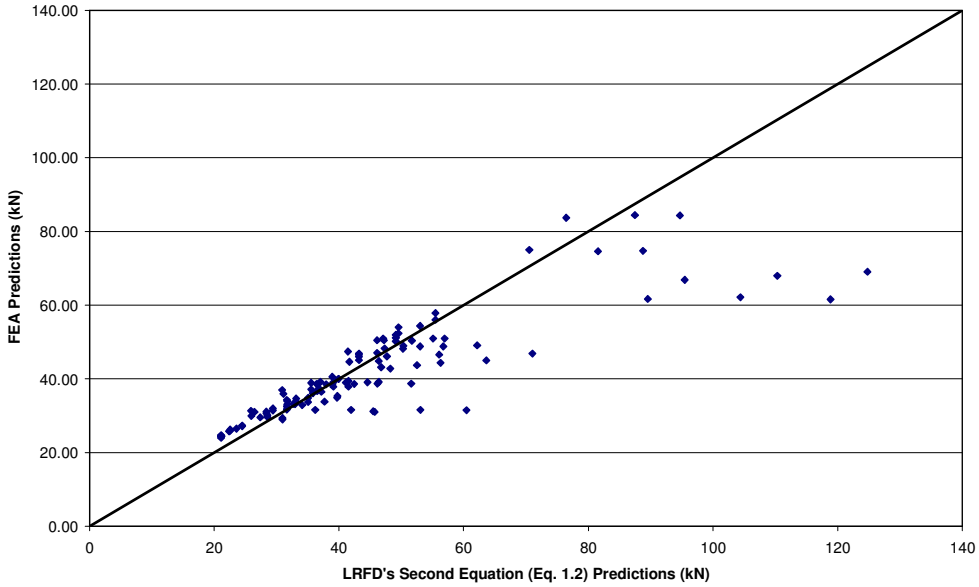

Figure 4.4 : Comparison of the LRFD's Second Equation (Equation 1.2) Predictions with FEA Predictions.

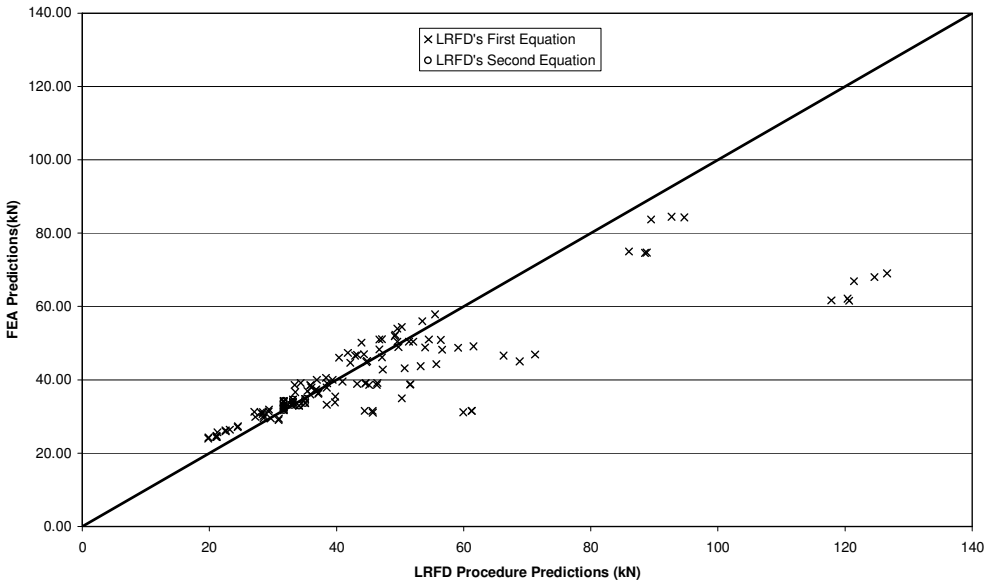

Figure 4.5 : Comparison of the LRFD Procedure Predictions with FEA Predictions

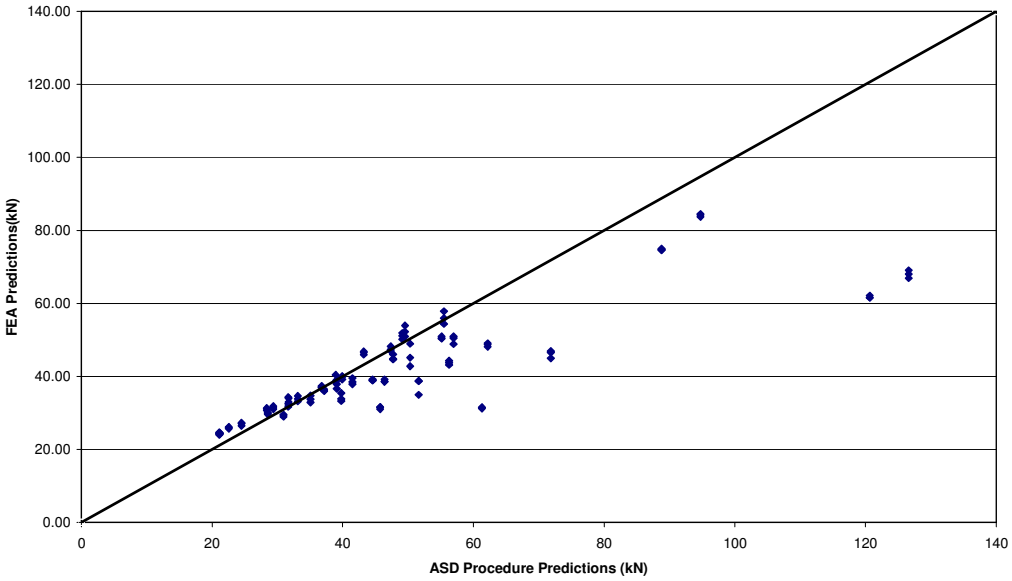

Figure 4.6 : Comparison of the ASD Procedure Predictions with FEA Predictions

Table 4.4 Professional Factor Statistics for AISC-LRFD and ASD Predictions

	Professional factor			
	LRFD1	LRFD2	LRFD	ASD
Mean	0.965	0.973	0.954	0.924
Standard deviation	0.184	0.152	0.177	0.168
Maximum	1.262	1.209	1.225	1.170
Minimum	0.501	0.518	0.510	0.509

According to the figures and statistical measures above, it is observed that both LRFD and ASD predictions overestimates the failure loads on average. Although, in LRFD predictions the equation with shear fracture term predicts more accurately the ultimate load of the specimens, except twelve cases the equation with tensile fracture term governed. The average professional factor for AISC-LRFD procedure is 0.954 and the standard deviation is 17.7%. According to the maximum and minimum professional factors, predictions of 22.5% understrength and 49% overstrength are possible. It is observed from the statistical measure that AISC-LRFD procedure predict the block shear load capacity of the staggered connection with acceptable accuracy with a big standard deviation value.

According to the statistical measures AISC-ASD highly overestimates the failure loads of the analyzed specimens. The average professional factor for AISC-ASD procedure is 0.924 with a standard deviation of 16.8%. According to the maximum and minimum professional factors 17% understrength and 49.1% overstrength are possible. AISC-ASD procedure predicts the block shear load capacity of the staggered connection worse than AISC-LRFD procedure predicts.

When the above figures are investigated LRFD and ASD equations highly overestimates the failure loads of some specimens. These specimens have high pitch to spacing ratios. Pitch to spacing ratio is a function of the angle (α) between spacing and pitch. As the angle (α) increases pitch to spacing ratio increases. The angle (α) is shown in the Figure 4.7. To investigate this phenomenon variation of professional factor with respect to above mentioned angle is graphed in Figure 4.8 and 4.9.

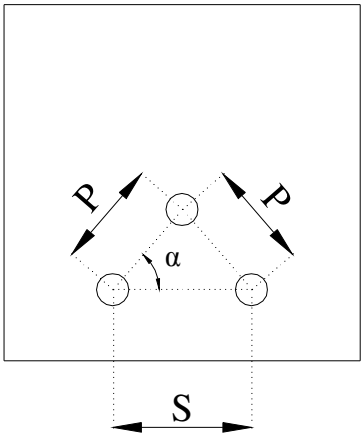

Figure 4.7 : Angle between Pitch and Spacing

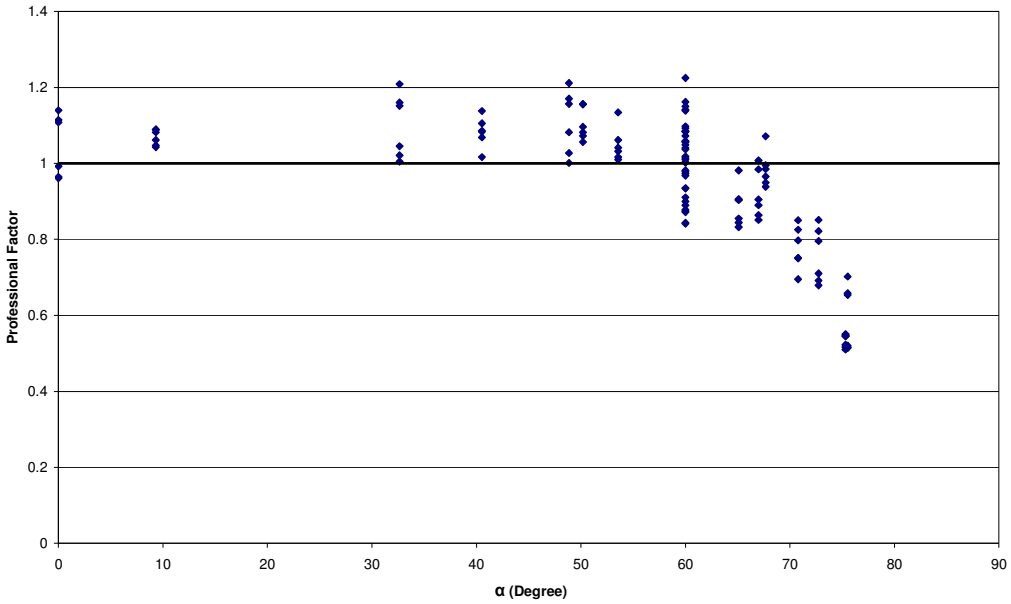

Figure 4.8 : Variation of Professional Factor of LRFD Equation with α

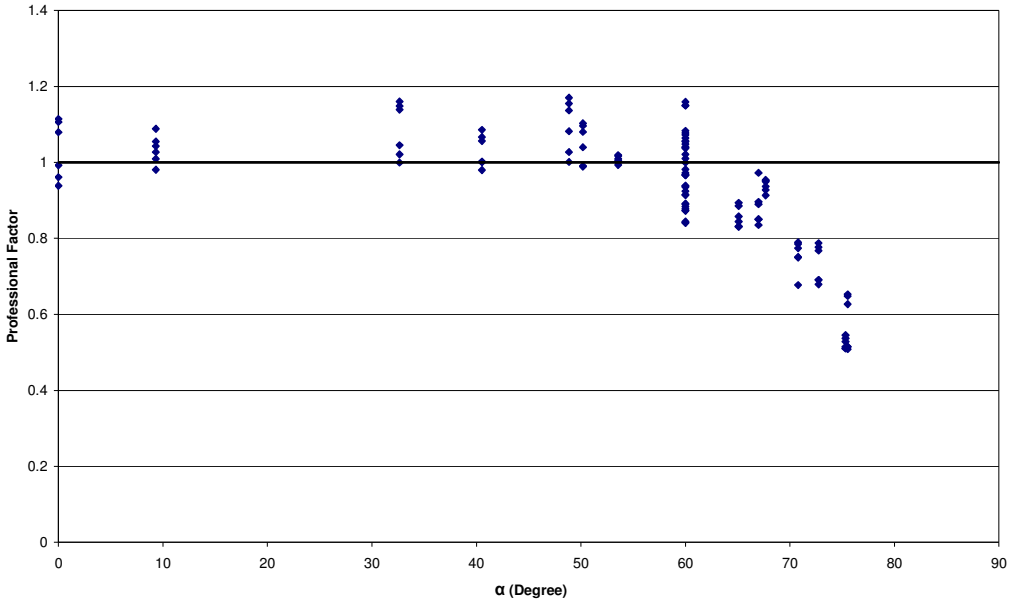

Figure 4.9 : Variation of Professional Factor of ASD Equation with α

According to the figures above it is observed that the decrease in professional factor is much more pronounced when α is more than 60^o. When the angle is smaller than 60^o professional factor is larger than unity which means that both LRFD and ASD procedures predict the failure loads conservatively on average. On the other hand, when the angle is more than 60^o both procedures predictions highly overestimate the failure loads of the specimens.

4.2.3 Development of the Block Shear Capacity Prediction Equations for Staggered Hole Connections

In the previous section analysis results of staggered hole connections were used to assess the quality of the AISC-LRFD and ASD predicting equations. In the computations, equations net area of the section was increased by using $s_t^2/4g$ rule as

recommended. In this section a new investigation will be performed to develop an equation to predict block shear capacity of the staggered connections.

In this equation, tensile capacity of the connection is defined as the tensile capacity of the pitch distance and the effective stress developed on this inclined area is a function of the angle (α) between pitch and spacing. On the other hand shear capacity of the connection is the shear capacity developed on the end distance as shown in Figure 4.10.

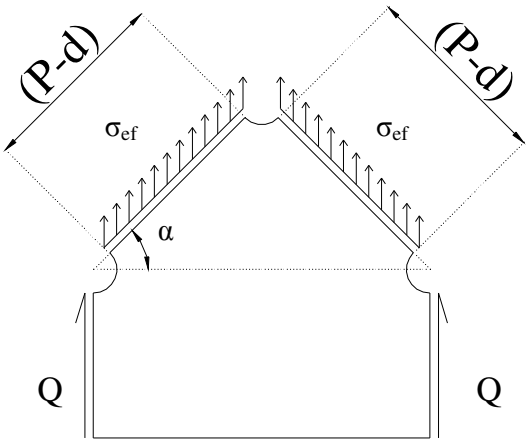

In where;

σ_{ef}= Effective stress

Q=Shear Resistance

Figure 4.10 : Effective Stress Developed on the Pitch Line and Shear Stress on the Shear Plane

In this argument to predict the block shear capacity equations variables are defined as the shear stress developed on the shear plane (Q), effective shear stress on the inclined distance (σ_{ef}), pitch distance (P), thickness of the plate (t), diameter of holes (d) and angle between the pitch and spacing (α). Pitch distance, thickness of the plate and diameter of the holes are the properties of the geometry and they are known. Shear stress developed on the shear plane can be found by the results of the finite element analysis.

To find the shear stress developed on the shear plane, a path was defined along the shear plane in each analysis. Shear stress developed on the shear plane is graphed and by integration, shear capacity (Q) of each specimen is found. Effective stress developed on the inclined area was found by subtracting the total shear capacity of the specimen from its ultimate load (U.L.-2*Q) divided by net inclined are ((p-d)*t). Shear capacity developed on one shear plane (Q) and effective stress (σ_{ef}) developed on the inclined area are presented in Tables 4.5 and 4.6 for all the specimens.

Table 4.5 : Shear Capacity and Effective Stresses of the Specimens with 27 mm. Holes

test #	E (mm)	P (mm)	S (mm)	Fu (MPa)	Fy (MPa)	U.L (kN)	Q (kN)	Ef. Str. (MPa)
1	50	76	76	352	210	46.0	8.6	293.4
2	50	150	76	352	210	61.6	8.6	180.7
3	50	76	150	352	210	50.9	8.4	349.4
4	50	150	150	352	210	75.0	6.5	252.0
5	64	76	76	352	210	50.2	10.7	293.5
6	64	150	76	352	210	66.9	10.8	184.0
7	64	76	150	352	210	54.4	10.2	346.5
8	64	150	150	352	210	83.7	9.7	261.2
9	50	76	76	352	252	46.6	8.8	296.6
10	50	150	76	352	252	62.2	8.8	180.7
11	50	76	150	352	252	52.3	9.0	349.5
12	50	150	150	352	252	74.6	5.5	259.0
13	64	76	76	352	252	51.1	11.1	294.8
14	64	150	76	352	252	68.0	11.0	187.0
15	64	76	150	352	252	56.0	10.5	357.3
16	64	150	150	352	252	84.4	9.1	269.3
17	50	76	76	352	293	46.8	8.9	295.5
18	50	150	76	352	293	61.6	9.0	176.8
19	50	76	150	352	293	54.0	9.1	364.6
20	50	150	150	352	293	74.7	5.6	258.5
21	64	76	76	352	293	51.9	11.4	296.7
22	64	150	76	352	293	69.0	11.2	189.2
23	64	76	150	352	293	57.8	11.4	357.5
24	64	150	150	352	293	84.3	9.1	269.2

To find the shear stress developed on the shear plane a new inspection is performed. Shear stresses developed on the shear plane were calculated by dividing the shear capacity with shear plane area. These shear stresses are normalized with ultimate strength of the material and the data points are presented in Figure 4.11.

Table 4.6 : Shear Capacity and Effective Stresses of the Specimens with 14 mm. Holes

Run #	E (mm)	P (mm)	S (mm)	Fu (Mpa)	Fy (Mpa)	U.L. (kN)	Q (kN)	Ef. Str. (MPa)
1	25	38	38	352	210	24.3	3.6	355.8
2	25	38	50	352	210	24.0	3.2	366.2
3	25	38	64	352	210	25.7	4.0	370.7
4	25	38	76	352	210	26.4	4.0	383.8
5	25	50	38	352	210	29.5	3.8	304.4
6	25	50	50	352	210	29.9	3.8	310.7
7	25	50	64	352	210	31.3	3.9	325.7
8	25	50	76	352	210	31.0	3.7	328.1
9	25	64	38	352	210	31.6	3.7	242.4
10	25	64	50	352	210	33.2	3.9	254.8
11	25	64	64	352	210	36.0	3.3	293.0
12	25	64	76	352	210	37.0	3.7	296.3
13	25	76	38	352	210	31.2	3.6	193.9
14	25	76	50	352	210	34.9	3.2	230.7
15	25	76	64	352	210	38.6	3.3	257.7
16	25	76	76	352	210	38.9	3.4	259.7
17	50	38	38	352	210	33.0	8.5	332.6
18	50	38	50	352	210	31.7	8.2	318.8
19	50	38	64	352	210	33.1	8.3	344.7
20	50	38	76	352	210	32.9	7.7	365.4
21	50	50	38	352	210	38.5	8.4	301.9
22	50	50	50	352	210	36.7	7.9	288.9
23	50	50	64	352	210	38.6	7.6	323.8
24	50	50	76	352	210	39.1	8.0	321.6
25	50	64	38	352	210	43.2	8.4	264.7
26	50	64	50	352	210	45.1	8.4	283.1
27	50	64	64	352	210	44.6	8.0	286.9
28	50	64	76	352	210	47.4	8.1	312.5
29	50	76	38	352	210	46.6	7.7	252.0
30	50	76	50	352	210	48.1	8.4	252.9
31	50	76	64	352	210	50.5	8.0	277.5
32	50	76	76	352	210	50.5	8.1	276.2
33	25	38	38	352	210	24.5	3.7	356.2
34	25	38	50	352	210	24.4	3.4	368.0
35	25	38	64	352	210	25.9	4.1	371.5
36	25	38	76	352	210	27.1	4.3	387.3
37	25	50	38	352	210	29.0	3.8	296.6
38	25	50	50	352	210	30.1	3.7	315.1
39	25	50	64	352	210	30.7	4.0	315.3
40	25	50	76	352	210	31.4	3.7	331.7
41	25	64	38	352	210	31.6	3.7	240.8
42	25	64	50	352	210	33.8	3.2	273.3
43	25	64	64	352	210	36.2	3.3	295.2
44	25	64	76	352	210	37.1	3.5	300.7
45	25	76	38	352	210	31.5	3.6	196.5
46	25	76	50	352	210	38.7	3.4	258.0
47	25	76	64	352	210	38.6	3.0	263.6
48	25	76	76	352	210	38.9	3.3	261.6

Run #	E (mm)	P (mm)	S (mm)	Fu (Mpa)	Fy (Mpa)	U.L. (kN)	Q (kN)	Ef. Str. (MPa)
49	50	38	38	352	210	32.1	8.9	298.4
50	50	38	50	352	210	32.6	8.5	325.8
51	50	38	64	352	210	33.8	8.4	353.8
52	50	38	76	352	210	33.7	7.8	375.5
53	50	50	38	352	210	37.9	8.7	284.4
54	50	50	50	352	210	37.8	8.4	292.4
55	50	50	64	352	210	38.5	8.4	301.9
56	50	50	76	352	210	40.0	8.4	321.6
57	50	64	38	352	210	43.7	8.0	276.3
58	50	64	50	352	210	42.8	7.8	271.1
59	50	64	64	352	210	44.8	8.4	281.0
60	50	64	76	352	210	47.0	8.4	303.1
61	50	76	38	352	210	45.0	5.6	272.6
62	50	76	50	352	210	48.8	7.9	266.5
63	50	76	64	352	210	48.8	7.6	271.2
64	50	76	76	352	210	50.4	8.0	277.6
65	25	38	38	352	210	24.3	4.2	333.7
66	25	38	50	352	210	24.7	3.7	359.5
67	25	38	64	352	210	26.2	4.2	370.8
68	25	38	76	352	210	27.3	4.5	382.4
69	25	50	38	352	210	29.4	4.3	288.0
70	25	50	50	352	210	29.6	4.3	291.1
71	25	50	64	352	210	31.1	4.3	313.1
72	25	50	76	352	210	31.9	3.9	335.5
73	25	64	38	352	210	31.1	3.8	233.9
74	25	64	50	352	210	35.4	3.7	280.5
75	25	64	64	352	210	36.5	3.5	295.2
76	25	64	76	352	210	37.4	3.6	301.8
77	25	76	38	352	210	31.5	3.7	193.9
78	25	76	50	352	210	38.8	3.3	259.5
79	25	76	64	352	210	39.2	3.1	265.3
80	25	76	76	352	210	39.1	2.8	269.7
81	50	38	38	352	210	34.0	8.7	345.8
82	50	38	50	352	210	34.3	8.6	355.4
83	50	38	64	352	210	34.6	8.7	360.8
84	50	38	76	352	210	34.8	8.5	371.8
85	50	50	38	352	210	39.5	8.7	305.5
86	50	50	50	352	210	39.1	8.5	306.1
87	50	50	64	352	210	40.5	8.5	326.5
88	50	50	76	352	210	40.0	8.4	321.4
89	50	64	38	352	210	44.3	8.6	271.6
90	50	64	50	352	210	49.0	8.4	320.7
91	50	64	64	352	210	46.1	8.1	298.9
92	50	64	76	352	210	48.3	8.0	322.6
93	50	76	38	352	210	46.9	7.8	252.3
94	50	76	50	352	210	49.1	8.6	257.9
95	50	76	64	352	210	50.9	8.3	277.3
96	50	76	76	352	210	51.0	8.0	282.0

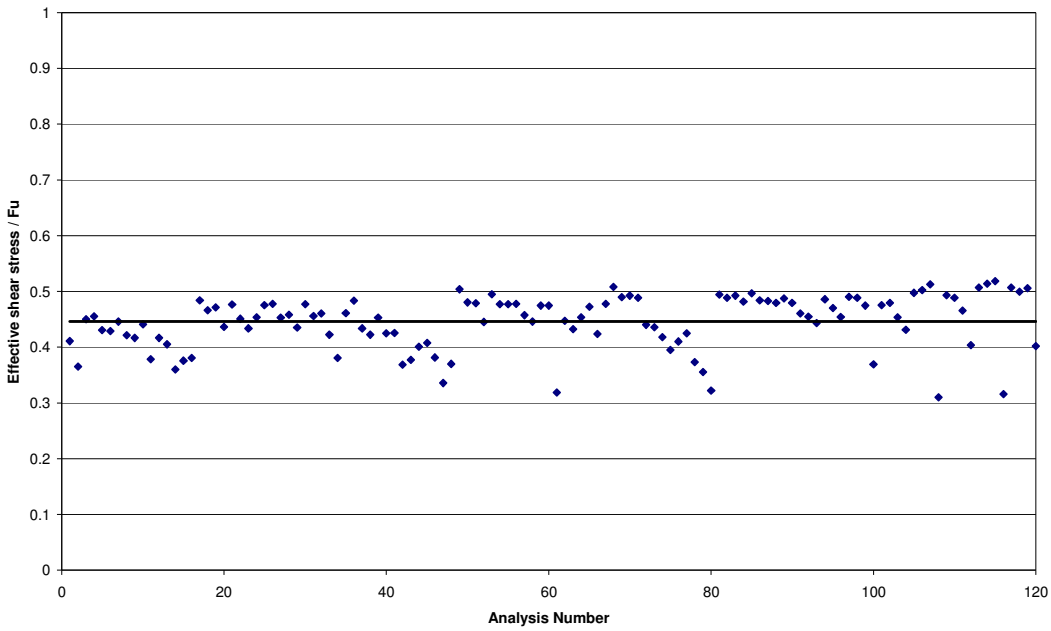

Figure 4.11 : Effective Shear Stress as a Function of Ultimate Strength

According to Figure 4.11, effective shear stress values falls within a band that is bounded by 31-51% of ultimate strength averaging a value of 44.6%. Average shear capacity developed on the shear area is calculated by Equation 4.2.

$$Q = 0.45 \cdot F_u \cdot E \cdot t \tag{4.2}$$

where

Q=shear capacity

E=end distance

t=thickness of the material

To formulize effective stress (σ_{ef}) developed on the inclined area, a new investigation is performed. Effective stress is normalized with ultimate strength of the material is graphed versus angle between the pitch and spacing normalized with 90^o ($\alpha/90^o$) in Figure 4.12.

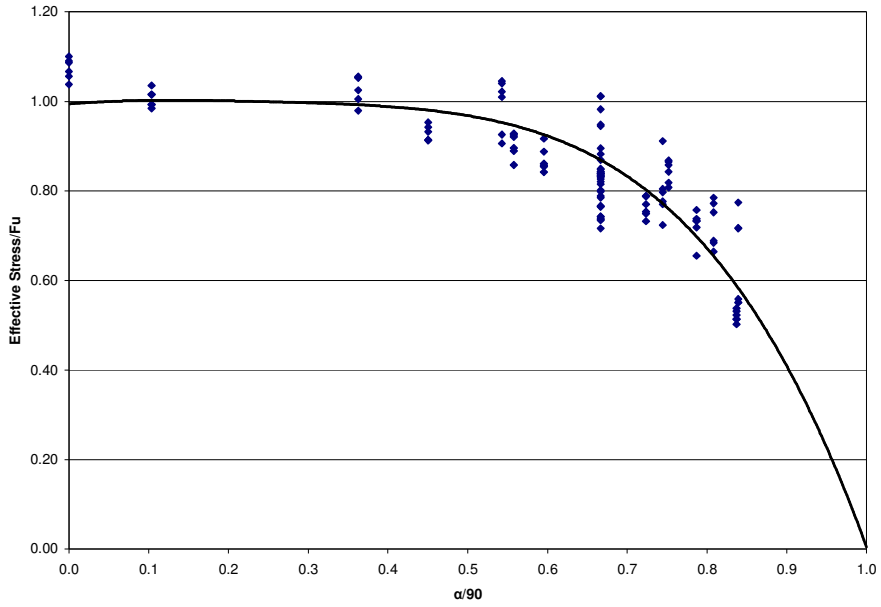

Figure 4.12 : Variation of Effective Stress Normalized by Ultimate Strength

A trend line is found for these data and effective stress ratio is calculated with Equation 4.3. If α is perpendicular, effective stress should be equal to the ultimate shear strength as calculated above and this bond is used in the equation.

$$\sigma_{ef} = \left[F_u \cdot \left(1 - \left(\frac{\alpha}{90} \right)^5 \right) \right] \geq \left[0.45 \cdot F_u \right] \tag{4.3}$$

Since shear capacity and effective stress is formulized, block shear capacity of the staggered hole connections is calculated as follows;

$$P_{ULT} = 2tF_u \left[\left(1 - \left(\frac{\alpha}{90} \right)^5 \right) \cdot (p - d) + 0.45 \cdot E \right] \geq 0.9tF_u \cdot \left[(p - d) + E \right] \tag{4.4}$$

The quality of the prediction equations presented is assessed by making comparisons with the finite element results. Failure loads of Equation 4.4 are plotted against the finite element analysis predictions in Figure 4.13. For each analyzed

specimen a professional factor is calculated and statistical measures of the predictions are presented in Table 4.7.

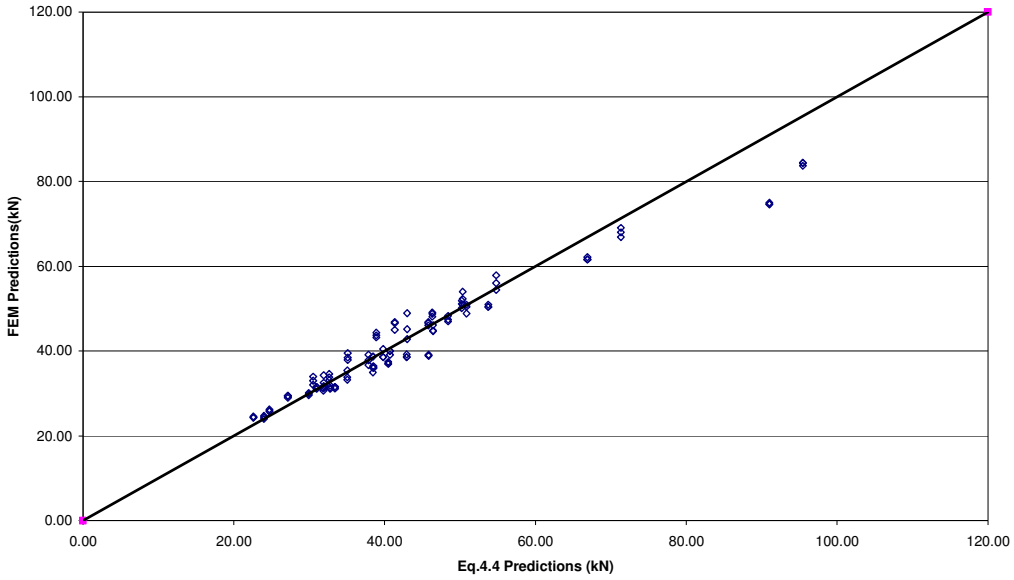

Figure 4.13 : Comparison of Equation 4.4. with FEM Results

Table 4.7 : Professional Factor Statistics for Equation 4.4 Predictions

	Professional factor
	Eq.4.4
Mean	0.994
Standard deviation	0.072
Maximum	1.139
Minimum	0.820

It is evident from the figures and the statistical measures that the developed equation predicts block shear load capacity with acceptable accuracy. The average professional factor for Equation 4.4 is very close to unity and the standard deviation is 7.2%. According to the maximum and minimum professional factors, predictions of 13.9% understrength and 18% overstrength are possible.

4.3 Investigation of Negative and Positive Stagger Pattern

To evaluate the application of the block shear capacity to different signed staggered connections a new investigation is performed. Totally 144, negatively and positively staggered four bolted connections were used in the analysis. The convention adopted for the sign of the stagger is shown in Figure 4.14. The included angle in the potential block shear path as shown "β" in Figure 4.14 is used in specifying the stagger sign. The connection is said to have a positive sign if the angle is greater than 90^o, negative stagger if less than 90^o.

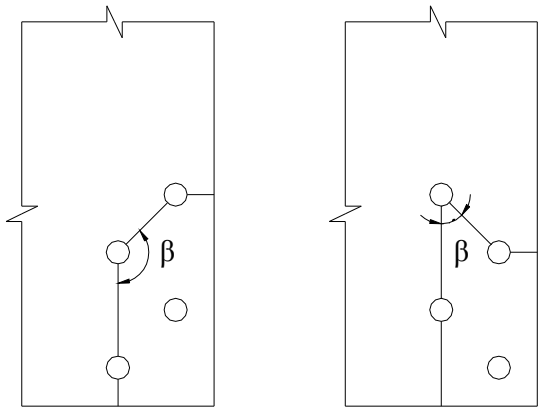

POSITIVE ($\beta > 90^O$) NEGATIVE ($\beta < 90^O$)

Figure 4.14 : Sign of Stagger

Half of the 144 connections had negative and positive stagger signs. Analyzed gusset plate specimens had a dimension of 500mm in width and length and thicknesses of the specimens were taken as unity. A fixed value of 14 mm was used to define the hole diameters. All the specimens had an end distance of 25, 50mm , pitch distance of 38, 50, 64 ,76 mm and an edge distance of 25, 50, 76 mm. As indicated in Figure 4.15, end distance (E) is defined as distance between the end of the gusset plate to the center of the hole closest to the end of the plate, pitch distance (P) is the inclined distance between the staggered holes and edge distance (A) is the

distance between the edge of the gusset plate to the center of the holes closest to the edge of the plate. Pitch distance is inclined with an angle of 45^o in all analyses.

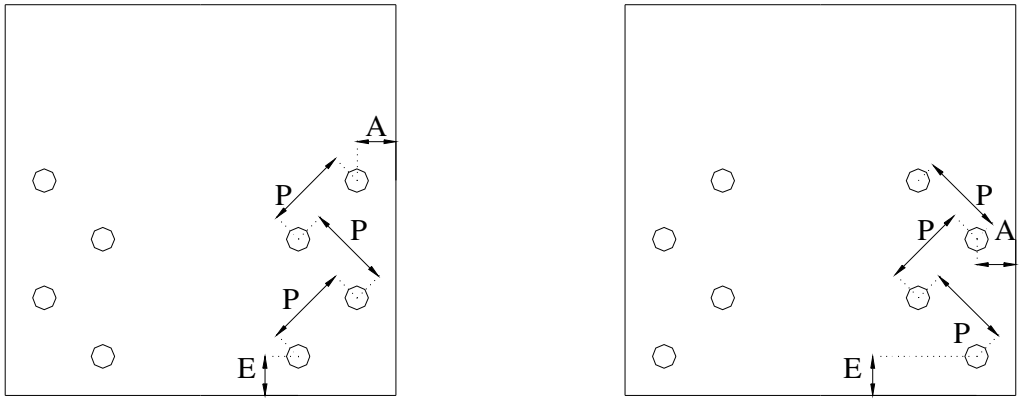

POSITIVE NEGATIVE

Figure 4.15 : General Analyzed Gusset Plate Connections

All the analyzed specimens had an ultimate strength value of 352 MPa. To see the effect of ultimate to yield ratio yield strength values of the specimens, yield strength values were varied as 210, 252 and 293 MPa. This values result in ultimate to yield strength ratios of 1.68, 1.40 and 1.20, respectively. The combination of all the variables considered in this study is listed in Table 4.8.

Table 4.8. Combinations of the Variables Used in Parametric Study

End distance	Edge distance	Pitch distance	F_u/F_y
Hole diameter (14mm)			
Positive Stagger			
25	25/50/76	38/50/64/76	1.68/1.4/1.2
50	25/50/76	38/50/64/76	1.68/1.4/1.2
			72 cases
Hole diameter (14mm)			
Negative Stagger			
25	25/50/76	38/50/64/76	1.68/1.4/1.2
50	25/50/76	38/50/64/76	1.68/1.4/1.2
			72 cases
Total number of cases			*144*

All dimensions are in mm

4.3.1 Results of the Analysis Cases

Previously mentioned geometries are used in the parametric study and Tables 4.9 and 4.10 shows the results of the connections with positive and negative staggers. In the tables below, end distances (E), pitch distances (P), edge distances (A), ultimate strengths (F_u), yield strength (F_y) and ultimate loads (U.L) of each specimens are presented.

Table 4.9 : Analysis Results for 72 Positive Staggered Specimens

Run #	E (mm)	A (mm)	P (mm)	Fu (Mpa)	Fy (Mpa)	U.L. (kN)
1	25	25	38	3.52	2.1	42.5
2	25	25	50	3.52	2.1	51.5
3	25	25	64	3.52	2.1	62.6
4	25	25	76	3.52	2.1	68.6
5	25	50	38	3.52	2.1	53.9
6	25	50	50	3.52	2.1	63.4
7	25	50	64	3.52	2.1	75.3
8	25	50	76	3.52	2.1	83.6
9	25	76	38	3.52	2.1	56.4
10	25	76	50	3.52	2.1	67.1
11	25	76	64	3.52	2.1	79.9
12	25	76	76	3.52	2.1	91.6
13	50	25	38	3.52	2.1	47.7
14	50	25	50	3.52	2.1	57.1
15	50	25	64	3.52	2.1	66.5
16	50	25	76	3.52	2.1	73.5
17	50	50	38	3.52	2.1	62.1
18	50	50	50	3.52	2.1	72.7
19	50	50	64	3.52	2.1	84.2
20	50	50	76	3.52	2.1	91.5
21	50	76	38	3.52	2.1	72.3
22	50	76	50	3.52	2.1	83.2
23	50	76	64	3.52	2.1	95.6
24	50	76	76	3.52	2.1	104.2
25	25	25	38	3.52	2.52	43.7
26	25	25	50	3.52	2.52	53.0
27	25	25	64	3.52	2.52	63.4
28	25	25	76	3.52	2.52	71.0
29	25	50	38	3.52	2.52	54.8
30	25	50	50	3.52	2.52	65.1
31	25	50	64	3.52	2.52	76.9
32	25	50	76	3.52	2.52	84.9
33	25	76	38	3.52	2.52	57.9
34	25	76	50	3.52	2.52	68.3
35	25	76	64	3.52	2.52	81.6
36	25	76	76	3.52	2.52	93.3

Run #	E (mm)	A (mm)	P (mm)	Fu (Mpa)	Fy (Mpa)	U.L. (kN)
37	50	25	38	3.52	2.52	49.9
38	50	25	50	3.52	2.52	59.5
39	50	25	64	3.52	2.52	69.3
40	50	25	76	3.52	2.52	76.8
41	50	50	38	3.52	2.52	64.9
42	50	50	50	3.52	2.52	75.4
43	50	50	64	3.52	2.52	86.7
44	50	50	76	3.52	2.52	93.9
45	50	76	38	3.52	2.52	72.5
46	50	76	50	3.52	2.52	83.8
47	50	76	64	3.52	2.52	96.4
48	50	76	76	3.52	2.52	106.0
49	25	25	38	3.52	2.52	45.3
50	25	25	50	3.52	2.52	53.0
51	25	25	64	3.52	2.52	65.4
52	25	25	76	3.52	2.93	73.7
53	25	50	38	3.52	2.93	56.2
54	25	50	50	3.52	2.93	66.6
55	25	50	64	3.52	2.93	79.1
56	25	50	76	3.52	2.93	88.1
57	25	76	38	3.52	2.93	59.1
58	25	76	50	3.52	2.93	70.1
59	25	76	64	3.52	2.93	83.9
60	25	76	76	3.52	2.93	95.6
61	50	25	38	3.52	2.93	53.1
62	50	25	50	3.52	2.93	61.9
63	50	25	64	3.52	2.93	72.5
64	50	25	76	3.52	2.93	81.6
65	50	50	38	3.52	2.93	70.8
66	50	50	50	3.52	2.93	81.1
67	50	50	64	3.52	2.93	91.4
68	50	50	76	3.52	2.93	99.9
69	50	76	38	3.52	2.93	79.3
70	50	76	50	3.52	2.93	89.8
71	50	76	64	3.52	2.93	101.6
72	50	76	76	3.52	2.93	115.8

Table 4.10 : Analysis Results for 72 Negative Staggered Specimens

Run #	E (mm)	A (mm)	P (mm)	Fu (Mpa)	Fy (Mpa)	U.L. (kN)
1	25	25	38	3.52	2.1	54.0
2	25	25	50	3.52	2.1	61.9
3	25	25	64	3.52	2.1	71.3
4	25	25	76	3.52	2.1	78.3
5	25	50	38	3.52	2.1	58.8
6	25	50	50	3.52	2.1	72.4
7	25	50	64	3.52	2.1	85.6
8	25	50	76	3.52	2.1	104.0
9	25	76	38	3.52	2.1	59.4
10	25	76	50	3.52	2.1	73.8
11	25	76	64	3.52	2.1	87.0
12	25	76	76	3.52	2.1	97.1
13	50	25	38	3.52	2.1	59.5
14	50	25	50	3.52	2.1	69.0
15	50	25	64	3.52	2.1	80.9
16	50	25	76	3.52	2.1	88.4
17	50	50	38	3.52	2.1	72.3
18	50	50	50	3.52	2.1	86.1
19	50	50	64	3.52	2.1	104.0
20	50	50	76	3.52	2.1	104.9
21	50	76	38	3.52	2.1	76.2
22	50	76	50	3.52	2.1	87.6
23	50	76	64	3.52	2.1	100.1
24	50	76	76	3.52	2.1	108.6
25	25	25	38	3.52	2.52	53.9
26	25	25	50	3.52	2.52	63.0
27	25	25	64	3.52	2.52	72.6
28	25	25	76	3.52	2.52	80.2
29	25	50	38	3.52	2.52	59.1
30	25	50	50	3.52	2.52	73.0
31	25	50	64	3.52	2.52	86.2
32	25	50	76	3.52	2.52	105.1
33	25	76	38	3.52	2.52	60.4
34	25	76	50	3.52	2.52	74.1
35	25	76	64	3.52	2.52	87.3
36	25	76	76	3.52	2.52	98.9

Run #	E (mm)	A (mm)	P (mm)	Fu (Mpa)	Fy (Mpa)	U.L. (kN)
37	50	25	38	3.52	2.52	60.7
38	50	25	50	3.52	2.52	70.5
39	50	25	64	3.52	2.52	81.7
40	50	25	76	3.52	2.52	89.3
41	50	50	38	3.52	2.52	73.0
42	50	50	50	3.52	2.52	88.0
43	50	50	64	3.52	2.52	104.6
44	50	50	76	3.52	2.52	105.9
45	50	76	38	3.52	2.52	77.1
46	50	76	50	3.52	2.52	88.3
47	50	76	64	3.52	2.52	101.5
48	50	76	76	3.52	2.52	109.0
49	25	25	38	3.52	2.52	54.3
50	25	25	50	3.52	2.52	64.7
51	25	25	64	3.52	2.52	75.2
52	25	25	76	3.52	2.93	82.8
53	25	50	38	3.52	2.93	59.9
54	25	50	50	3.52	2.93	72.9
55	25	50	64	3.52	2.93	87.8
56	25	50	76	3.52	2.93	107.4
57	25	76	38	3.52	2.93	61.1
58	25	76	50	3.52	2.93	74.3
59	25	76	64	3.52	2.93	89.3
60	25	76	76	3.52	2.93	102.2
61	50	25	38	3.52	2.93	62.2
62	50	25	50	3.52	2.93	73.0
63	50	25	64	3.52	2.93	85.1
64	50	25	76	3.52	2.93	93.4
65	50	50	38	3.52	2.93	74.2
66	50	50	50	3.52	2.93	87.5
67	50	50	64	3.52	2.93	101.5
68	50	50	76	3.52	2.93	112.0
69	50	76	38	3.52	2.93	76.6
70	50	76	50	3.52	2.93	89.2
71	50	76	64	3.52	2.93	101.9
72	50	76	76	3.52	2.93	111.2

4.3.2. Assessment of the Existing Capacity Equations

When dealing with positive staggers a unique block shear path seems to occur. This block shear path follows the stagger line. But, in negative stagger path, there are two block shear paths to define, one following the stagger line (Path 1), the other one with rectangular block (Path 2). These paths are shown in Figure 4.16.

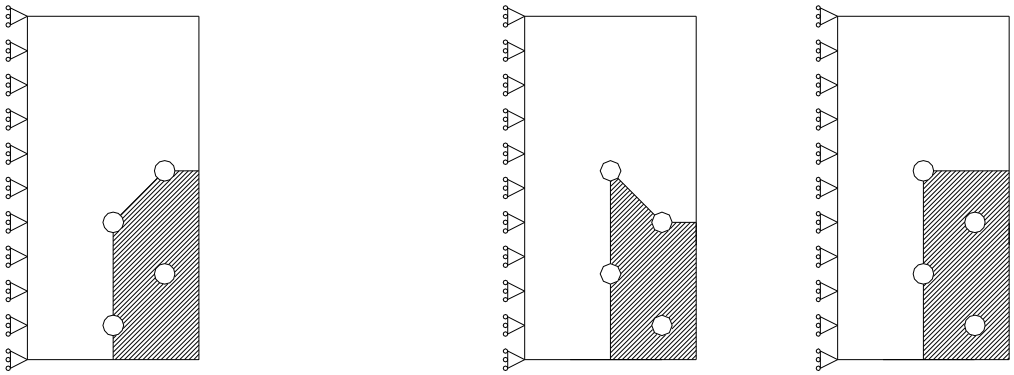

(PATH 1) (PATH 2)

(POSITIVE) (NEGATIVE)

Figure 4.16 : Block Shear Paths for Connections with Positive and Negative Stagger.

Based on AISC-LRFD and ASD specifications block shear capacities of the analyzed 144 specimens with defined block shear paths were calculated and the quality of the prediction equations was assessed by making comparisons with the finite element results. As mentioned in previous section, $s_t^2/4g$ correction for stagger is used when dealing with net tension of the specimens, as AISC recommends. Failure loads of equation predictions are plotted against the finite element analysis predictions in Figures 4.17 to 4.24. Data points appearing below the diagonal line indicate that AISC-LRFD and ASD equations overestimate the failure loads while points above the diagonal line indicate that equations underestimate the failure loads. For each analyzed specimen a professional factor is calculated and statistical measures of the predictions are presented in Tables 4.11 to 4.14.

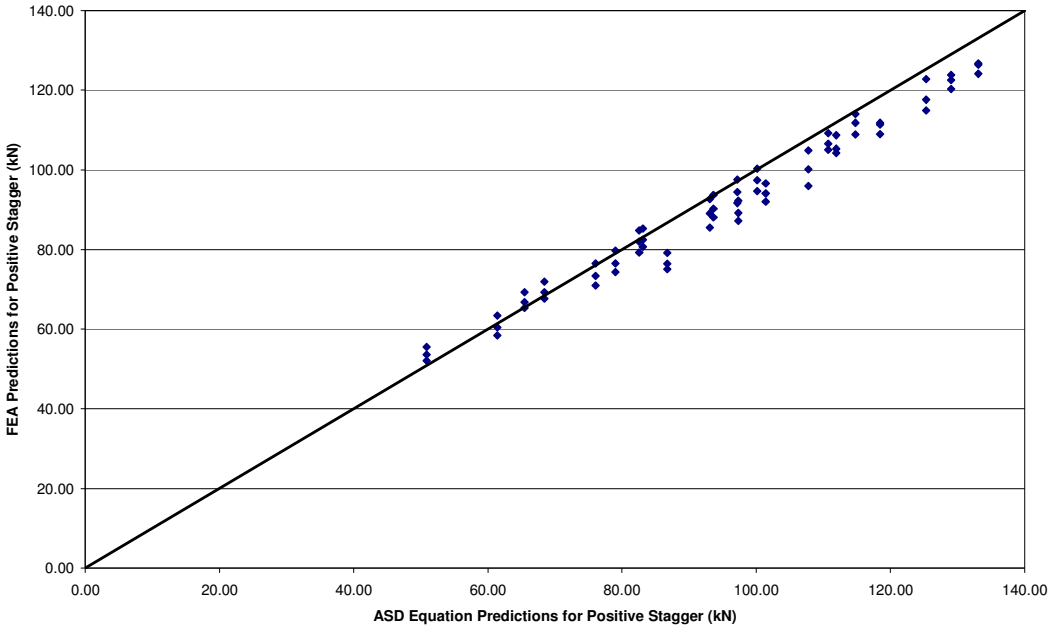

Fig.4.17 : Comparison of ASD Prediction with FEA Predictions for Positive Stagger

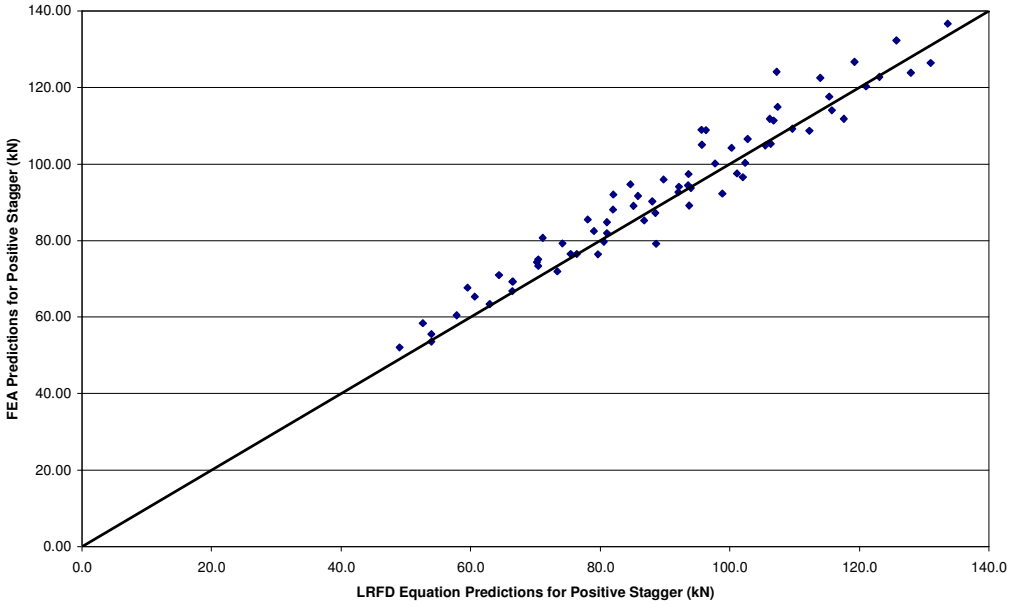

Figure 4.18 : Comparison of LRFD Prediction with FEA predictions for Positive Stagger

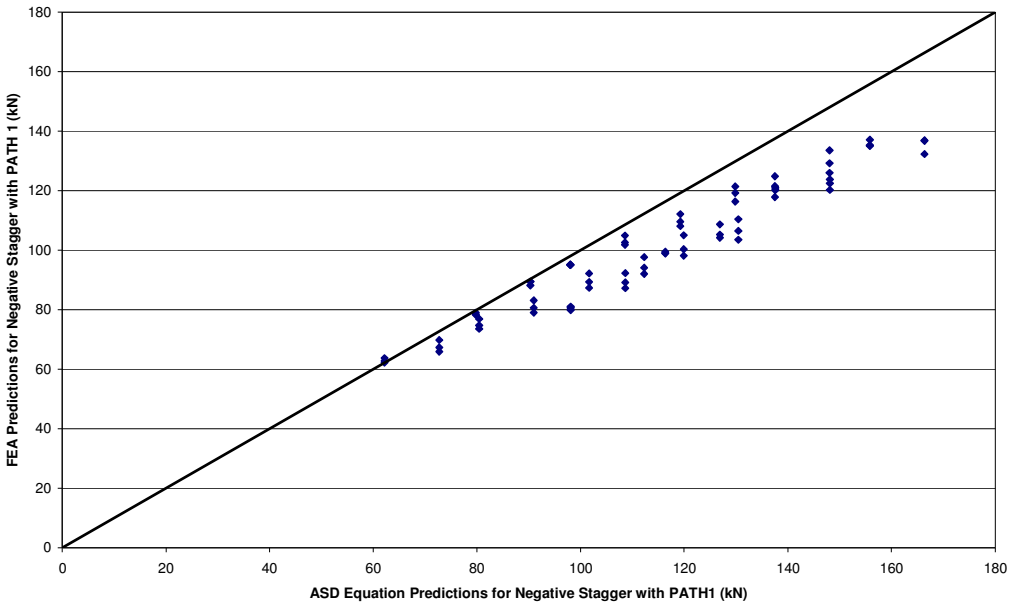

Figure 4.19 : Comparison of ASD Prediction with FEA Predictions for Negative Stagger with PATH1

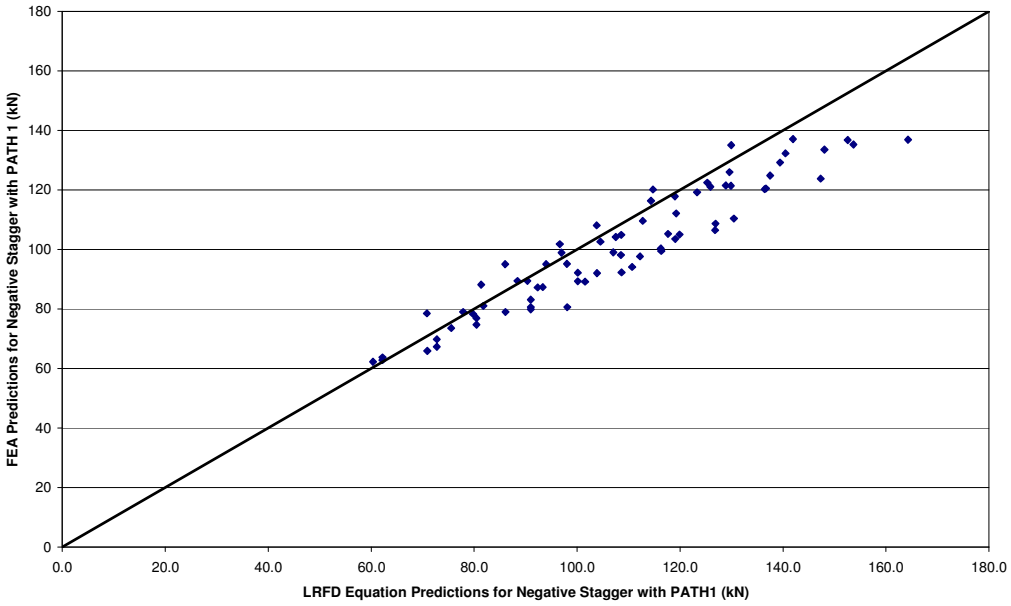

Figure 4.20 : Comparison of LRFD Prediction with FEA Predictions for Negative Stagger with PATH1

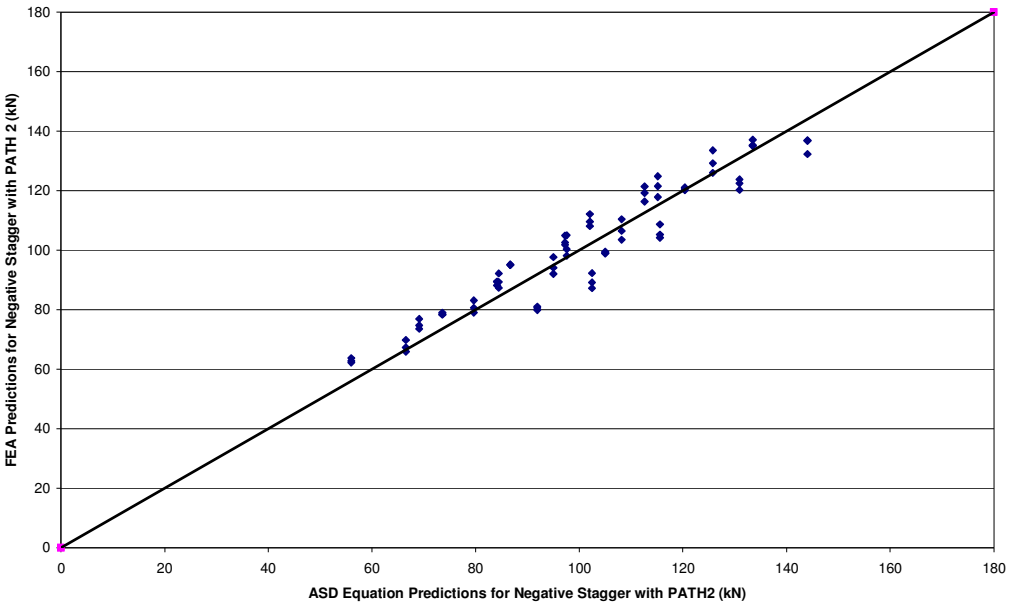

Figure 4.21 : Comparison of ASD Prediction with FEA Predictions for Negative Stagger with PATH2

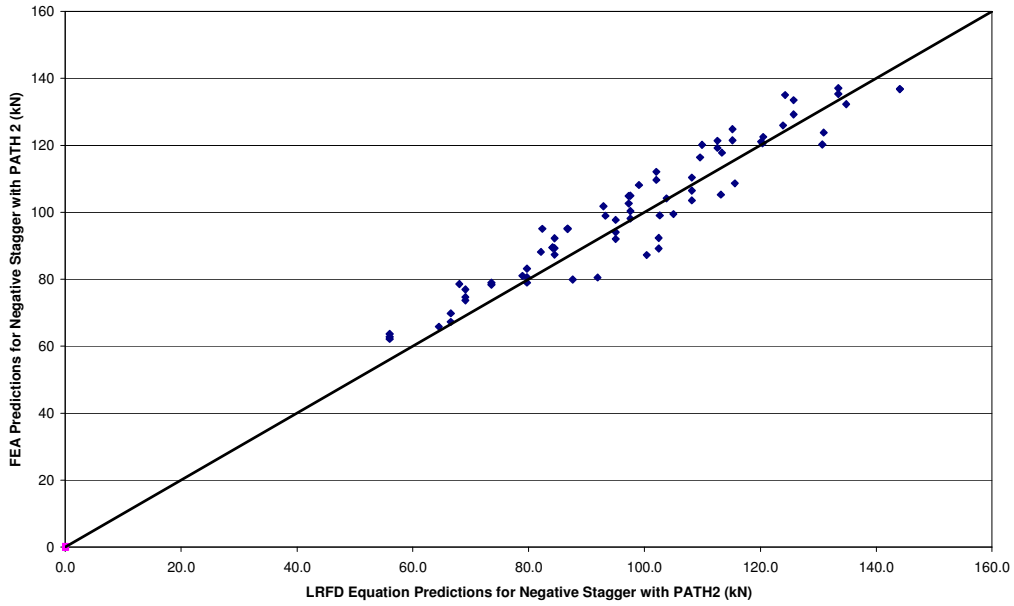

Figure 4.22 : Comparison of LRFD Prediction with FEA Predictions for Negative Stagger with PATH2

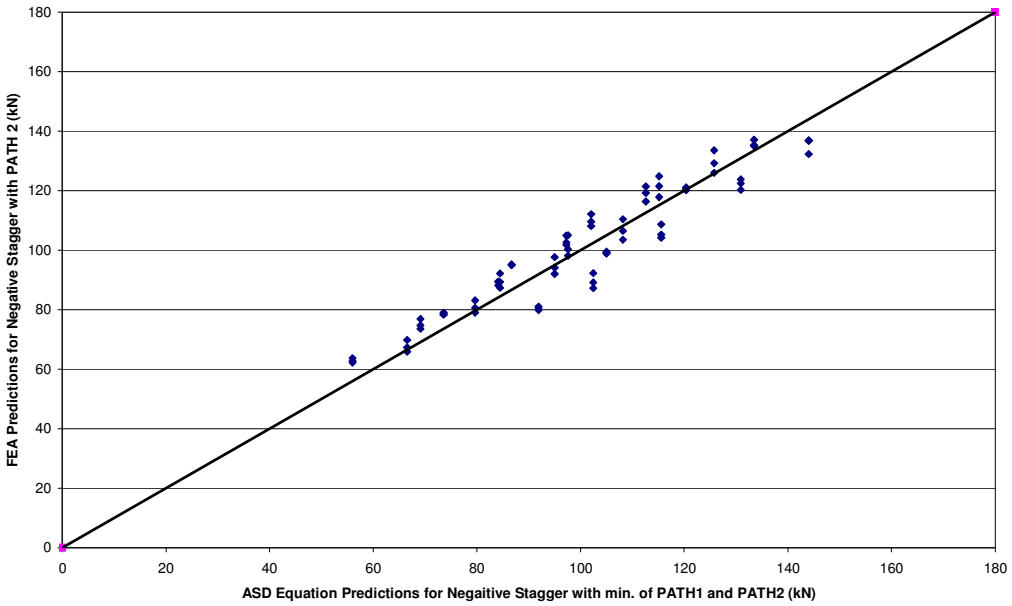

Figure 4.23 : Comparison of ASD Prediction with FEA Predictions for Negative Stagger with min. of PATH1 and PATH2.

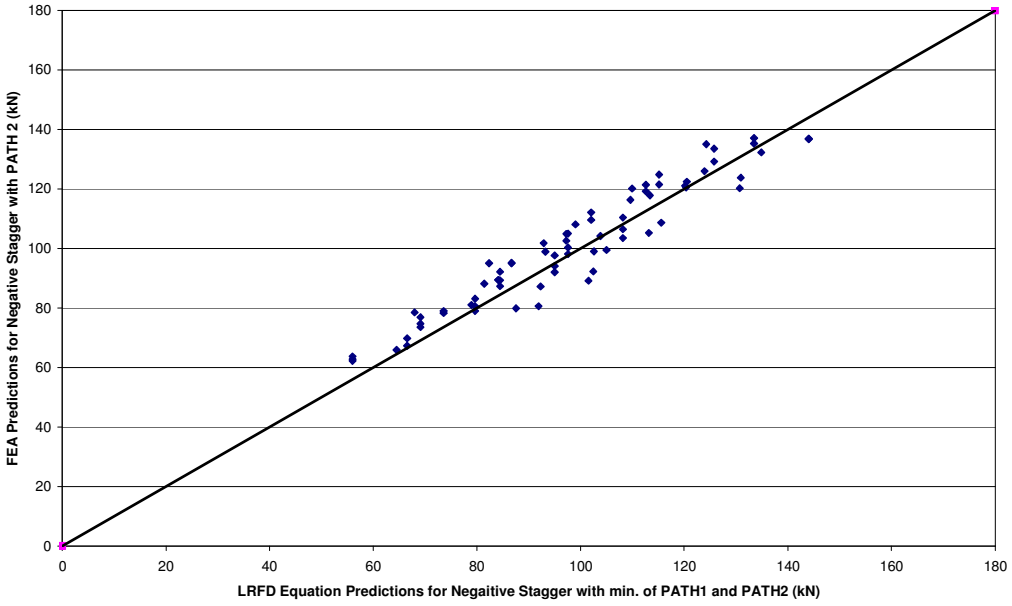

Figure 4.24 : Comparison of LRFD Prediction with FEA Predictions for Negative Stagger with min. of PATH1 and PATH2

Table 4.11 : Professional Factor Statistics of LRFD-ASD Predictions for Positive Stagger

	Professional factor	
	LRFD	ASD
Mean	1.031	0.965
Standard deviation	0.055	0.043
Maximum	1.158	1.093
Minimum	0.893	0.895

Table 4.12 : Professional Factor Statistics of LRFD-ASD Predictions for Negative Stagger (PATH1)

	Professional factor	
	LRFD	ASD
Mean	0.942	0.890
Standard deviation	0.068	0.060
Maximum	1.109	1.024
Minimum	0.821	0.793

Table 4.13 : Professional Factor Statistics of LRFD-ASD Predictions for Negative Stagger (PATH2)

	Professional factor	
	LRFD	ASD
Mean	1.029	1.014
Standard deviation	0.066	0.069
Maximum	1.155	1.138
Minimum	0.869	0.851

Table 4.14 : Professional Factor Statistics of LRFD-ASD Predictions for Negative Stagger (min. of PATH1 and PATH2)

	Professional factor	
	LRFD	ASD
Mean	1.030	1.014
Standard deviation	0.064	0.069
Maximum	1.155	1.138
Minimum	0.877	0.851

It is evident from the figures and and the statistical measures that the both, AISC and ASD equations predict block shear load capacity of the specimens with acceptable accuracy. For positively staggered connections, the average professional factor is 1.031 and 0.965 and standard deviations are 5.5% and 4.3% for AISC-LRFD and AISC-ASD predictions, respectively. According to the maximum and minimum professional factors 15.8% understrength and 10.7% overstrength is possible for LRFD predictions and 9.3% understrength and 10.5% overstrength is possible for ASD predictions.

For negatively staggered connections both LRFD and ASD equations result in more acceptable predictions when PATH2 is used to define block shear path. According to statistical measures, the average professional factor is 1.029 and 1.014 with standard deviations of 6.6% and 6.9% for AISC-LRFD and ASD predictions, respectively. According to the maximum and minimum professional factors 15.5% and 13.8% understrength, 13.1% and 14.9% overstrength is possible for LRFD and ASD predictions, respectively. When smallest of the predictions of PATH1 and PATH2 are observed, for ASD predictions all PATH2 values are less than PATH1 values. For LRFD predictions, PATH2 is the dominated block shear path except three cases again. It can be said that governing block shear path was PATH2 which follows the net horizontal tensile area for negatively staggered connections. It is recommended to use the smallest values of the PATH1 and PATH2 results of ASD and LRFD equations when dealing with negative bolt stagger patterns.

CHAPTER 5

SUMMARY AND CONCLUSIONS

5.1 Summary

Block shear failure is a limit state that should be accounted for during the design of steel tension members. When connections are relatively short block shear failure is usually the mode of the failure. Code treatments present equations to predict block shear load capacities of the connections. But significant differences in failure mode are found in previous test results from code treatment predictions. In this thesis an analytical parametric study has been conducted to investigate the block shear failure in multiple bolt line connections and staggered connections.

In this study, finite element method is employed to study the behavior of the structural members subject to block shear failure mode. An accurate prediction of the block shear failure load is essential to develop design equations and evaluate the existing design equations. Finite element methodology used by Topkaya (2004) was used in the analyses. The quality of the finite element results were assessed by comparing with the previous experimental results performed by Gross (1995), Orbison (1998) and Hardash (1985).

In Chapter 3, analysis of 576 connections with multiple bolt lines was performed. Effects of certain parameters on block shear capacity of the multiple bolt line connections were investigated and defined. The quality of the equations presented in codes and the ones developed by Topkaya (2004) were assessed by

making comparisons with finite element analysis results. Based on analytical investigations, three new equations were developed.

In Capter 4, a new investigation was performed to study stagger effects on block shear load capacity. Code treatments for staggered connections are not explicitly defined, but use of "$s_t^2/4g$" rule is recommended when defining the net tensile section. The quality of the code predictions, by using"$s_t^2/4g$" rule, was assessed by using the finite element results. A new treatment for staggered bolt connections was presented and a new equation (Equation 4.4) was developed based on analytical findings.

Four bolt connections with positive and negative stagger were analyzed. The analysis results were used to test the quality of code provisions and recommendations were given for calculating the block shear paths of staggered connections.

5.2 Conclusions

The following conclusions were drawn based on the results of the study:

- Finite element methodology used by Topkaya (2004) gives good predictions when compared with test results performed by Gross (1995), Orbison (1998) and Hardash & Bjorhovde (1985).
- Both AISC-LRFD and ASD predicts the inaccurate failure mechanism.
- For multiple bolt line connections, effect of end distance pitch distance and block aspect ratio could be ignored in predicting capacities.
- Block shear capacity of the multiple bolt line connections is mostly influenced by connection length and ultimate to yield ratio.
- It is not accurate to use a single effective shear stress value as used in LRFD specification.

- The developed equations provide load capacity estimates of multiple bolt line connections with acceptable accuracies. These equations could be alternative to more traditional code equations.
- When dealing with the stagger, the net area could be increased by $s_t^2/4g$ if the angle between pitch and spacing is less than 60°.
- A new equation was developed for staggered three bolt patterns that encompass all the angle range.
- Sign of the stagger should be taken into account for accurate predictions of the failure load. For positive stagger it is recommended that block shear path should follow the stagger line. On the other hand, for negative stagger it is recommended that minimum of two block shear paths should be considered to find the capacity.

REFERENCES

American Institute of Steel Construction Inc. (AISC), *Allowable Stress Design Specification for Structural Steel Buildings*, 9th Edition, Chicago (IL): American Institute of Steel Construction, 1989.

American Institute of Steel Construction Inc. (AISC), *Load and Resistance Factor Design Specification for Structural Steel Buildings*, 3rd Edition, Chicago (IL): American Institute of Steel Construction, 2001.

Cochrane V.H., *Rules for Rivet Hole Deduction in Tension Members*, Eng News Record, Nov. 1922.

Cunnigham T.J., Orbison J.G., Ziemian R.D., *Assessment of American Block Shear Load Capacity Predictions*, Journal of Constructional Steel Research 1995; 35: 323-38

Epstein H.I., Chamarajanagar R., *Finite Element Studies for Correlation with Block Shear Tests*, Computers and Structures 1996; 61 (5); 967-74.

Gross J.M., Orbison J.G., Ziemian R.D., *Block Shear Tests in High-Strength Steel Angles,* AISC Engineering Journal 1995; 32 (3);117-22.

Hardash S.G., Bjorhovde R., *New Design Criteria for Gusset Plates in Tension*, AISC Engineering Journal 1985; 22(2); 77-94.

Kulak G.L., Grondin G.Y., *AISC Rules for Block Shear in Bolted Connections*, Engineering Journal 4th Quarter, 2001; 199-203.

Kulak G.L., Wu E.Y., *Shear Lag in Bolted Angle Tension Members*, ASCE Journal of Structural Engineering 1997; 123(9): 1144-52.

Munse, W. H., and W. H. Chesson, Jr., *Riveted and Bolted Joints: Net Section Design*, ASCE Journal of the Structural Division, Vol.89, No. ST1, Feb.1963; 107-126.

Orbison J.G., Wagner M.E., Fritz W.P., *Tension Plane Behavior in Single-Row Bolted Connections Subjected to Block Shear*, Journal of Constructional Steel Research 1999; 49; 225-39.

Ricles J.M., Yura J.A., *Strength of Double-Row Bolted-Web Connections*, ASCE Journal of Structural Engineering 1983; 109 (1).

Smith, J.C., *Structural Steel Design: LRFD Method*, New York: Harper&Row,1989.

Topkaya C, *A Finite Element Parametric Study on Block Shear Failure of Steel Tension Members*, Journal of Constructional Steel Research 2004; 1615-35

Yura, J.A., *Elements for Teaching Load and Resistance Factor Design*, American Institute of Steel Construction, 1988.